Analysis of Cirrus Cloud Microphysical Data

Final Report

NASA Grant NAG1-1706

Michael R. Poellot

Cedric A Grainger

Department of Atmospheric Sciences

University of North Dakota

P.O. Box 9006

Grand Forks, ND 58202-9006

October 15, 1999

TABLE OF CONTENTS

1. Introduction

The FIRE program has the goal of improving our capabilities to understand, model and detect the properties of climatically-important clouds. This is being undertaken through a three-pronged effort of modeling, long-term observations and short-term intensive field studies. Through examination of satellite and other data it is apparent that stratus and cirrus cloud types have the greatest impact on climate due to their radiative effects and ubiquitous nature. As a result, the FIRE program has developed two paths of investigation, each having its own subset of research objectives and measurement programs. The work conducted under this grant was directed toward furthering our understanding of cirrus cloud systems.

While it is known that cirrus are climatically important, the magnitude and even sign of the impact is unclear. Cirrus clouds affect the transfer of radiation according to their physical depth and location in the atmosphere and their microphysical composition (Liou, 1986). However, significant uncertainties still exist in how cirrus clouds form and how they are maintained, what their physical properties are and how they can be parameterized in numerical models. Better remote sensing techniques for monitoring cirrus cloud systems and improved modeling of radiative transfer through ice particles are also needed. A critical element in resolving these issues is a better understanding of cirrus cloud microphysical properties and how they vary.

Important microphysical parameters include ice water content and integrated ice water path, particle size distribution and crystal habit; the significance of these parameters has been shown in a number of applications. For example, Starr and Cox (1985) found notable interactions between cloud processes and microphysical properties in their modeling studies. They concluded that the bulk physical properties of cirrus are affected by crystal habit and size distribution, and that cirrus cannot be represented by analogy to warmer stratiform clouds. Stackhouse and Stephens (1994) illustrated how biases in particle size parameterizations can lead to biases in model results and interpretations. Model results of Mitchell and Arnott (1994) showed a strong dependence of cirrus cloud radiative properties on particle habit. Significant differences resulted from the use of non-spherical particles versus equivalent spheres. Another critical area is the retrieval of cloud properties from remote measurements which requires some assumptions concerning the composition of the clouds. For example, Intrieri, et al, (1993), have developed a method for determining cirrus cloud particle sizes using lidar and radar measurements based on a modified gamma distribution of particle sizes. Other retrievals such as those using satellite data are also dependent on similar assumptions (e.g., Ackerman, et al, 1993).

Our understanding of cirrus cloud microphysical characteristics has lagged to a large extent because of the relative inaccessibility of these upper-tropospheric cloud systems and a lack of adequate instrumentation for their measurement. Prior to 1991, only a limited number of in situ measurement programs had been conducted, and these included a variety of cirrus types and geographical locations. Perhaps not surprisingly, analyses of these data sets have found a high degree of variability in particle sizes and

concentrations (for reviews, see Liou, 1986, and Dowling and Radke, 1990). While there have been some parameterizations derived for modeling use (Heymsfield and Platt, 1984, Stephens, et al, 1990), there remains a significant amount of uncertainty as to the source and nature of this variability. This is particularly true at the small end of the size spectrum because most of the particle probes used in the past could not detect particles smaller than approximately 50 μm. There is evidence which suggests that there are enough ice particles in cirrus at sizes smaller than this to have a significant radiative impact (e.g., Platt, et al, 1989). The shape of the particle spectrum in this range is also needed for accurate retrievals of cirrus properties from remote sensors. Fortunately, the microphysical data collected in situ during the FIRE Cirrus IFO II included measurements of small ice particles. Analysis of these data was conducted to help reduce the uncertainties in cirrus microphysical properties.

The focus of the research to be conducted under this grant was the data collected in situ by the University of North Dakota Citation aircraft. The goals of this research were to:

- add to the body of knowledge of cirrus cloud microphysics, particularly at the small end of the size spectrum; and
- analyze the spatial variation of cirrus clouds.

2. Microphysical Data

The FIRE Cirrus IFO II was conducted over southeastern Kansas in late fall of 1991, to sample clouds of a more sub-tropical origin and to expand upon the knowledge gained from the first IFO. Sampling was conducted simultaneously by active and passive remote sensors and by in situ aircraft and sonde-born instruments. The mission of the UND Citation aircraft was to collect cloud microphysical and supporting data. A compliment of cloud particle sizing probes included a continuous formvar replicator and four standard Particle Measuring Systems (PMS) instruments:

FSSP	Cloud water droplets	3 - 47 μm
1D-C	Cloud particles	20 - 600 μm
2D-C	Cloud particles	33 - 1056 μm
1D-P	Large particles	0.3 - 4.5 mm.

The replicator, supplied by the University of Nevada Desert Research Institute (DRI), is capable of capturing particles as small as approximately 7 μm. The FSSP is a light scattering instrument and its response to ice particles is uncertain (but it still may be possible to use its data to derive small particle information under some conditions). The other three are optical array probes. Liquid and supercooled water contents were measured with a Johnson-Williams probe and Rosemount ice detector, respectively. Other measured parameters included the state parameters (temperature, pressure and dew point), three-dimensional wind flow and turbulence, condensation nuclei (CN), ozone and NO_X concentrations, and aircraft dynamics.

A variety of mid and upper-tropospheric cirriform clouds were sampled during the IFO. A thorough overview of the conditions encountered is given in a technical report by Poellot and Henderson (1994); the highlights may be summarized as follows. Ten missions were flown for a total of 35 flight hours at cloud altitudes ranging from approximately 6.6 to 12.2 km with in-cloud temperatures of - 23 °C to -64 °C. The typical flight profile consisted of step climbs and descents on an along-wind track; several spiral descents were also performed. Cirrus conditions sampled included layers which were optically thin, optically thick, "patchy", multi-layered, deepening or dissipating. Supercooled water was encountered on two flights. Many of the clouds appeared to contain an abundance of small (<100 μm diameter) ice particles.

A recent analysis of a portions of these data compared the performance of the 2D-C optical array probe, which is the type most often used in previous measurement programs, and the formvar replicator (Arnott, et al, 1994). The comparison of 2D-C and replicator data revealed that for this sample cloud there were some tens to hundreds of small particles which went undetected by the 2D-C. Calculations showed that these particles could significantly contribute to and even dominate the solar extinction and infrared emission of cirrus. Therefore, the replicator data were used in the analyses to extend our knowledge of cirrus microphysics to the smaller sizes.

3. Approach

3.1 Microphysical Characterization of Cirrus

Ice water content, particle size distribution and habit are microphysical parameters important to the proper modeling and monitoring of cirrus clouds and their radiative effects. The method of analysis followed that of Heymsfield and Platt (1984; hereafter referred to as HP), where pass average values of particle concentrations by size were calculated. Data from the DRI replicator were used to count and size particles with diameters up to 150 μm and the 2D-C for larger ones. Crystal habits were determined from the replicator data for particles smaller than 300 μm and from the 2D-C data for larger ones through the use of an automatic classification scheme (Heymsfield and Parrish 1979). (Particles larger than about 300 μm tend to fragment when impacting the replicator film surface.) Ice water contents (IWC) were calculated using the pass-averaged concentrations and crystal habits using relationships cited in Heymsfield (1977) and Mitchell (1994).

Following HP, the size distributions were parameterized for each 5 °C temperature range analyzed, and the pass average IWC used to normalize the spectra. Values obtained for the clouds sampled in this study were compared with those derived by HP. Some differences were expected due to the cloud types sampled and the instrumentation used to collect the data. The data set used by HP was taken from primarily deep, uniform cirrus generally associated with synoptic depressions, while the FIRE samples were mostly thin, banded features associated with jet stream circulations or

baroclinic ascent. Also in contrast with the present study, the small particle size spectra (down to 20 μm) were derived by HP from 1D probe data.

In addition to the stratification by temperature, an effort was made to determine relationships between the microphysical and macrophysical cloud properties such as cloud depth, distance from cloud boundary, and large-scale forcing. A review of complimentary aircraft, lidar and radar data was performed to determine the study clouds' top and base heights and the relative position of each Citation sample leg within cloud. Supporting synoptic descriptions and satellite data were also reviewed to determine the large scale forcing of the sampled cirrus cloud systems.

Analysis of the replicator data for this study was accomplished under subcontract with DRI. The tedious job of counting and sizing particle replica has been somewhat streamlined by the acquisition of equipment and development of software to make the process semi-automatic (Arnott and Hallett, 1994). Even so, it is still a time-consuming procedure and on the order of a half million frames of replicator film were exposed during the FIRE IFO alone. Therefore, it was not within the scope of this proposal to analyze all of the replicator data; rather, portions of the film from a representative portion of each data leg were processed.

3.2 Analysis of the Spatial Variation of Cirrus Clouds.

The variation of the microphysical characteristics of the cirrus clouds over distances of a few meters to tens of kilometers is important when trying to interpret data with relatively coarse resolution, such as radiometric measurements of cloud characteristics. The manner in which the cirrus microphysical characteristics vary would be expected to be closely related to the dynamics of the generating mechanism. Sassen et al. (1989) have shown by a spectral analysis of aircraft-derived vertical velocities that there is an apparent convective structure present in cirrus with a horizontal scale of approximately 1-2 km. Therefore, an analysis of the vertical velocities derived from the UND Citation data for the legs flown in the FIRE cirrus was accomplished. The purpose of this analysis was to see if the type of convective structures reported by Sassen et al. are apparent in this larger data base. In addition, similar analyses were performed on several of the cirrus microphysical parameters. The parameters included ice crystal concentration, crystal size, and ice water content. The output of this work was a description of the variation of these parameters as a function of scale, to see if the apparent fluctuations in vertical velocity at the 1 km scale are indicative of fluctuations in cloud microphysical characteristics of the same scale.

In a similar vein, if there are sustained convective structures responsible for the peaks in the spectral density described earlier (rather than random fluctuations on that scale) there would be a reasonable likelihood of finding a significant positive eddy flux of ice crystals (or of ice water content) that is independent of the larger scale (i.e., >100 km) vertical motions. This would be expected since a sustained downdraft would contain

crystals that are sublimating while the updraft would contain crystals that are growing. Non-sustained vertical motions, lasting for relatively short time periods would result in very little vertical displacement and any effects would not be likely to be seen in the microphysics data. Therefore, the eddy flux computations should be near zero. The presence or absence of sustained convective elements within the cirrus would be of major importance in understanding the microphysical characteristics of these clouds

4. Results

4.1 Cloud Microphysics

The detailed results of the cirrus cloud microphysics are given in Poellot, et al., 1998. The following is a summary of these results.

This analysis of the cloud microphysical data collected during FIRE II by the UND Citation found that there are a number of factors which influence cirrus cloud microphysics and which must be taken into account for parameterization of these cloud systems. These include but are not necessarily limited to temperature, synoptic forcing, position in cloud and cloud ice water content. The key results are summarized as follows: 1) A dependence of particle size spectra shape on temperature was found which differed from that previously reported for deeper, frontal overrunning cirrus. 2) There was no marked dependence of crystal habit on temperature other than columns were most prevalent in clouds colder than – 50°C. 3) When synoptic forcing was considered, clouds generated by closed low systems and the sub-tropical jet (southwesterly flow cases) contained many more particles at all sizes than those produced by short wave and baroclinic lift (northwesterly flow cases). 4) A position-in-cloud stratification supported earlier studies with evidence that ice particles are nucleated in the upper portion of the cirrus cloud, grow by diffusion and aggregation as they fall, and finally evaporate as they reach cloud base. 5) A look at the variation of spectral form with ice water content (IWC, a common model-predicted variable) found that as IWC increased, an increase in particle number concentration was accompanied by a broadening of the distribution to larger sizes. 6) Analysis of the replicator data suggests that the small particle end of the size spectrum may be best represented by a modified Gamma distribution.

4.2 Spectral Analysis

The spectral analysis performed on each of the components of the wind velocity showed that, with few exceptions, the shape of the spectra was similar and the turbulence intensities were comparable. The slopes of the power spectra for each of the wind velocity components were close to $-\frac{5}{3}$ for the high wavenumber end of the spectrum. The vertical velocity spectra were run on most of the days. Some examples of the vertical component spectra are shown in figures 1-3. These spectra are unfiltered, so there are no known biases for any particular portion of the spectrum. On many of the time blocs

investigated, the spectra showed a significant change in the slope for wavenumbers corresponding to wavelengths of between 1 and 2 km (wavenumbers of between .003 and .006 m^{-1}). Generally, the slope became closer to zero at the very low wavenumbers. This would indicate that there was an input of energy at the 1-2 km scale.

The spectral analyses on the microphysics data showed little consistent difference from one parameter to another in terms of the shapes of the curves. That is, the power spectra for the 2D-C concentrations were not markedly different from the spectra of the 1D-C concentrations. Some typical spectral density curves for the 1D-C probe are shown in figures 4-6. These are for data taken in the same time periods as was done for the vertical velocity spectra in figures 1-3. In general, the spectra of the hydrometeor concentrations tended to be fairly flat (i.e., near zero slope) at the high wavenumber end of the spectrum. This "whiteness" of the spectrum implies that there are no preferences for variations in the microphysical data for one size scale to another. There was substantial variability at the low wavenumber end of the spectrum and some variability in the point where the slope of the spectra began to deviate from zero. There was also significant day to day differences in the magnitude of the variations as indicated by the spectral magnitudes.

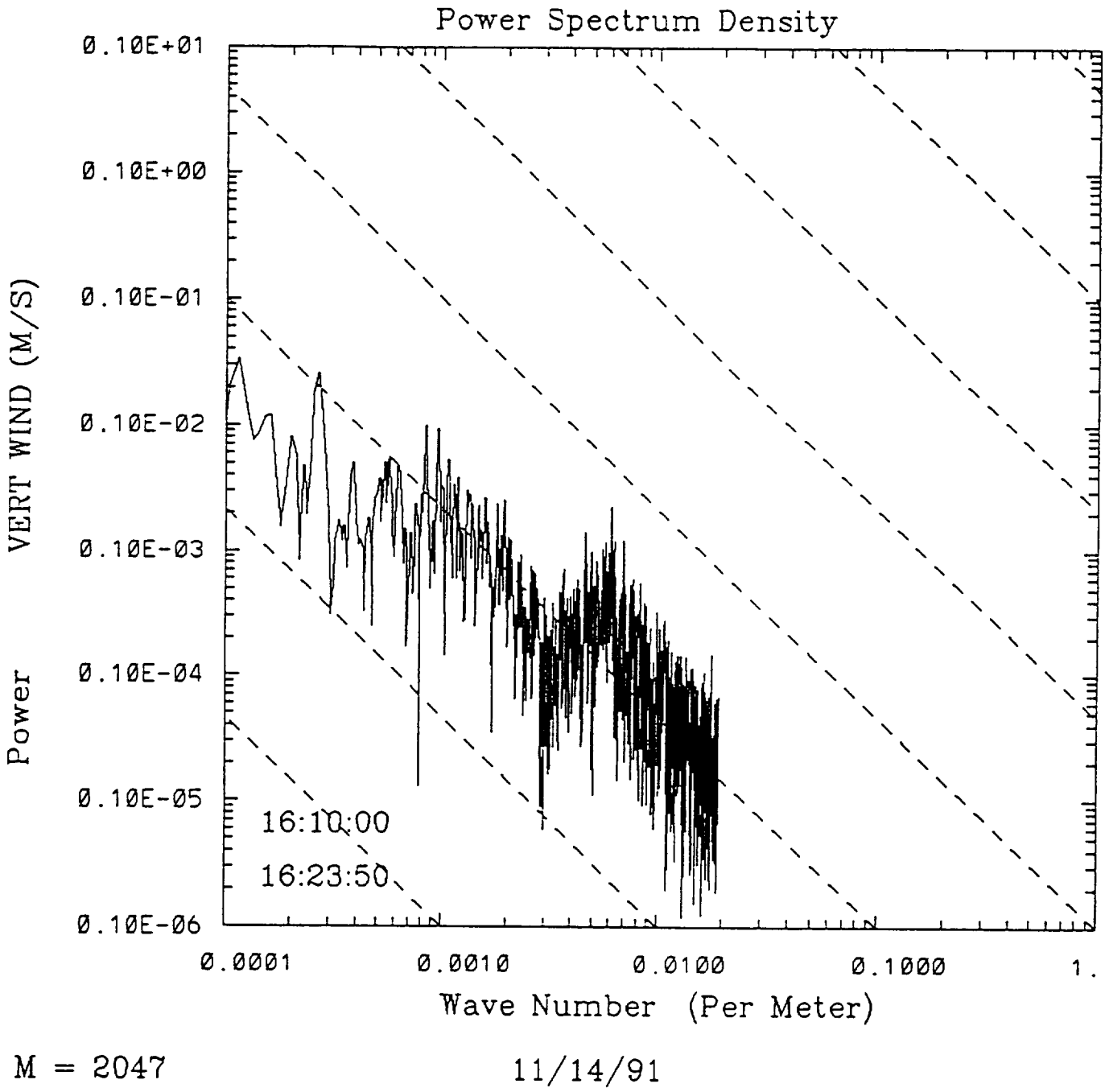

Figure 1. Spectral density for the vertical velocity as a function of wavenumber for the period 16:10:00 to 16:23:50 on 14 November 1991. The dashed lines represent a –5/3 slope.

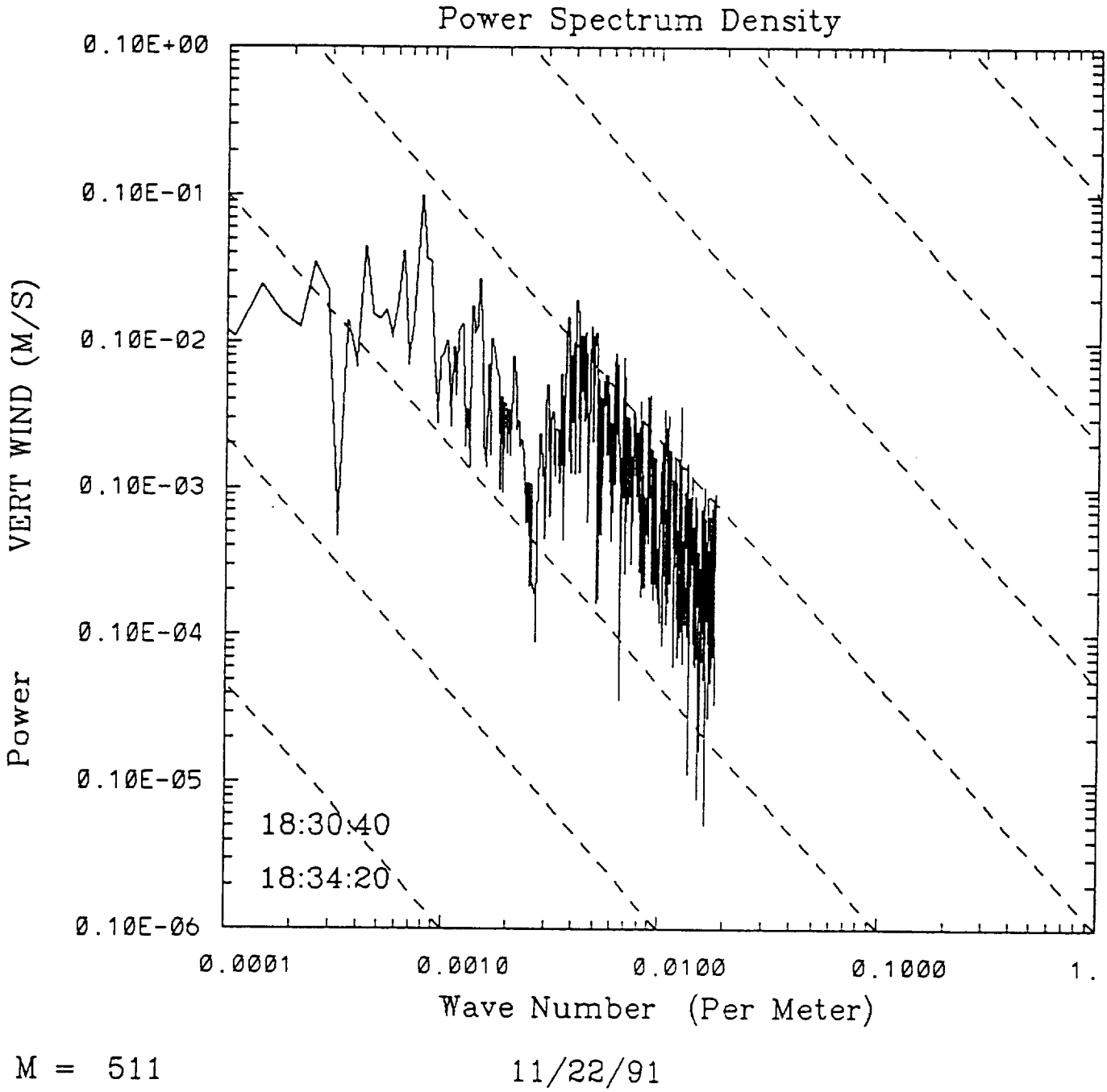

Figure 2. Same as Figure 1, but for the time period 18:30:40 to 18:34:20 on 22 November 1991.

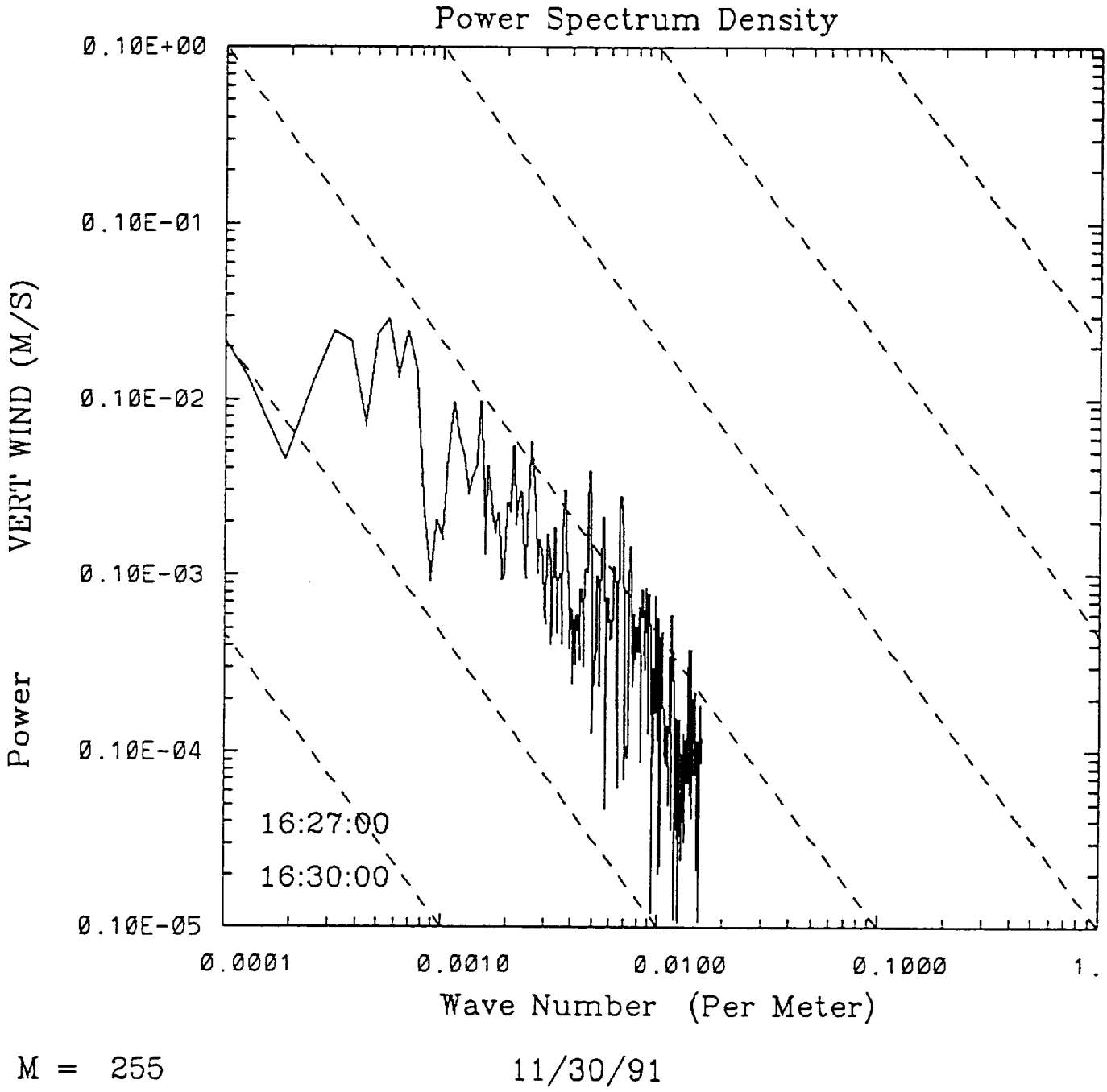

Figure 3. Same as Figure 1, but for the time period 16:27:00 to 16:30:00 on 30 November 1991.

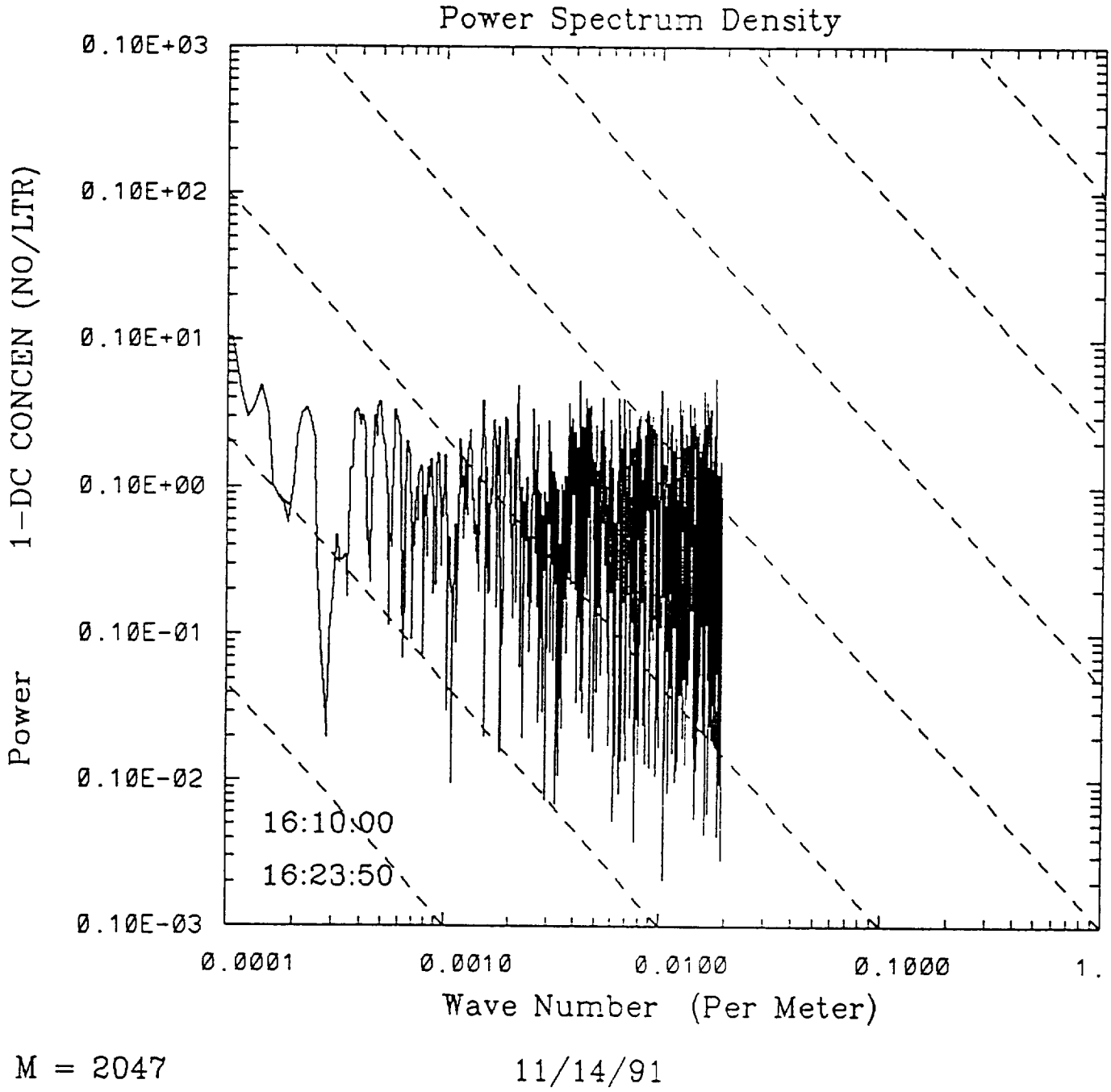

Figure 4. Spectral density for the 1D-C concentrations as a function of wavenumber for the period 16:10:00 to 16:23:50 on 14 November 1991. The dashed lines represent a –5/3 slope.

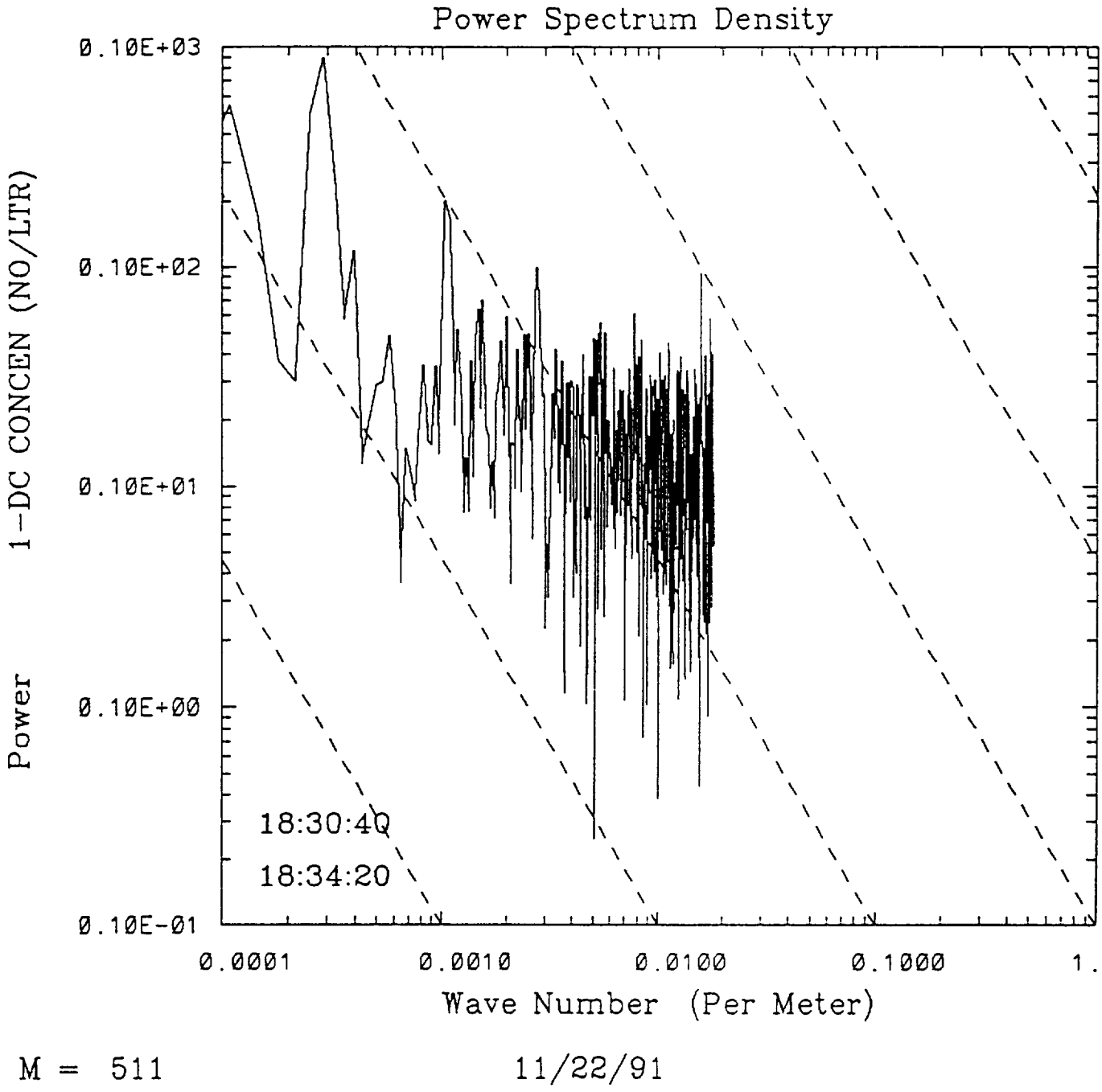

Figure 5. Same as Figure 4, but for the time period 18:30:40 to 18:34:20 on 22 November 1991.

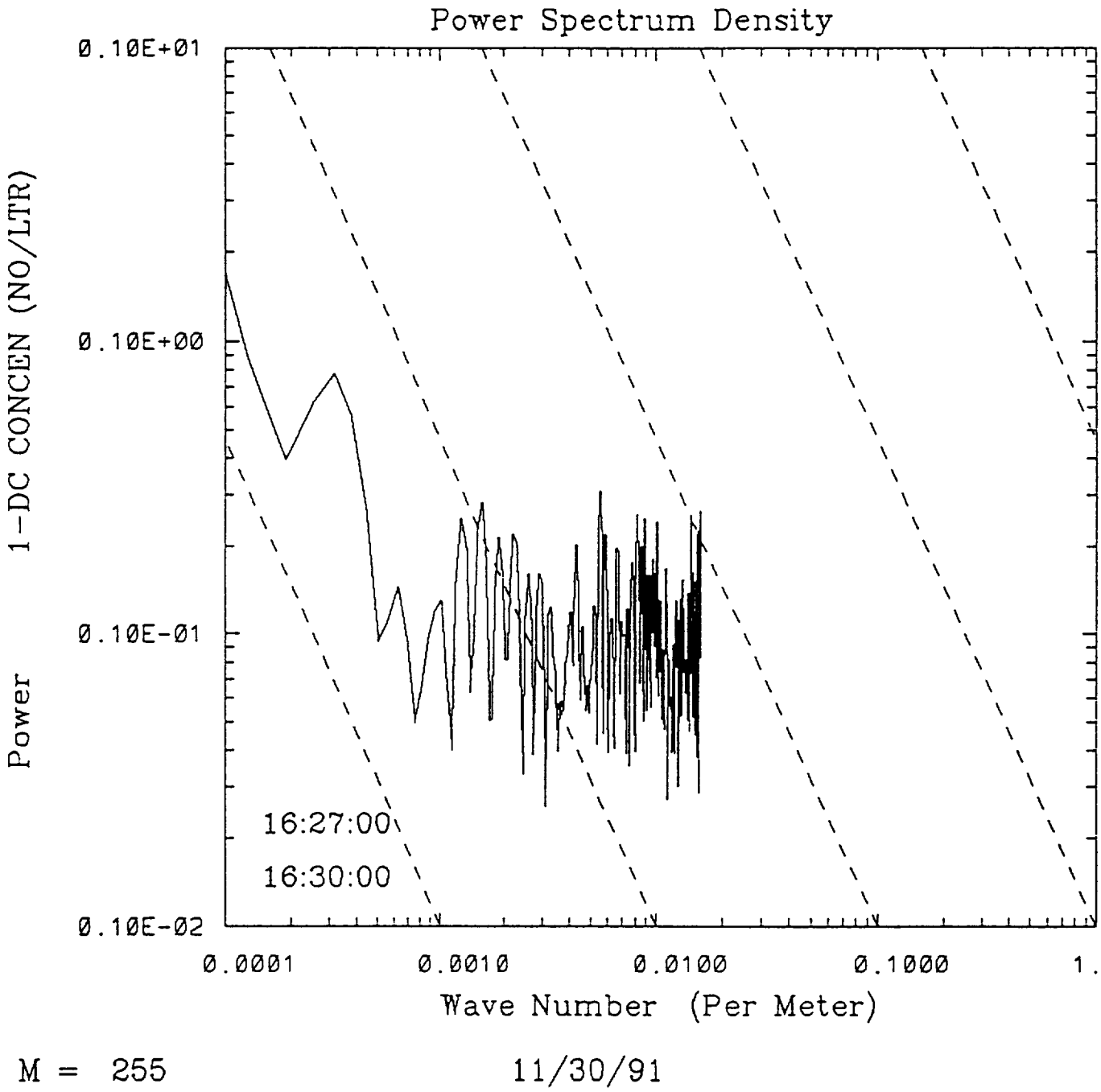

Figure 6. Same as Figure 4, but for the time period 16:27:00 to 16:30:00 on 30 November 1991.

5. References

Ackerman, S., W. Smith, X. Ma, R. Knuteson and H. Revercomb, 1993: Cirrus cloud retrievals from HIS observations during FIRE II. Proceedings, FIRE Cirrus Science Conf., Breckenridge, CO, June 14-17, 1993, pp 88-92.

Arnott, W., Y. Dong, J. Hallett and M. Poellot, 1994: Role of small ice crystals in radiative properties of cirrus: a case study, FIRE II, November 22, 1991. *J. Geophys. Res,*. **99**, 1371-1381.

Arnott, W. and J. Hallett, 1994: Automation of replicator data analysis. Progress report to NASA, Contract NAG-1-1546, Desert Research Institute, Reno, NV, 18 pp.

Dowling, D. and L. Radke, 1990: A summary of the physical properties of cirrus clouds. *J. Appl. Meteor.*, **29**, 970-978.

Heymsfield, A., 1977: Precipitation development in stratiform ice clouds: a microphysical and dynamical study. *J. Atmos. Sci.*, **34**, 367-381.

Heymsfield, A. and J. Parrish, 1979: Techniques employed in the processing of particle size spectra and state parameter data obtained with the T-28 aircraft platform. NCAR/TN-137+1A, National Center for Atmospheric Research, Boulder, CO, 89 pp.

Heymsfield, A. and C. Platt, 1984: A parameterization of the particle size spectrum of ice clouds in terms of the ambient temperature and the ice water content. *J. Atmos. Sci.*, **41**, 846-855.

Intrieri, J., G. Stephens, W. Eberhard and T. Uttal, 1993: A method for determining cirrus cloud particle sizes using lidar and radar backscatter technique. *J. Appl. Meteor.*, **32**, 1074-1082.

Liou, K., 1986: Influence of cirrus clouds on weather and climate processes: a global perspective. *Mon. Wea. Rev.*, **114**, 1167-1199.

Mitchell, D., 1994: A model predicting the evolution of ice particle size spectra and radiative properties of cirrus clouds. Part I: microphysics. *J. Atmos. Sci.*, **51**, 797-816.

Mitchell, D. and W. Arnott, 1994: A model predicting the evolution of ice particle size spectra and radiative properties of cirrus clouds. Part II: dependence of absorption and extinction on ice crystal morphology. *J. Atmos. Sci.*, **51**, 817-832.

Platt, C., J. Spinhirne and W. Hart, 1989: Optical and microphysical properties of a cold cirrus cloud: evidence for regions of small ice particles. *J. Geophys. Res.*, **94**, 11,151-11,164.

Poellot, M. and B. Henderson, 1994: University of North Dakota Citation FIRE Cirrus II mission summary and data report. report to NASA, Grant NAG-1-1351, University of North Dakota, Grand Forks, ND, 182 pp.

Poellot, M., R. Zerr, W.P. Arnott, and J. Hallett, 1998: A microphysical characterization of cirrus from the FIRE-II Cirrus IFO. *Preprints, Conference on Cloud Physics*, Everett, WA, pp. 3-6.

Sassen, K., D. Starr and T Uttal, 1989: Mesoscale and microscale structure of cirrus clouds: three case studies. *J. Atmos. Sci.*, **43**, 371-396.

Stackhouse, P. and G. Stephens, 1994: Investigation of the effects of the macrophysical and microphysical properties of cirrus clouds on the retrieval of optical properties: results from FIRE II. Preprints, 8th Conf. on Atmospheric Radiation, Amer. Meteor. Soc., (Nashville), pp. 225-227.

Starr, D., and S. Cox, 1985: Cirrus clouds. Part II: numerical experiments on the formation and maintenance of cirrus. *J. Atmos. Sci.*, **42**, 2682-2694.

Stephens, G., S. Tsay, P. Stackhouse and P. Flatau, 1990: The relevance of the microphysical and radiative properties of cirrus clouds to climate and climatic feedback. *J. Atmos. Sci.*, **47**, 1742-1753.

Conference Preprints/Presentations

Arnott, W.P., T. Ulrich, R. Cole, J. Hallett, and M. Poellot, 1998: Summary of in situ observations of cirrus microphysics during FIRE II: Instrumental response. Preprints, Conference on Cloud Physics, Everett, WA, pp. 7-10.

Poellot, M., R. Zerr, W.P. Arnott, and J. Hallett, 1998: A microphysical characterization of cirrus from the FIRE-II Cirrus IFO. Preprints, Conference on Cloud Physics, Everett, WA, pp. 3-6.

Appendix: Particle Size Spectra

This appendix contains a series of graphs showing detailed particle size spectra and distribution parameters derived from the Citation microphysical data. The data consisted of aircraft pass-averaged spectra, which were divided into temperature categories and location in cloud categories. The temperature categories were intervals of 5 C, the location categories were either bottom, bottom-middle, middle, top-middle, or top. These data are summarized in the attached figures.

In the case of the 1DC and 2DC data set, exponential distributions were fit to the data in a manner similar to that used by Heymsfield and Platt (1984). The parameters they discussed are compared with the data collected here and summarized in the attached figures and table.

The empirical corrections made to the 1DC data were then removed and a gamma distribution was fit to this uncorrected 1DC and 2DC data. These can be found in the attached figures for both temperature and location in cloud categories. The figures titled "1DC Gamma Distribution Parameters vs. Temperature" and "1DC Gamma Distribution Parameters vs. Location in Cloud" give a graphical representation of the parameters obtained from the best-fit gamma distribution. The parameter labeled Gamma is representative of the 'average' concentration in the distribution and the parameter labeled Peak is representative of the size at which the maximum concentration in the distribution occurred. Similar figures are given for gamma distributions fit to the replicator and 2DC data.

Replicator ice particle habits: the ice particle habit data from the replicator was also obtained and partially analyzed. Two figures are included from this limited analysis.

Particle Size Distributions

by Temperature and Location in Cloud

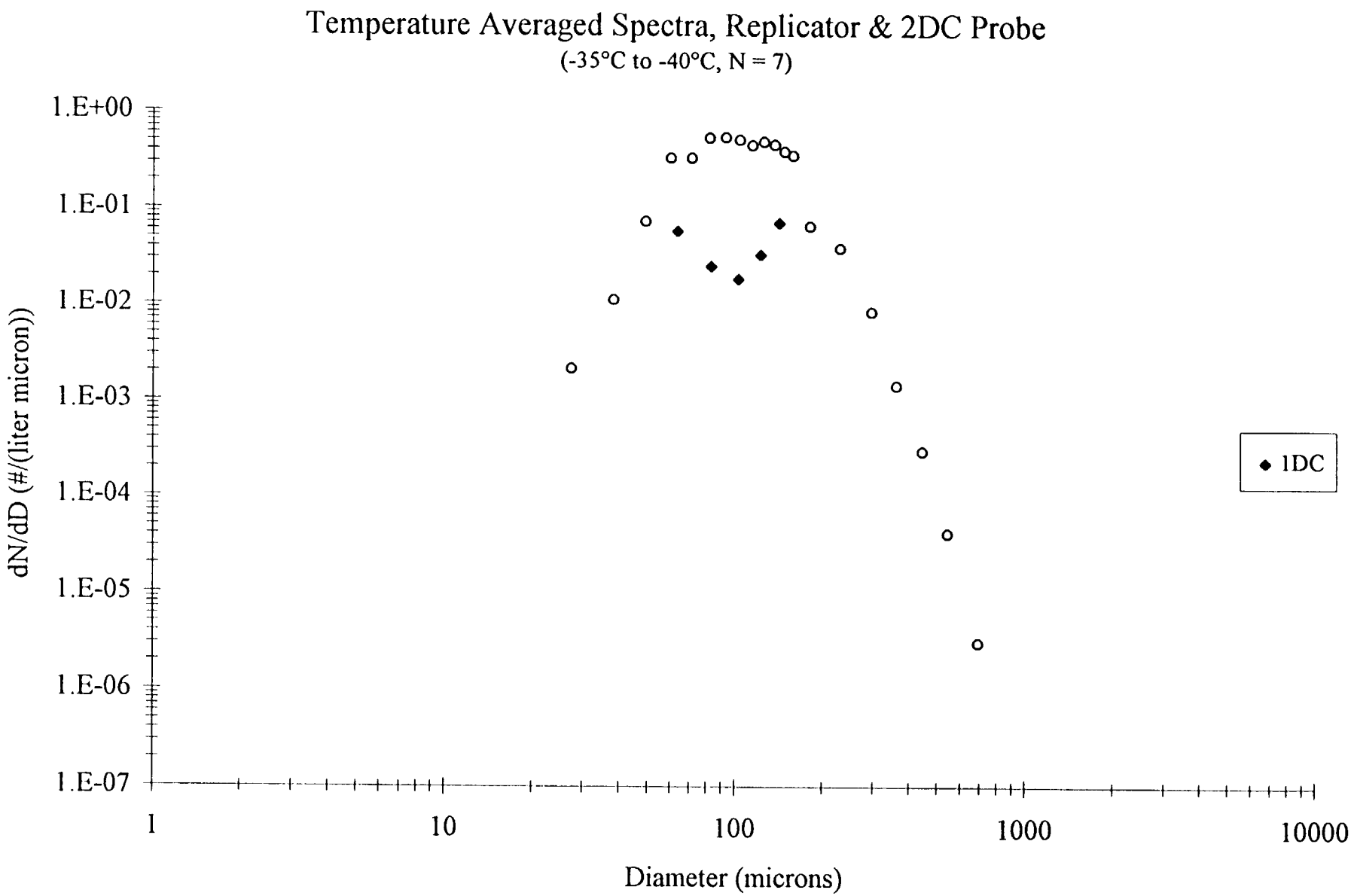
Temperature Averaged Spectra, Replicator & 2DC Probe
(-35°C to -40°C, N = 7)
1.E+00
1.E-01
1.E-02
1.E-03
1.E-04
1.E-05
1.E-06
1.E-07
dN/dD (#/(liter micron))
1
10
100
1000
10000
Diameter (microns)
1DC

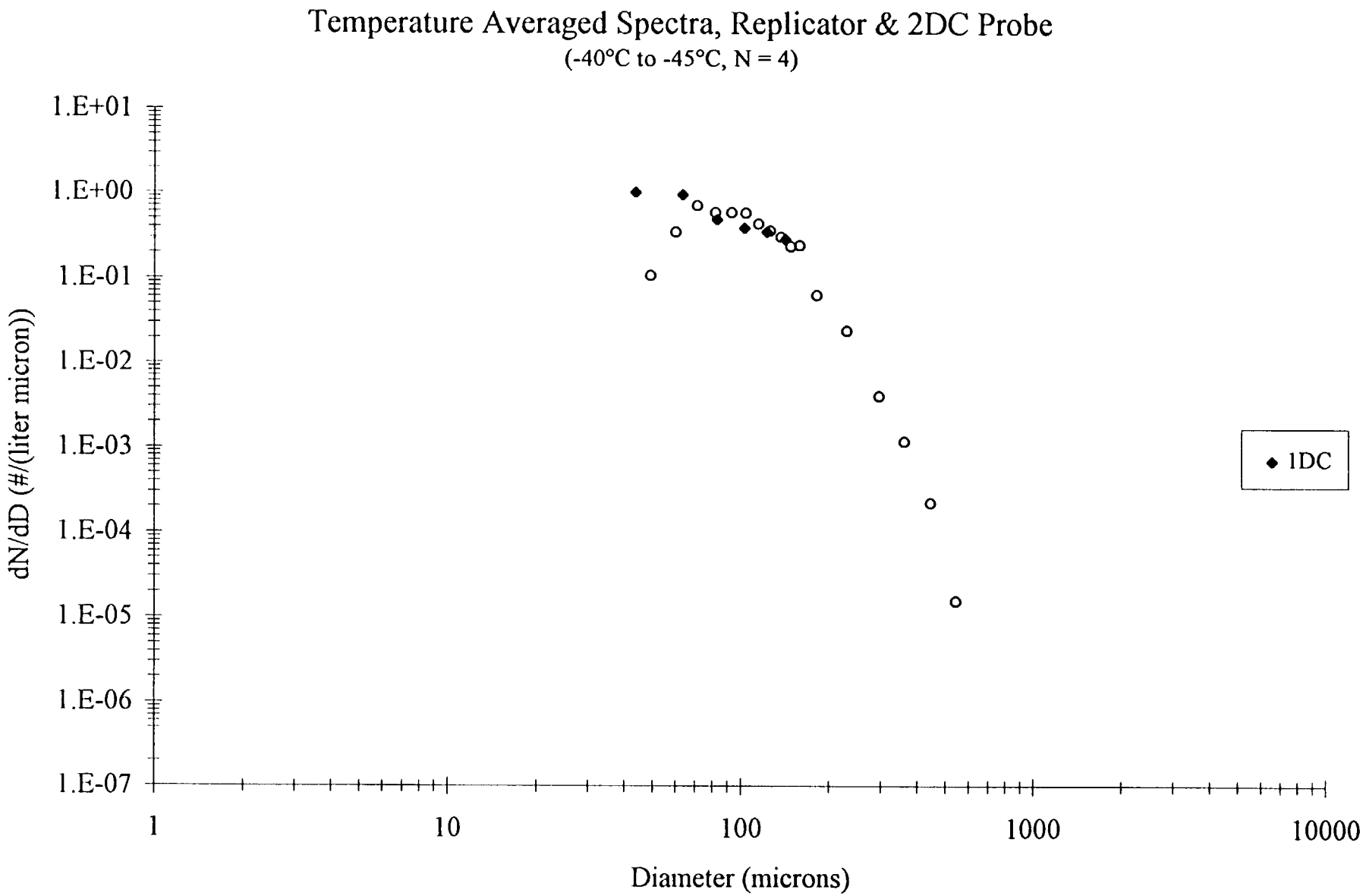
Temperature Averaged Spectra, Replicator & 2DC Probe
(-40°C to -45°C, N = 4)
1.E+01
1.E+00
1.E-01
1.E-02
1.E-03
1.E-04
1.E-05
1.E-06
1.E-07
dN/dD (#/(liter micron))
1
10
100
1000
10000
Diameter (microns)
1DC

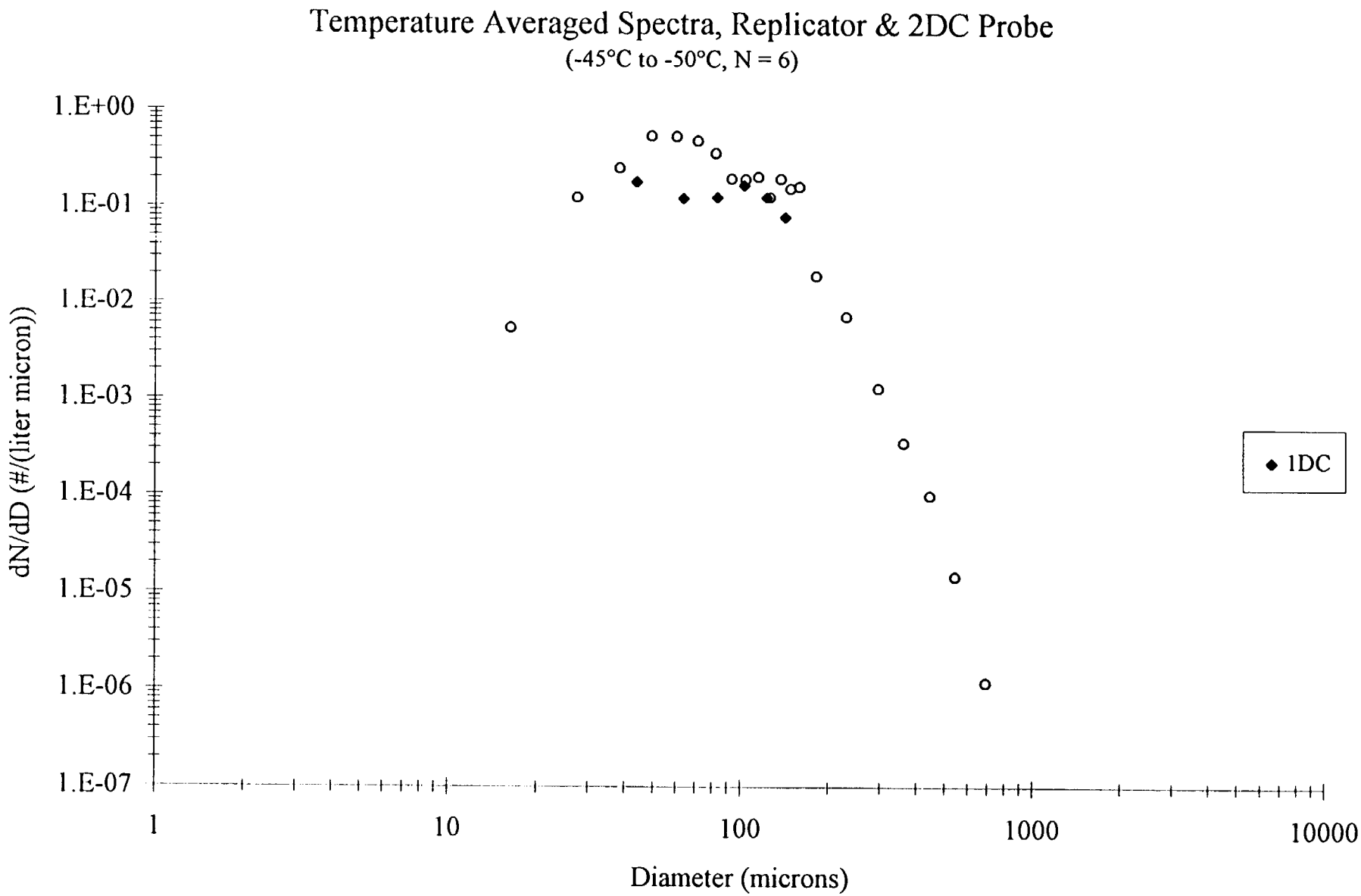
Temperature Averaged Spectra, Replicator & 2DC Probe
(-45°C to -50°C, N = 6)
dN/dD (#/(liter micron))
1.E+00
1.E-01
1.E-02
1.E-03
1.E-04
1.E-05
1.E-06
1.E-07
1
10
100
1000
10000
Diameter (microns)
1DC

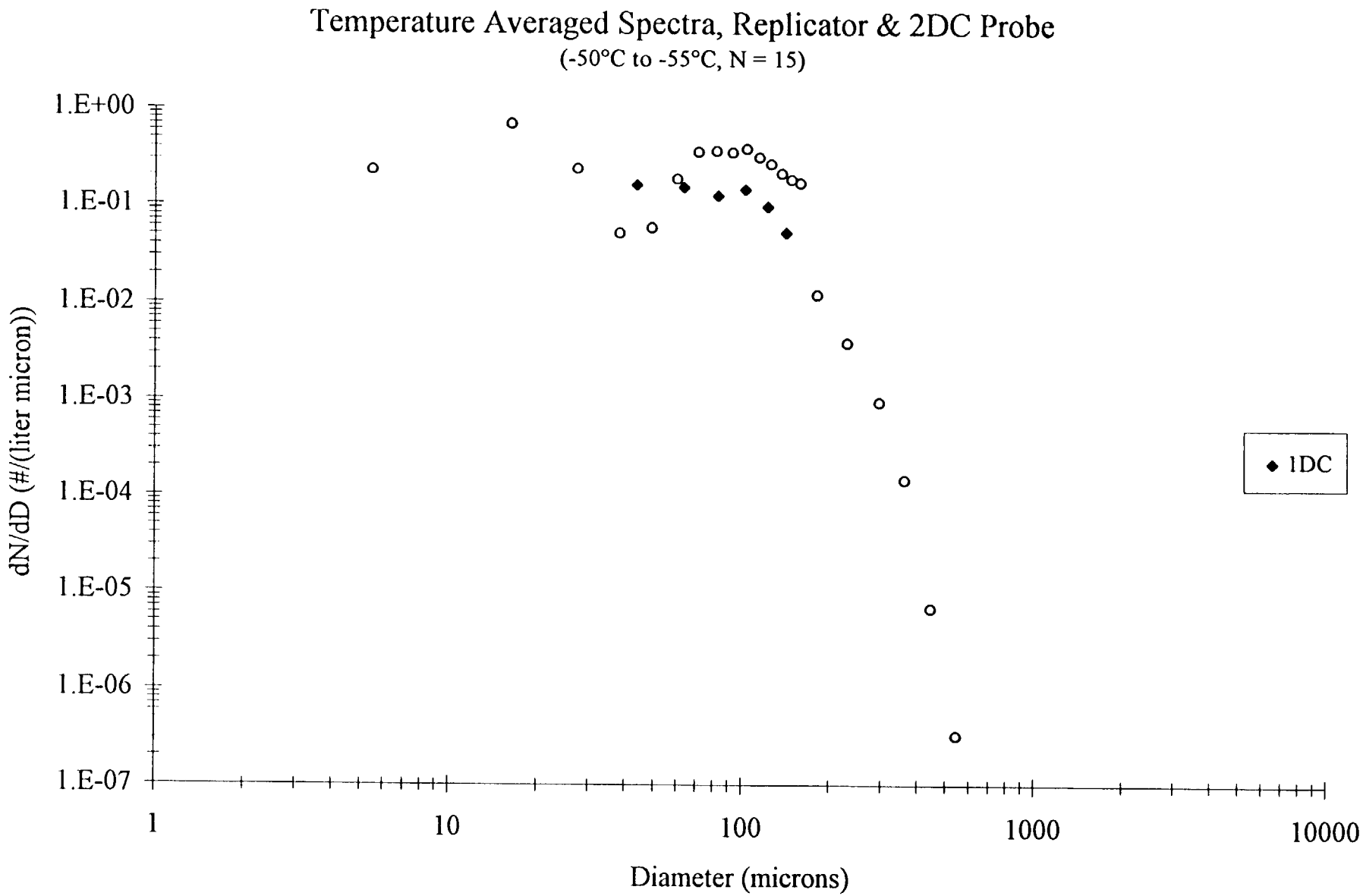
Temperature Averaged Spectra, Replicator & 2DC Probe
(-50°C to -55°C, N = 15)
1.E+00
1.E-01
1.E-02
1.E-03
1.E-04
1.E-05
1.E-06
1.E-07
dN/dD (#/(liter micron))
1
10
100
1000
10000
Diameter (microns)
1DC

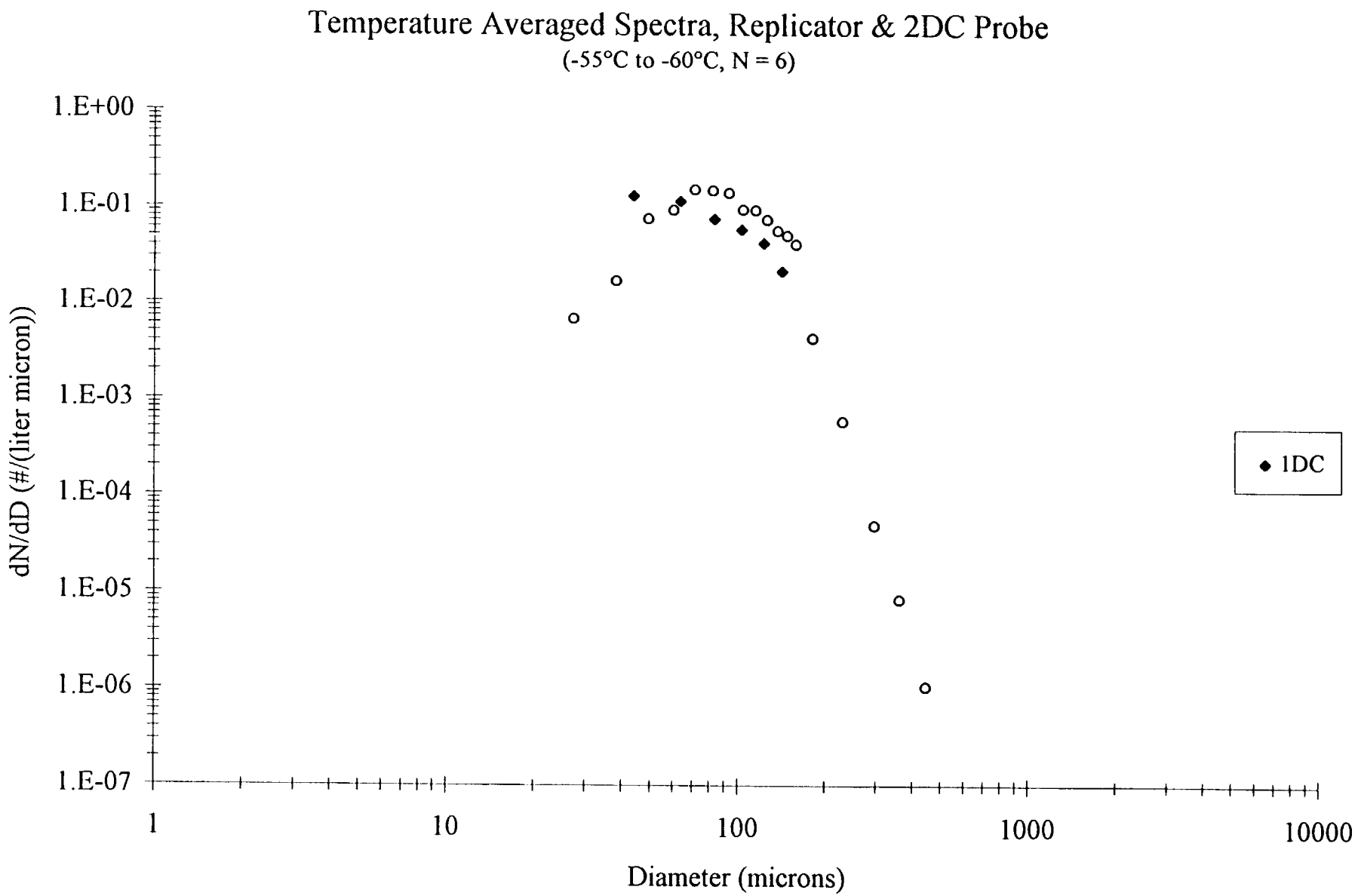
Temperature Averaged Spectra, Replicator & 2DC Probe
(-55°C to -60°C, N = 6)
1.E+00
1.E-01
1.E-02
1.E-03
1.E-04
1.E-05
1.E-06
1.E-07
dN/dD (#/(liter micron))
1
10
100
1000
10000
Diameter (microns)
1DC

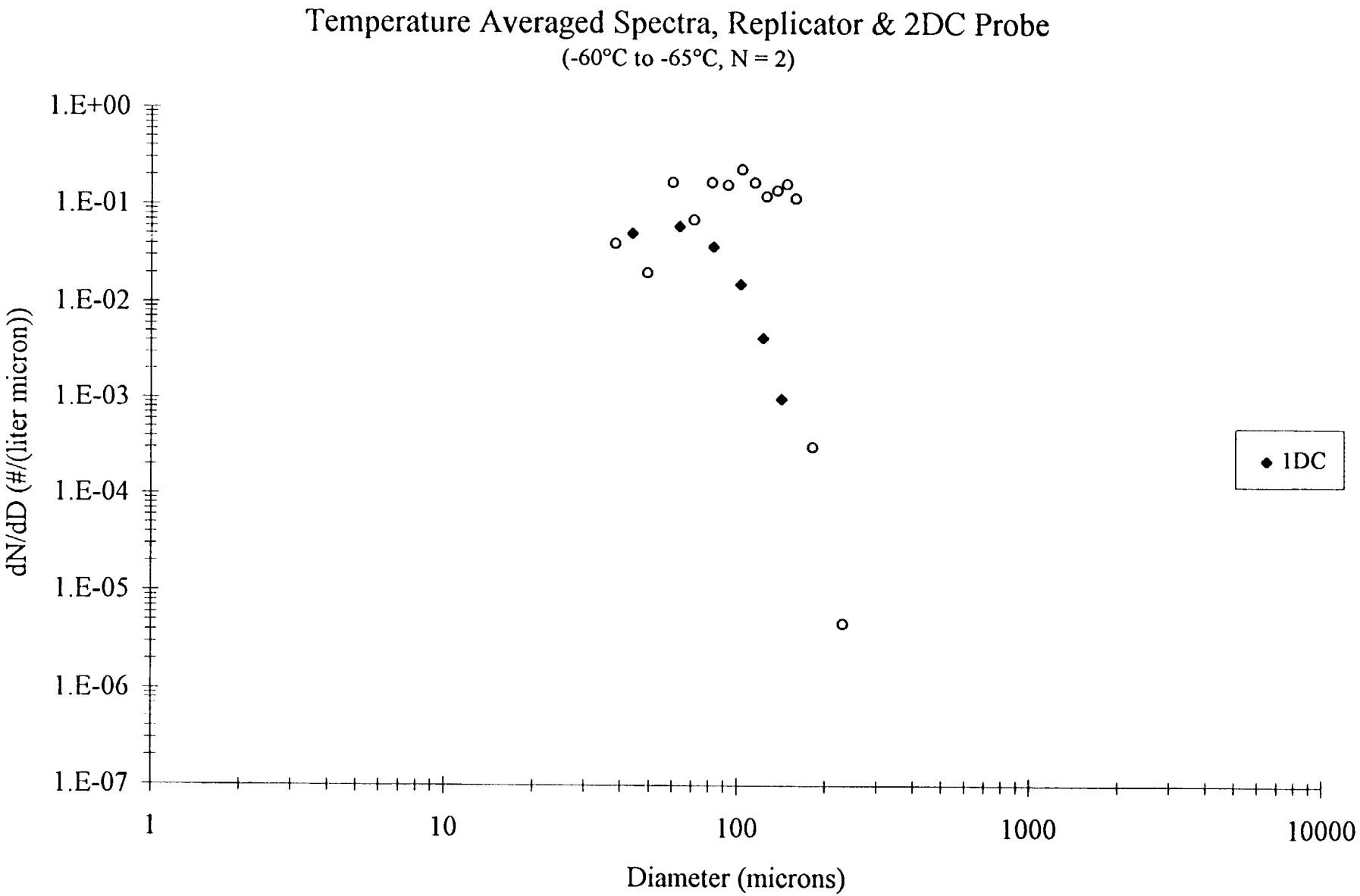
Temperature Averaged Spectra, Replicator & 2DC Probe
(-60°C to -65°C, N = 2)
1.E+00
1.E-01
1.E-02
1.E-03
1.E-04
1.E-05
1.E-06
1.E-07
dN/dD (#/(liter micron))
1
10
100
1000
10000
Diameter (microns)
1DC

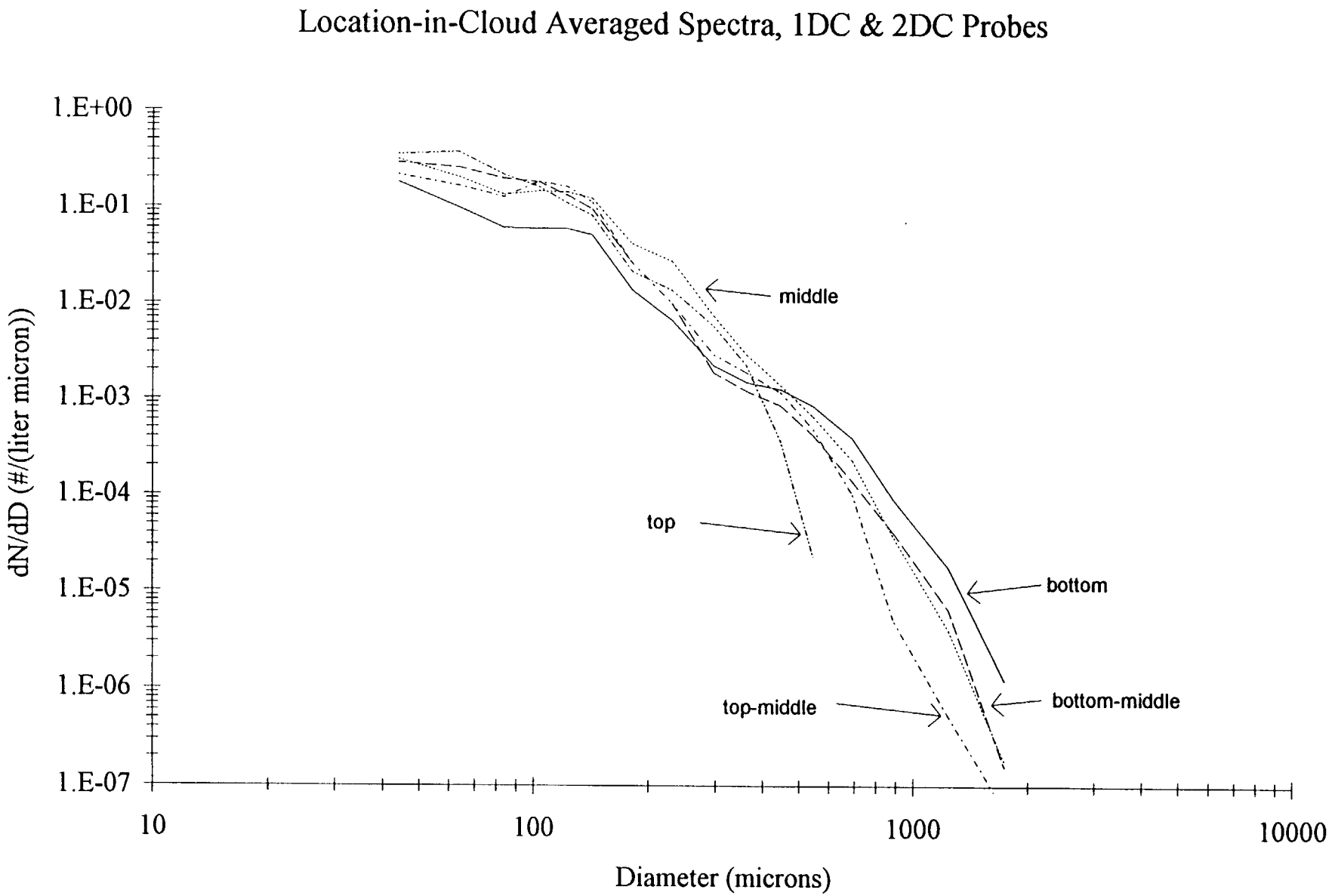
Location-in-Cloud Averaged Spectra, 1DC & 2DC Probes
1.E+00
1.E-01
1.E-02
1.E-03
1.E-04
1.E-05
1.E-06
1.E-07
dN/dD (#/(liter micron))
middle
top
bottom
top-middle
bottom-middle
10
100
1000
10000
Diameter (microns)

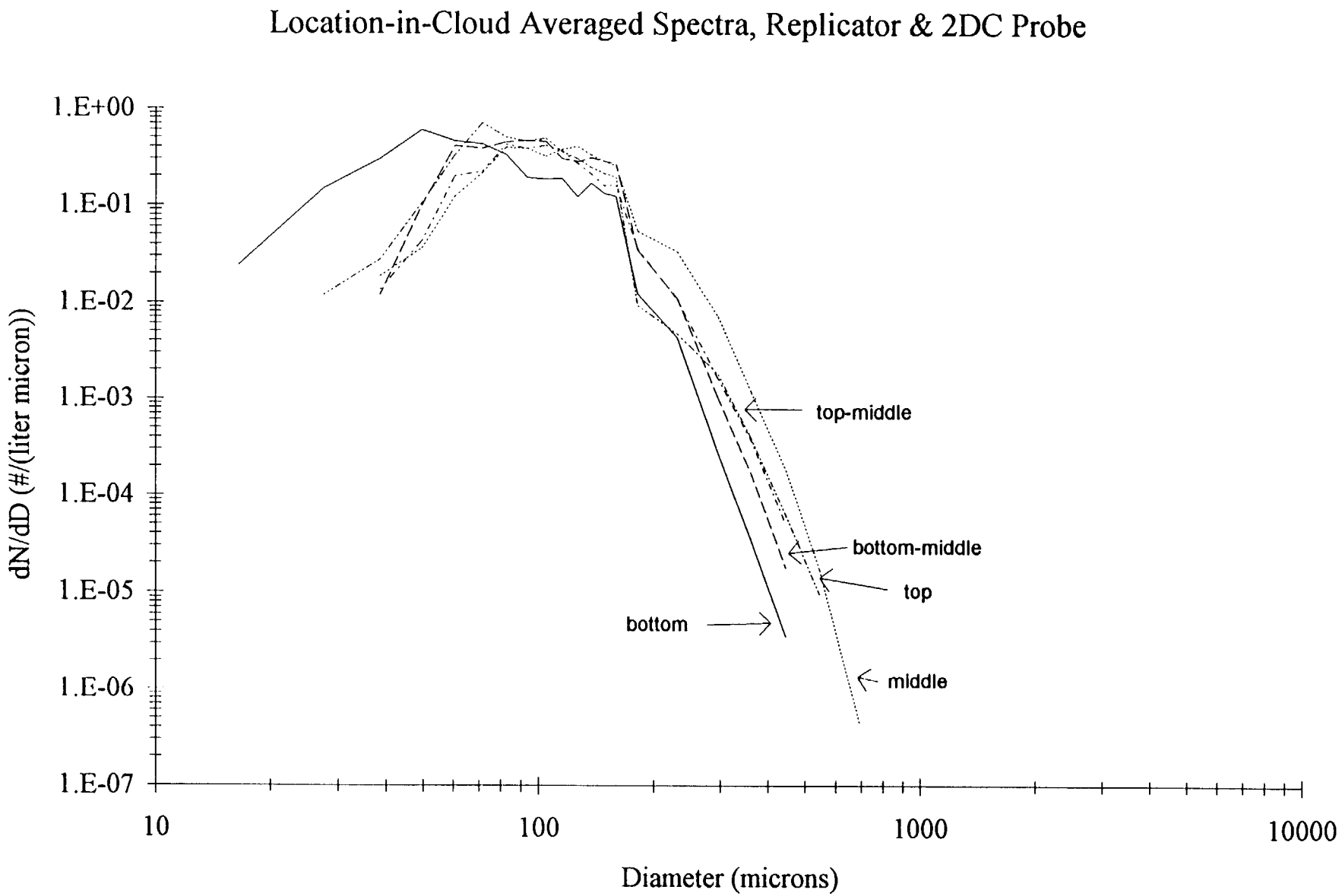
Location-in-Cloud Averaged Spectra, Replicator & 2DC Probe
1.E+00
1.E-01
1.E-02
1.E-03
1.E-04
1.E-05
1.E-06
1.E-07
dN/dD (#/(liter micron))
10
100
1000
10000
Diameter (microns)
top-middle
bottom-middle
top
bottom
middle

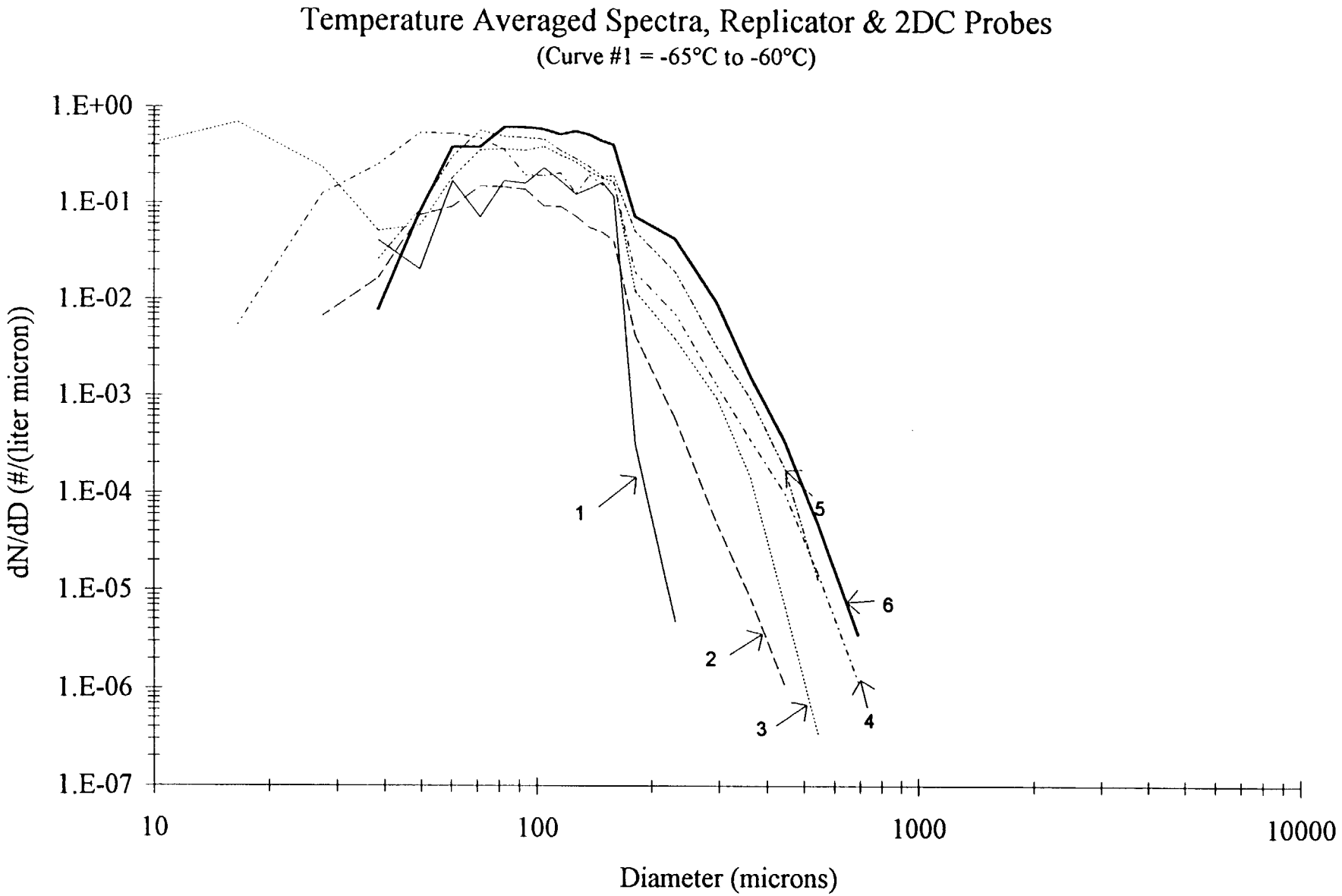
Temperature Averaged Spectra, Replicator & 2DC Probes
(Curve #1 = -65°C to -60°C)
1.E+00
1.E-01
1.E-02
1.E-03
1.E-04
1.E-05
1.E-06
1.E-07
dN/dD (#/(liter micron))
10
100
1000
10000
Diameter (microns)
1
2
3
4
5
6

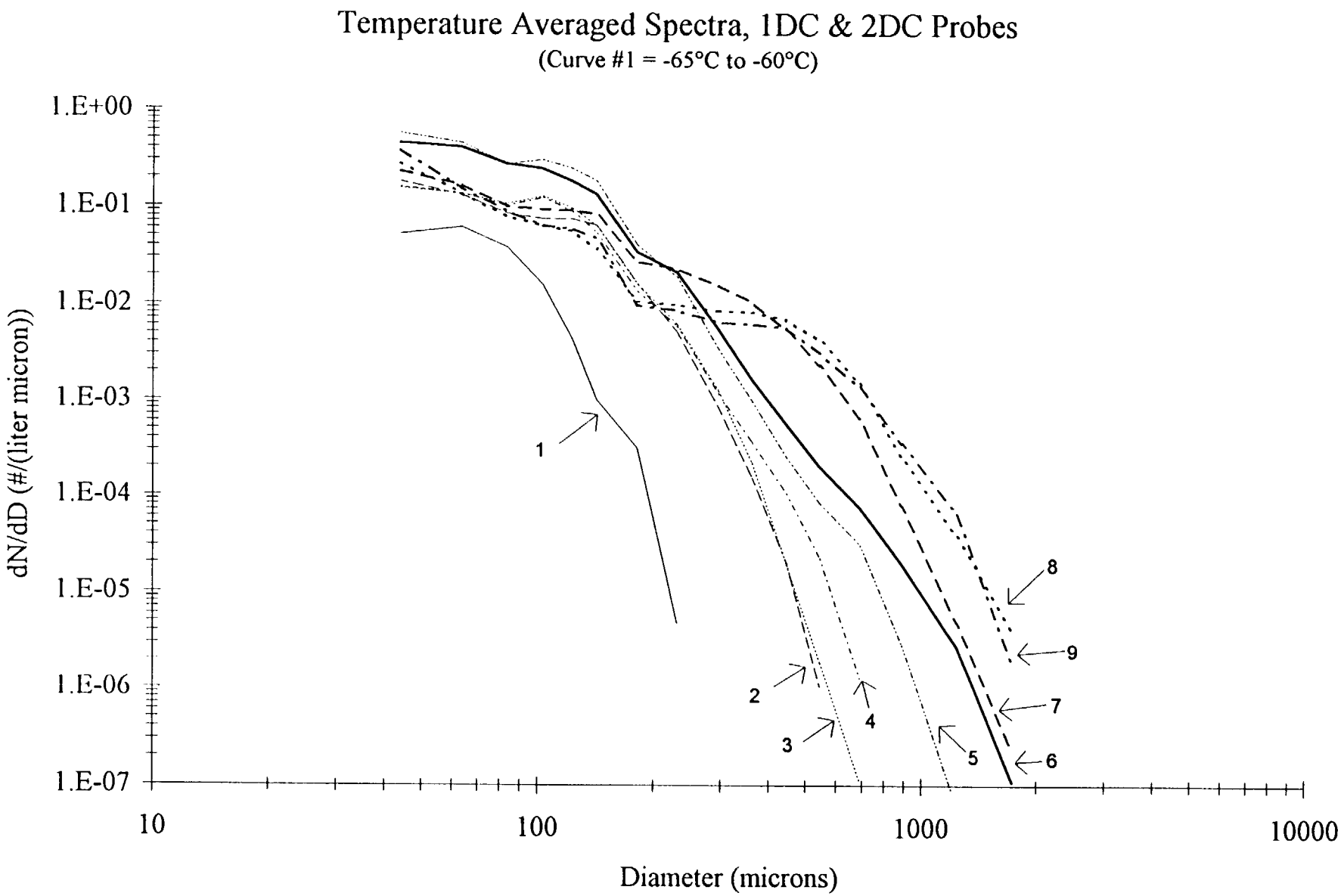
Temperature Averaged Spectra, 1DC & 2DC Probes
(Curve #1 = -65°C to -60°C)
1.E+00
1.E-01
1.E-02
1.E-03
1.E-04
1.E-05
1.E-06
1.E-07
dN/dD (#/(liter micron))
10
100
1000
10000
Diameter (microns)
1
2
3
4
5
6
7
8
9

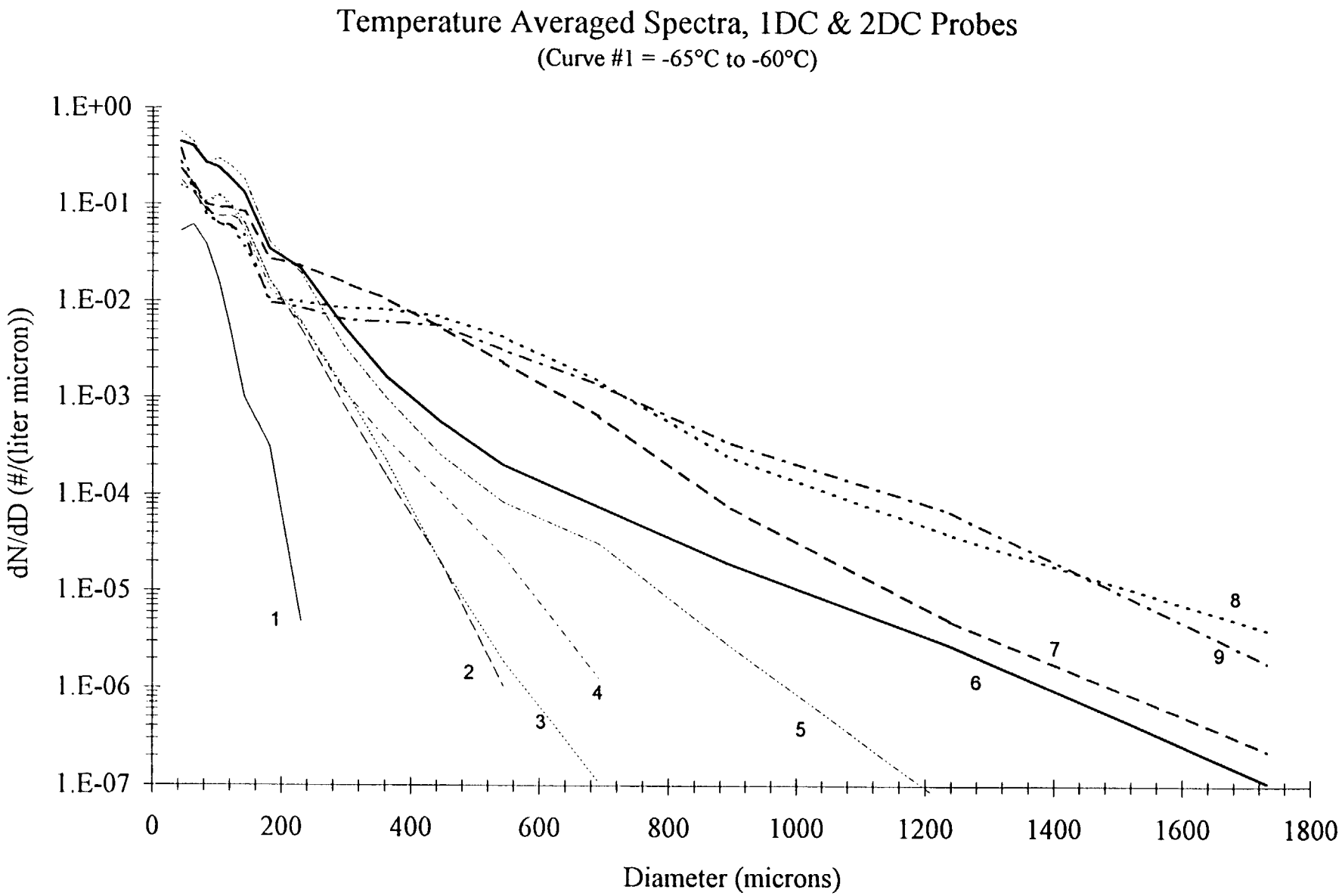
Temperature Averaged Spectra, 1DC & 2DC Probes
(Curve #1 = -65°C to -60°C)
dN/dD (#/(liter micron))
1.E+00
1.E-01
1.E-02
1.E-03
1.E-04
1.E-05
1.E-06
1.E-07
0
200
400
600
800
1000
1200
1400
1600
1800
Diameter (microns)
1
2
3
4
5
6
7
8
9

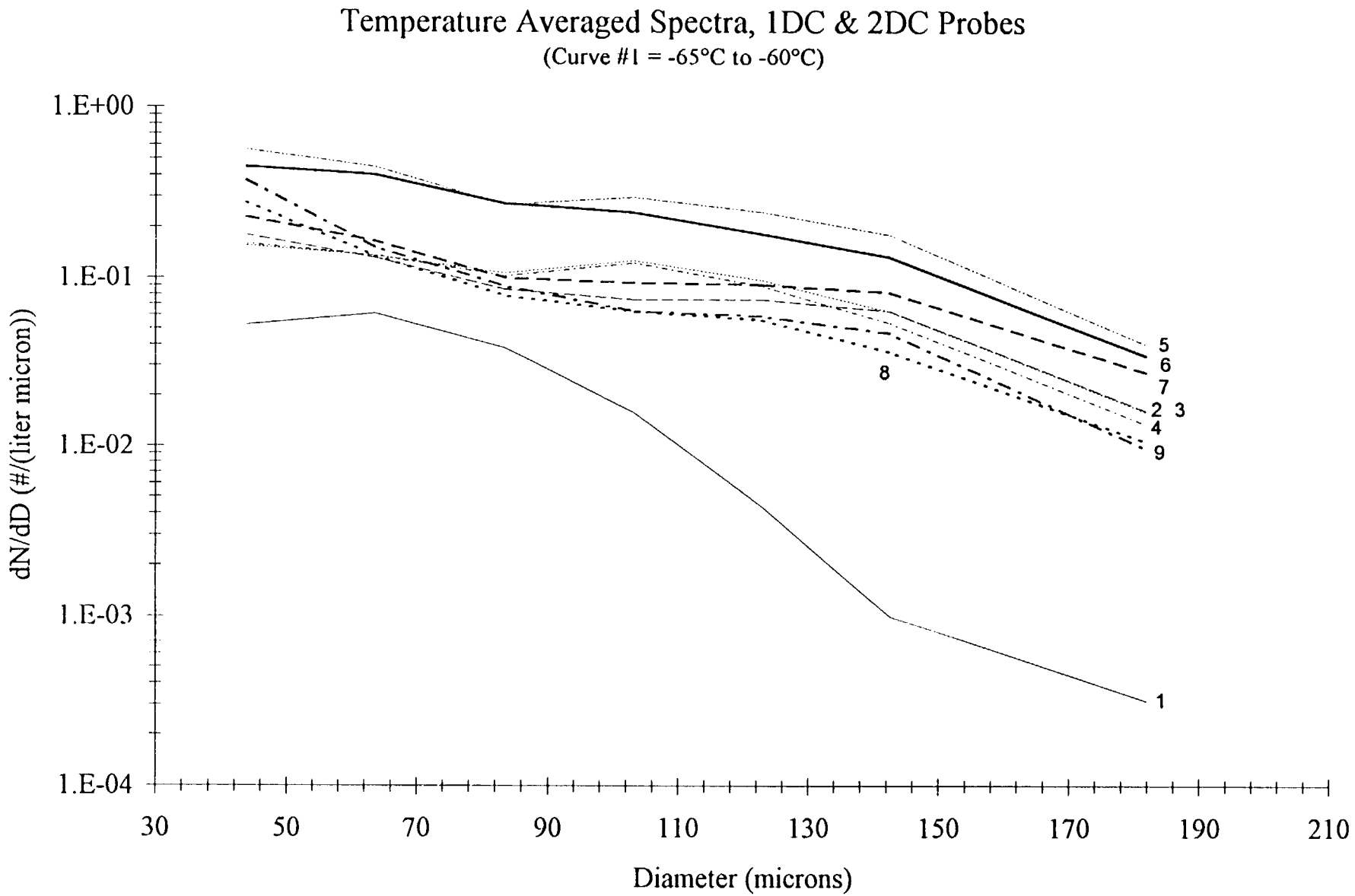
Temperature Averaged Spectra, 1DC & 2DC Probes
(Curve #1 = -65°C to -60°C)
1.E+00
1.E-01
1.E-02
1.E-03
1.E-04
dN/dD (#/(liter micron))
30
50
70
90
110
130
150
170
190
210
Diameter (microns)
5
6
7
2
3
4
8
9
1

Exponential Distribution Fit to Size Spectra

Temp Range	Number of Samples	Max IWC ($g\ m^{-3}$)	Min IWC ($g\ m^{-3}$)	Avg IWC ($g\ m^{-3}$)	N_{100} ($m^{-3}\ \mu m^{-1}$)	N_{100}/IWC ($g^{-1}\ \mu m^{-1}$)	B1	N_{1000} ($m^{-3}\ \mu m^{-1}$)	N_{1000}/IWC ($g^{-1}\ \mu m^{-1}$)	B2
-20 to -25	4	0.039749	0.010797	0.022327	66.1	2960.4845	-1.913	0.125	5.5984956	-6.268
-25 to -30	5	0.033549	0.011848	0.023491	60.5	2575.4916	-1.669	0.108	4.5975717	-6.089
-30 to -35	16	0.083412	0.000288	0.02045	86.3	4220.0855	-1.611	0.0222	1.085584	-7.551
-35 to -40	21	0.086635	0.000507	0.016647	224.4	13479.977	-1.013	0.00676	0.4060813	-5.338
-40 to -45	12	0.050385	0.000588	0.017805	275.1	15450.315	-0.9056	0.00107	0.0600939	-6.483
-45 to -50	12	0.015015	0.00065	0.006093	106.5	17478.15	-0.4887	0.000482	0.079103	-6.106
-50 to -55	21	0.023245	0.000206	0.006313	101	15998.019	-0.612	1.77E-05	0.0028036	-8.351
-55 to -60	8	0.022735	0.000524	0.005164	83.6	16189.327	-0.886	3.63E-05	0.0070296	-7.914
-60 to -65	2	0.001468	0.000186	0.000827	40.3	48738.001	-0.442	7.58E-08	9.167E-05	-8.474

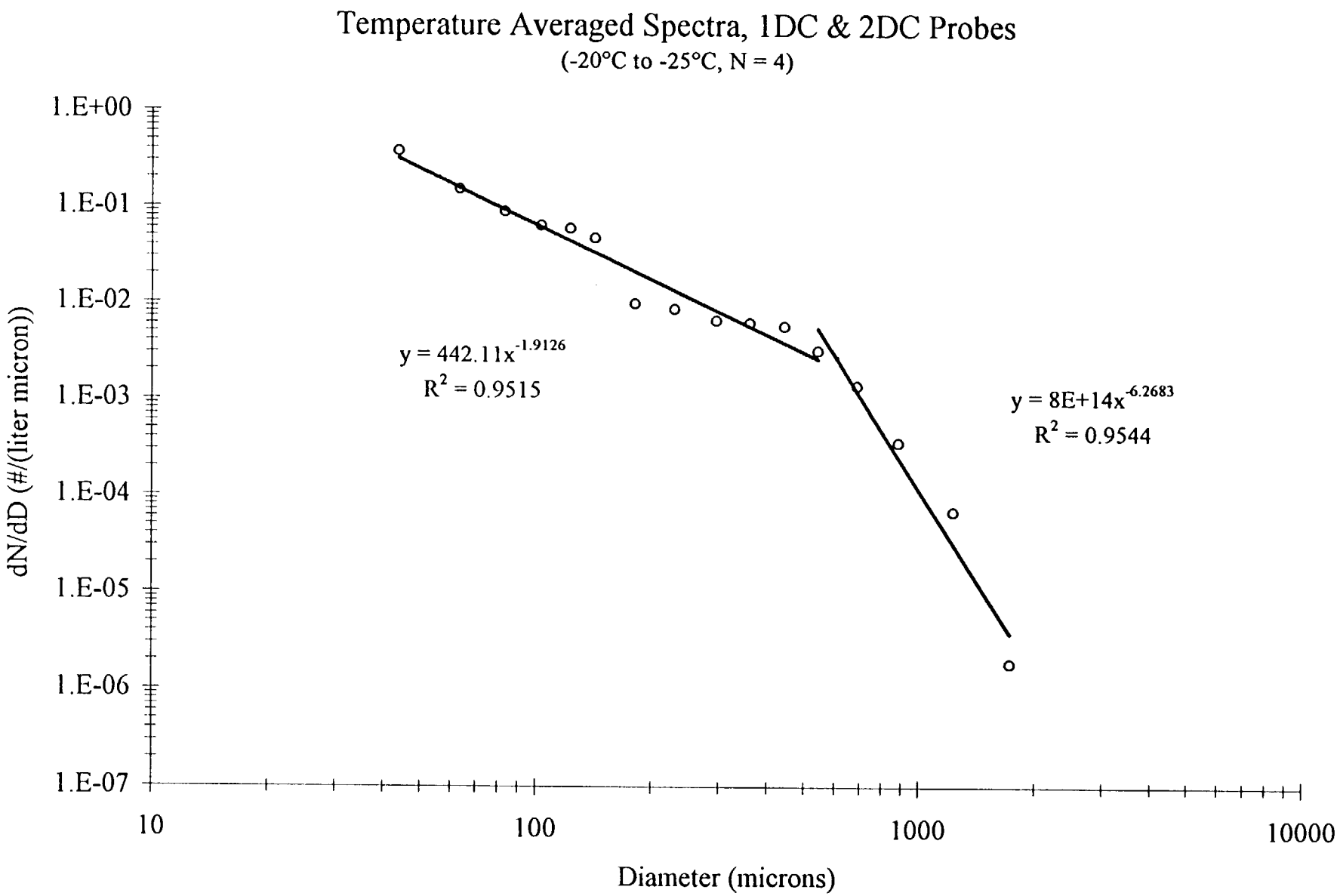
Temperature Averaged Spectra, 1DC & 2DC Probes
(-20°C to -25°C, N = 4)
1.E+00
1.E-01
1.E-02
1.E-03
1.E-04
1.E-05
1.E-06
1.E-07
dN/dD (#/(liter micron))
y = 442.11x^-1.9126
R^2 = 0.9515
y = 8E+14x^-6.2683
R^2 = 0.9544
10
100
1000
10000
Diameter (microns)

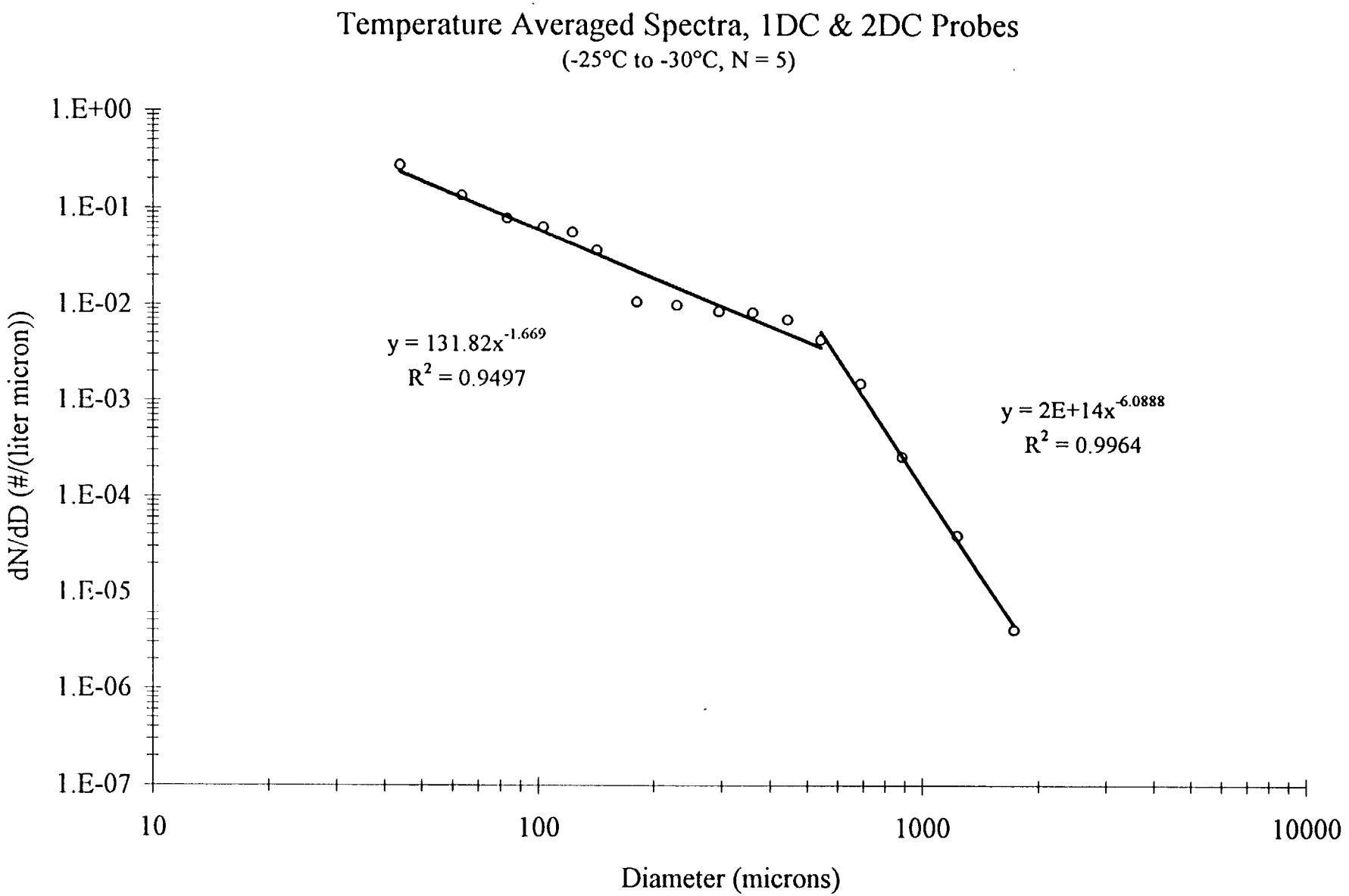
Temperature Averaged Spectra, 1DC & 2DC Probes
(-25°C to -30°C, N = 5)
1.E+00
1.E-01
1.E-02
1.E-03
1.E-04
1.E-05
1.E-06
1.E-07
dN/dD (#/(liter micron))
y = 131.82x^-1.669
R^2 = 0.9497
y = 2E+14x^-6.0888
R^2 = 0.9964
10
100
1000
10000
Diameter (microns)

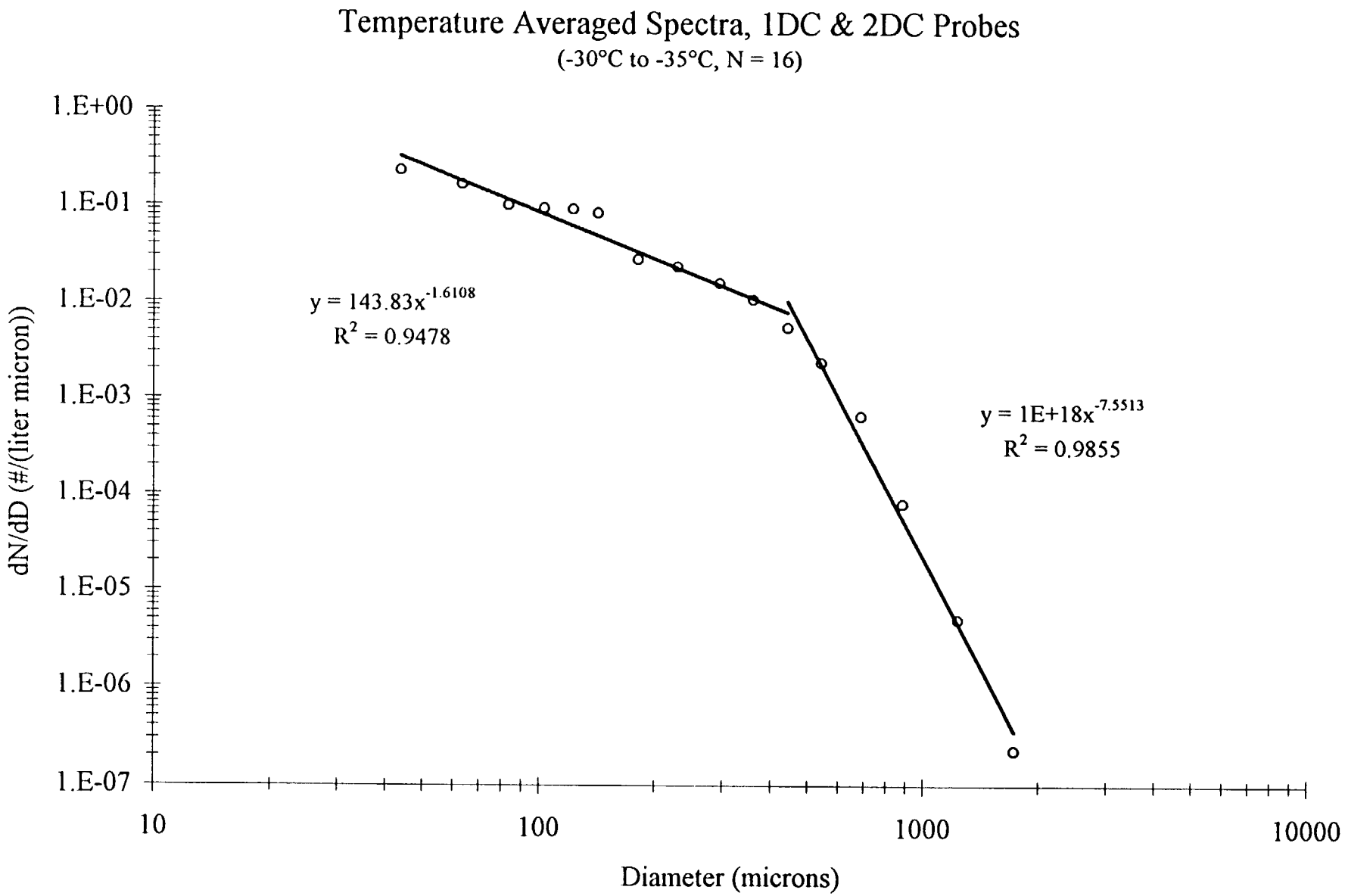
Temperature Averaged Spectra, 1DC & 2DC Probes
(-30°C to -35°C, N = 16)
1.E+00
1.E-01
1.E-02
1.E-03
1.E-04
1.E-05
1.E-06
1.E-07
dN/dD (#/(liter micron))
y = 143.83x^-1.6108
R^2 = 0.9478
y = 1E+18x^-7.5513
R^2 = 0.9855
10
100
1000
10000
Diameter (microns)

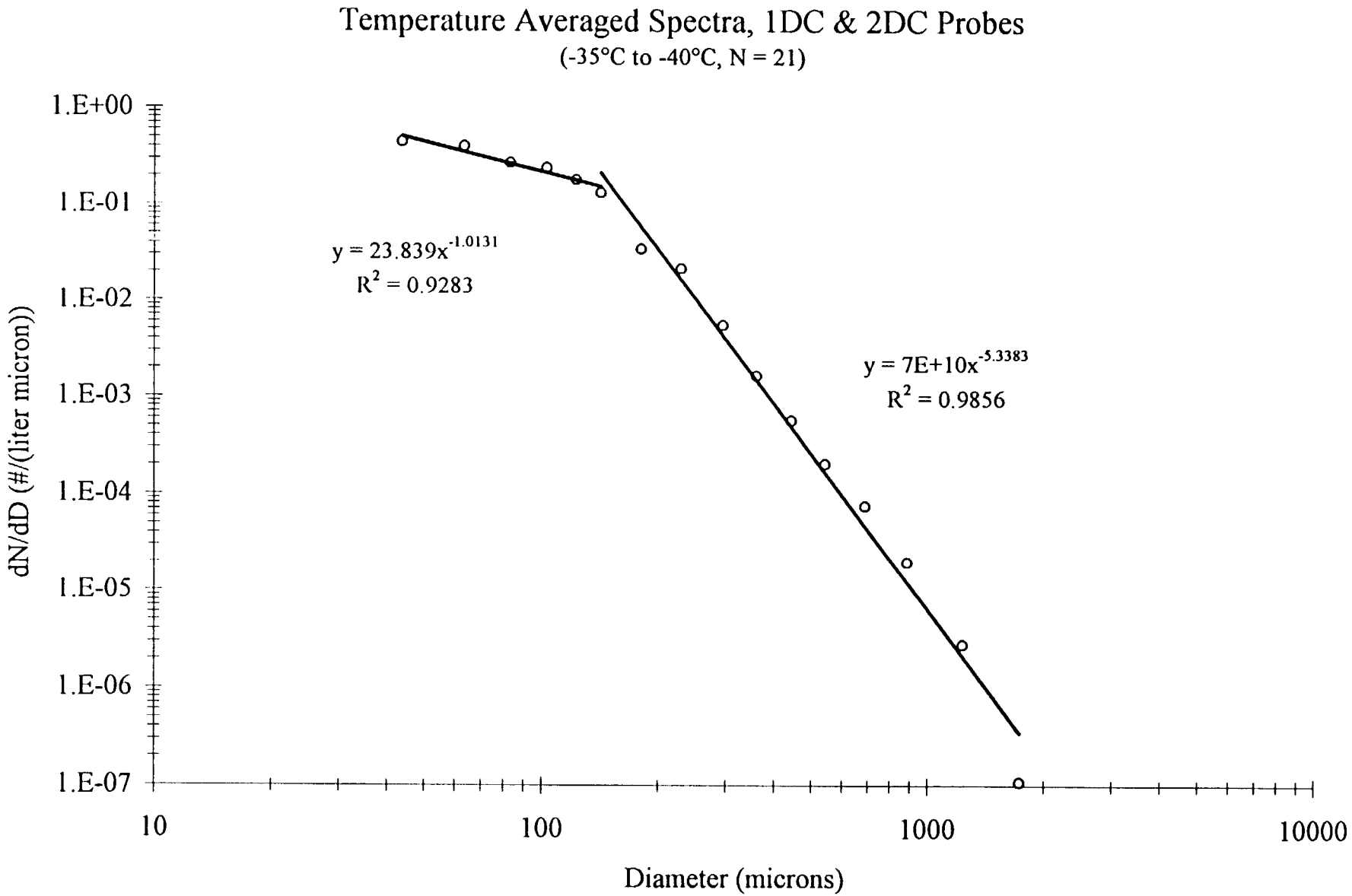
Temperature Averaged Spectra, 1DC & 2DC Probes
(-35°C to -40°C, N = 21)
1.E+00
1.E-01
1.E-02
1.E-03
1.E-04
1.E-05
1.E-06
1.E-07
dN/dD (#/(liter micron))
y = 23.839x^-1.0131
R^2 = 0.9283
y = 7E+10x^-5.3383
R^2 = 0.9856
10
100
1000
10000
Diameter (microns)

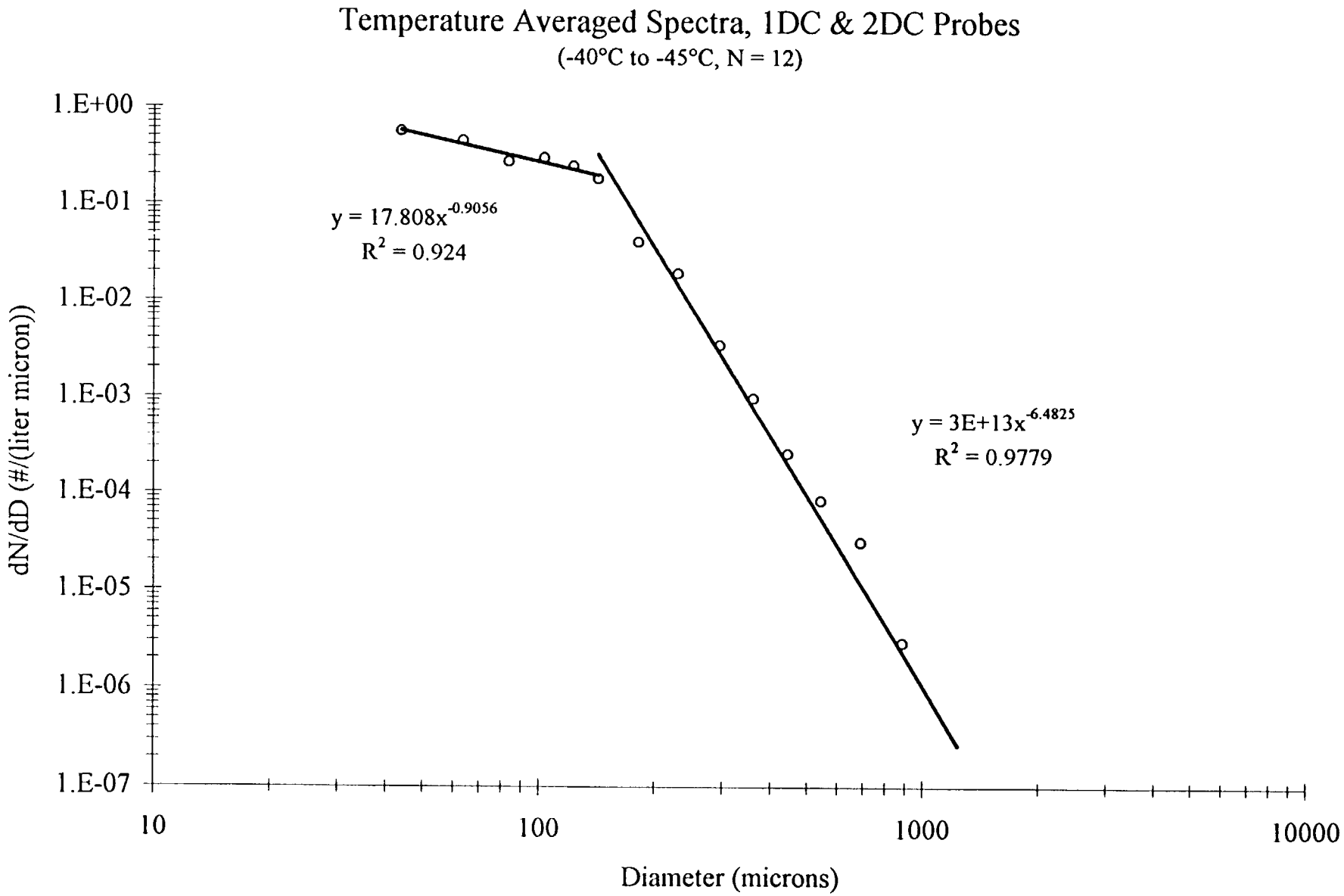
Temperature Averaged Spectra, 1DC & 2DC Probes
(-40°C to -45°C, N = 12)
1.E+00
1.E-01
1.E-02
1.E-03
1.E-04
1.E-05
1.E-06
1.E-07
dN/dD (#/(liter micron))
y = 17.808x^-0.9056
R^2 = 0.924
y = 3E+13x^-6.4825
R^2 = 0.9779
10
100
1000
10000
Diameter (microns)

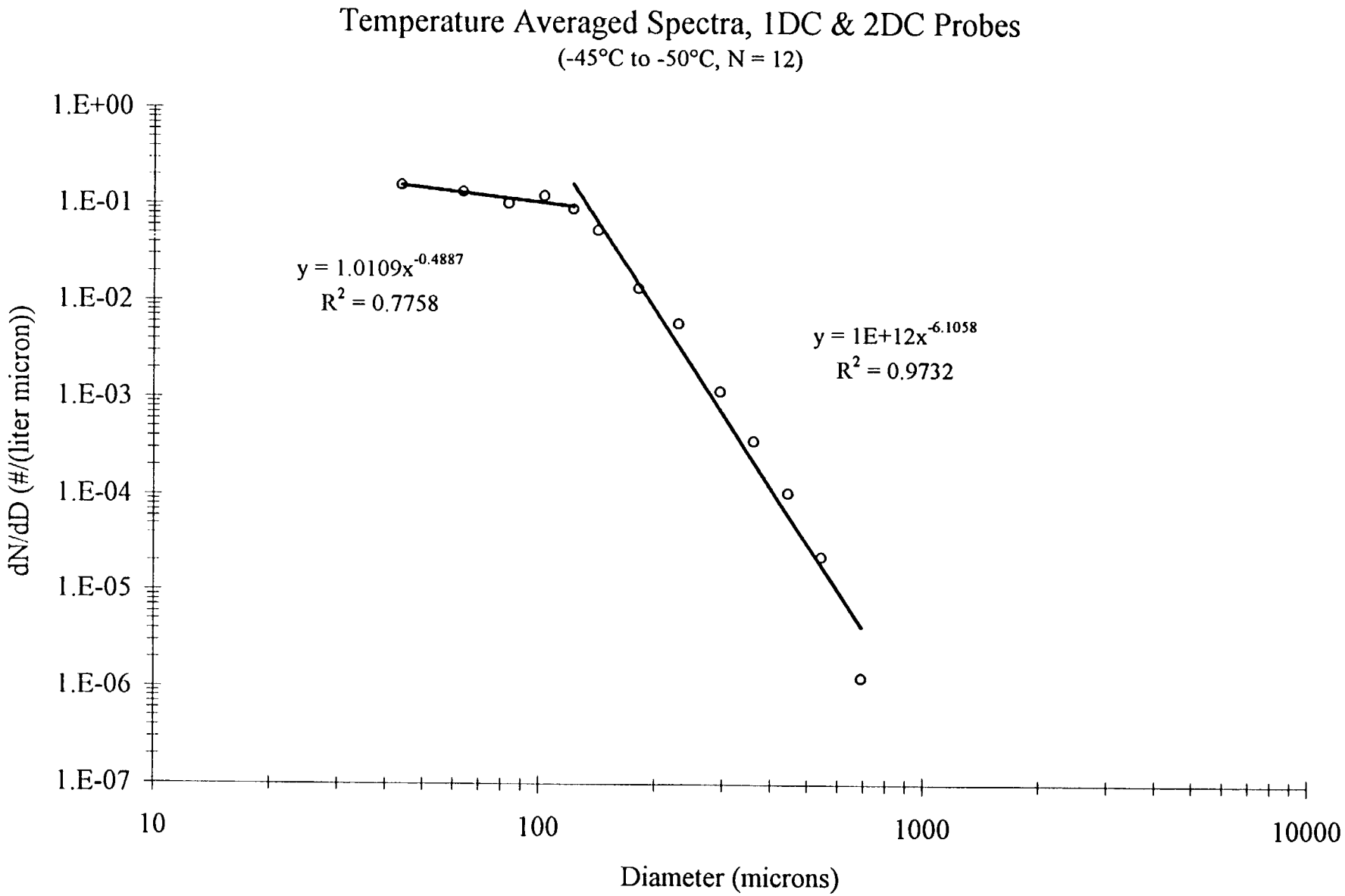
Temperature Averaged Spectra, 1DC & 2DC Probes
(-45°C to -50°C, N = 12)
1.E+00
1.E-01
1.E-02
1.E-03
1.E-04
1.E-05
1.E-06
1.E-07
dN/dD (#/(liter micron))
y = 1.0109x^-0.4887
R^2 = 0.7758
y = 1E+12x^-6.1058
R^2 = 0.9732
10
100
1000
10000
Diameter (microns)

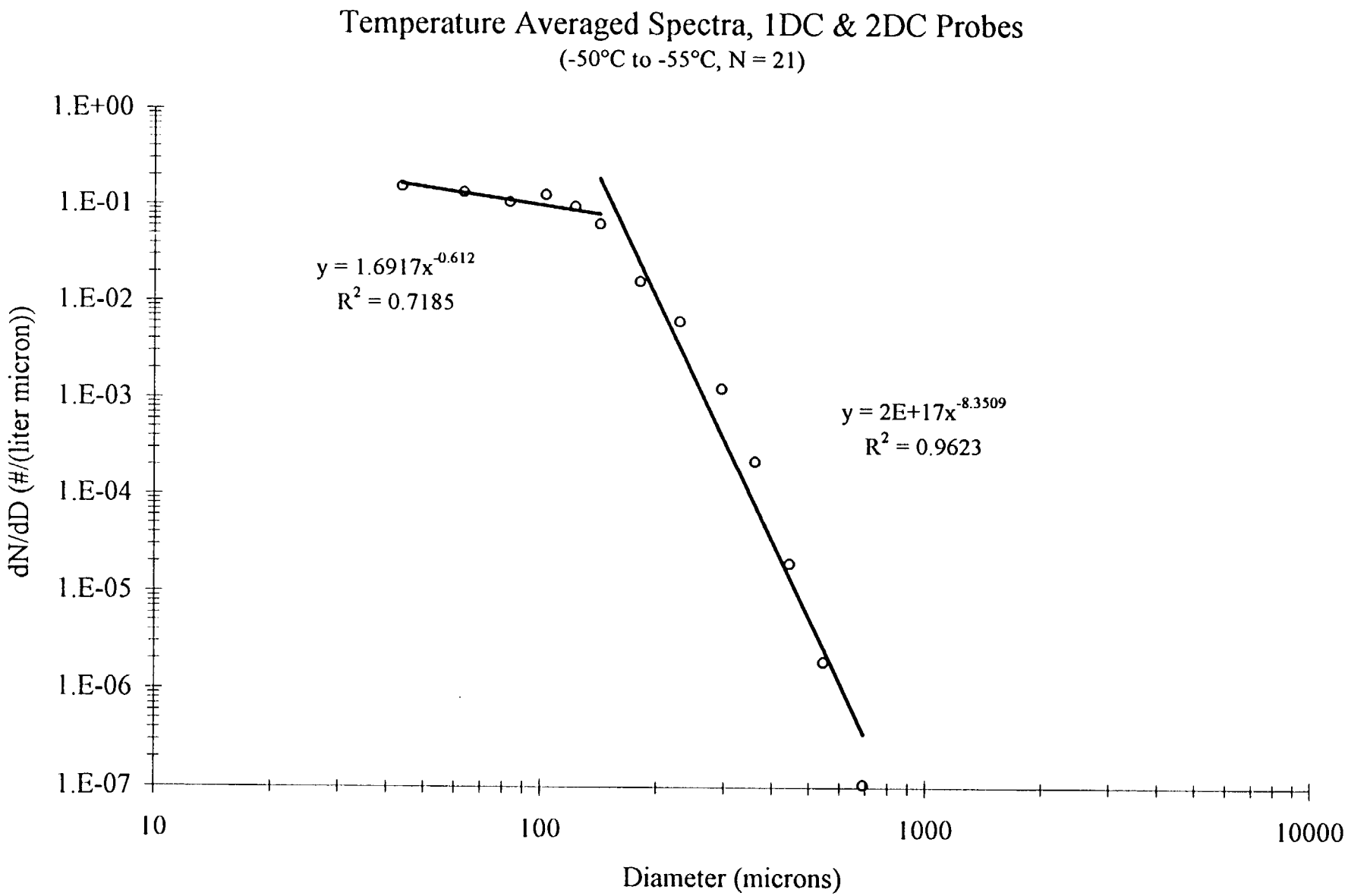
Temperature Averaged Spectra, 1DC & 2DC Probes
(-50°C to -55°C, N = 21)
1.E+00
1.E-01
1.E-02
1.E-03
1.E-04
1.E-05
1.E-06
1.E-07
dN/dD (#/(liter micron))
y = 1.6917x^-0.612
R^2 = 0.7185
y = 2E+17x^-8.3509
R^2 = 0.9623
10
100
1000
10000
Diameter (microns)

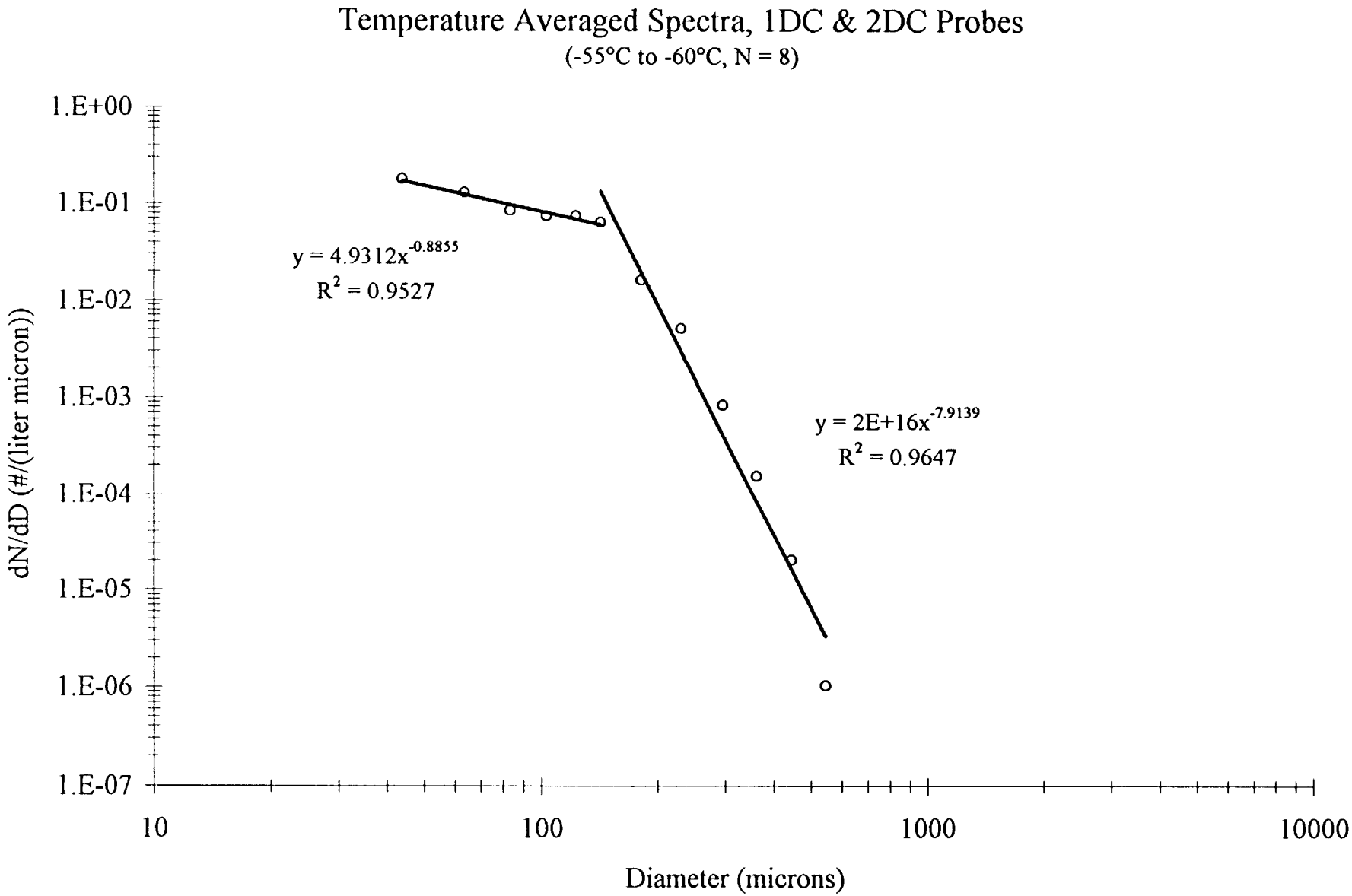
Temperature Averaged Spectra, 1DC & 2DC Probes
(-55°C to -60°C, N = 8)
1.E+00
1.E-01
1.E-02
1.E-03
1.E-04
1.E-05
1.E-06
1.E-07
dN/dD (#/(liter micron))
y = 4.9312x^-0.8855
R^2 = 0.9527
y = 2E+16x^-7.9139
R^2 = 0.9647
10
100
1000
10000
Diameter (microns)

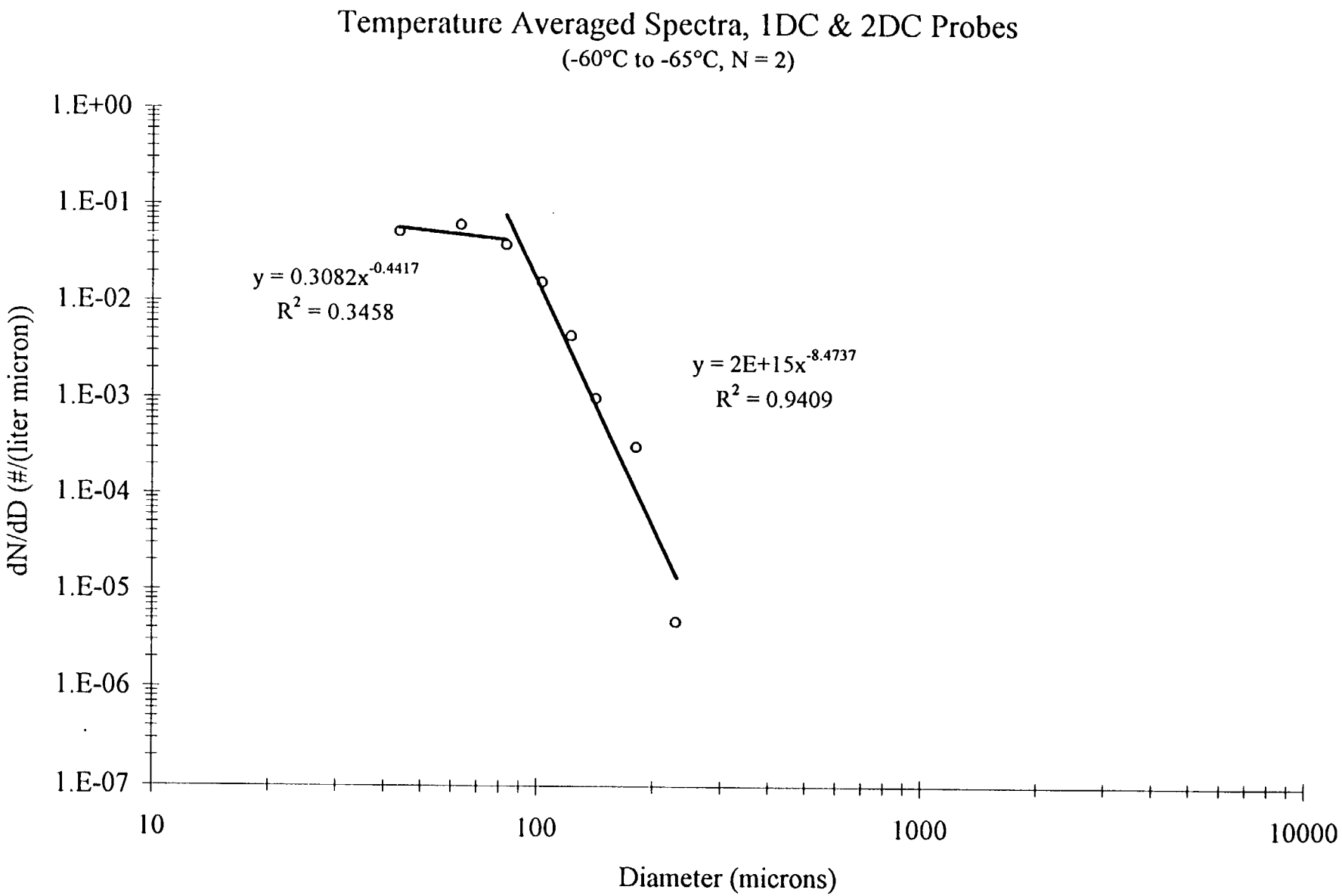
Temperature Averaged Spectra, 1DC & 2DC Probes
(-60°C to -65°C, N = 2)
1.E+00
1.E-01
1.E-02
1.E-03
1.E-04
1.E-05
1.E-06
1.E-07
dN/dD (#/(liter micron))
y = 0.3082x^-0.4417
R^2 = 0.3458
y = 2E+15x^-8.4737
R^2 = 0.9409
10
100
1000
10000
Diameter (microns)

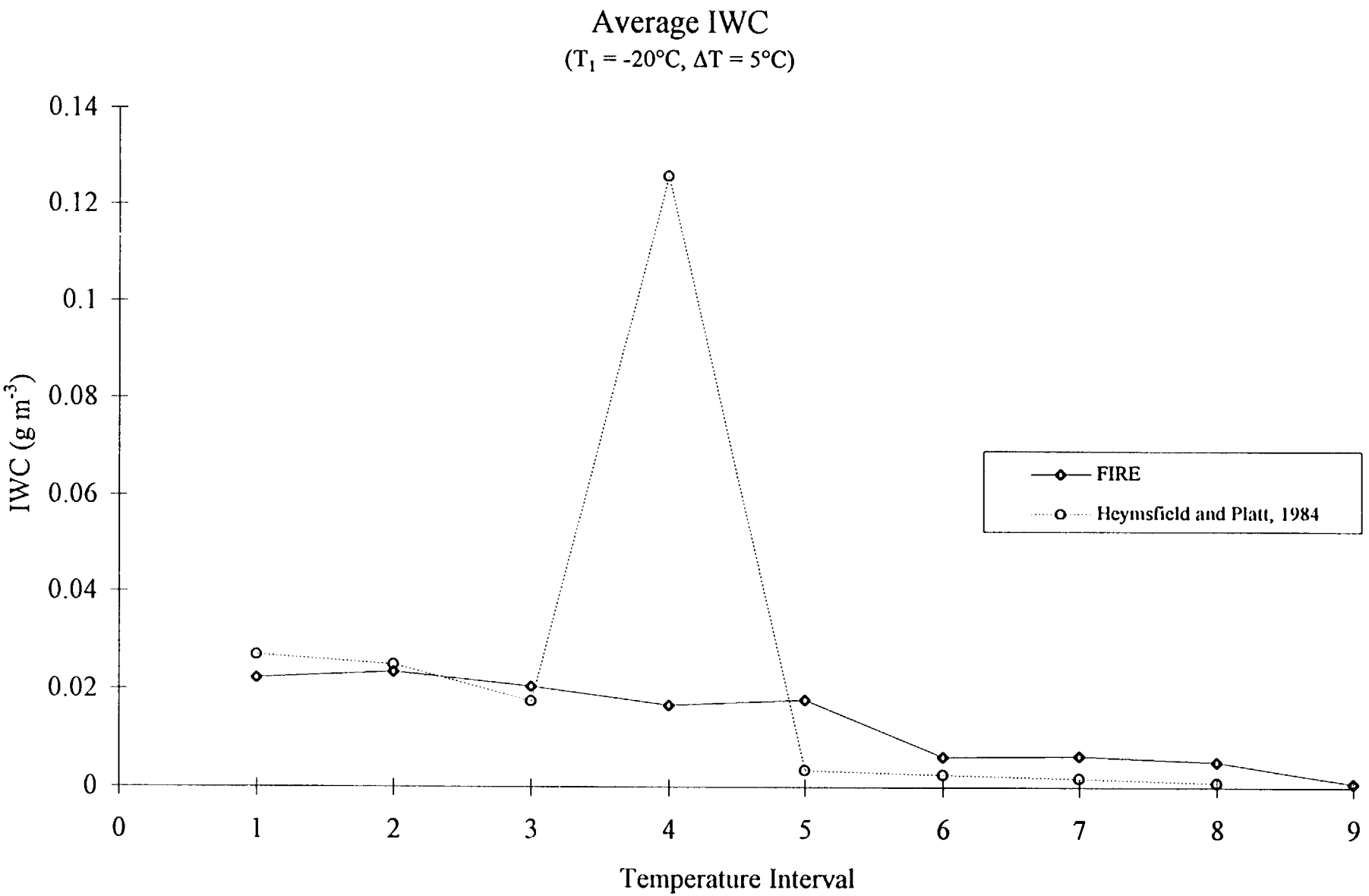
Average IWC
(T_1 = -20°C, ΔT = 5°C)
IWC (g m^{-3})
0.14
0.12
0.1
0.08
0.06
0.04
0.02
0
0
1
2
3
4
5
6
7
8
9
Temperature Interval
FIRE
Heymsfield and Platt, 1984

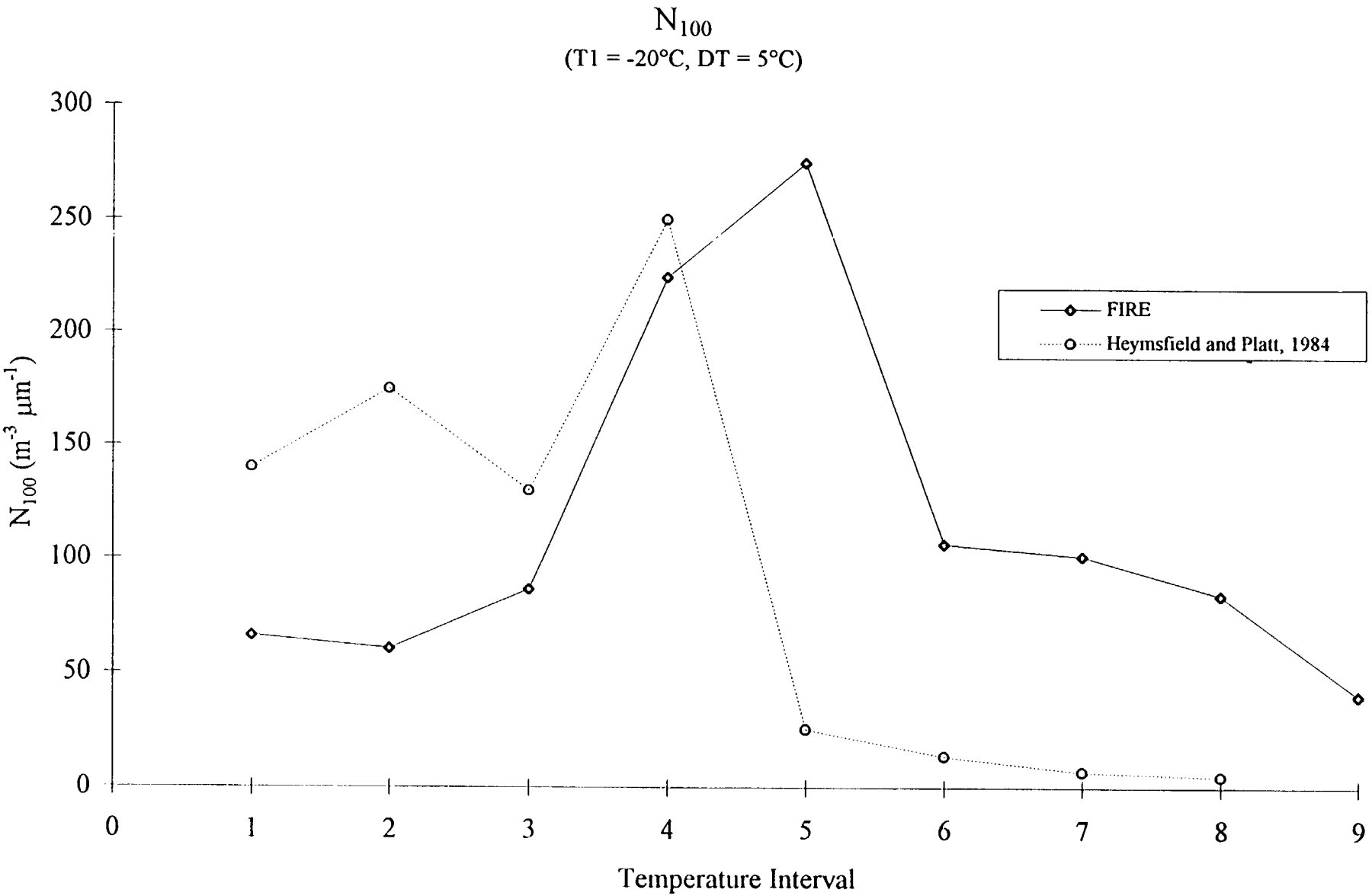
N_{100}
(T1 = -20°C, DT = 5°C)
N_{100} (m^{-3} μm^{-1})
300
250
200
150
100
50
0
0
1
2
3
4
5
6
7
8
9
Temperature Interval
FIRE
Heymsfield and Platt, 1984

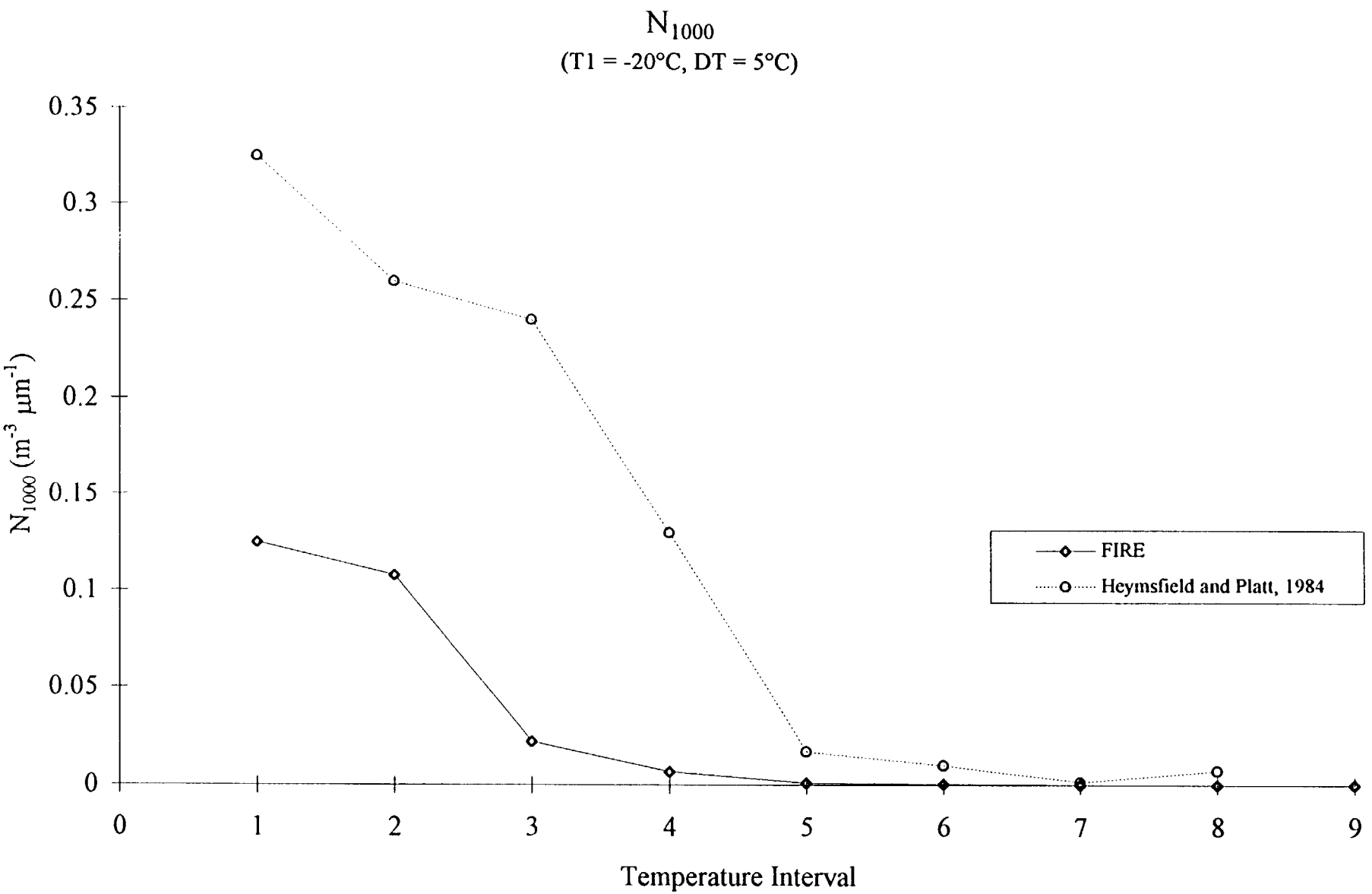
N_{1000}
(T1 = -20°C, DT = 5°C)
0.35
0.3
0.25
0.2
0.15
0.1
0.05
0
N_{1000} (m^{-3} μm^{-1})
0
1
2
3
4
5
6
7
8
9
Temperature Interval
FIRE
Heymsfield and Platt, 1984

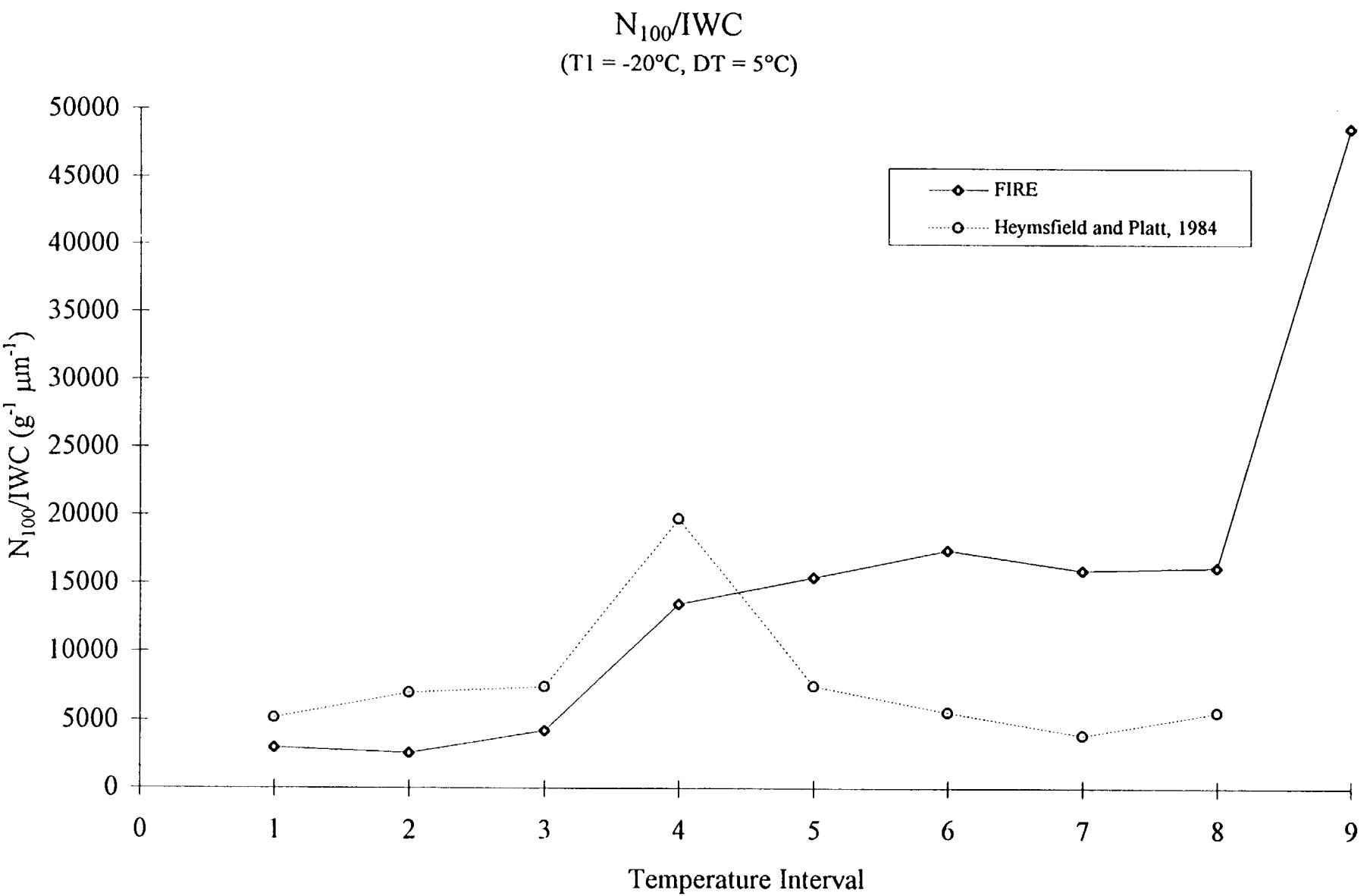
N_{100}/IWC
(T1 = -20°C, DT = 5°C)
N_{100}/IWC (g^{-1} μm^{-1})
50000
45000
40000
35000
30000
25000
20000
15000
10000
5000
0
0
1
2
3
4
5
6
7
8
9
Temperature Interval
FIRE
Heymsfield and Platt, 1984

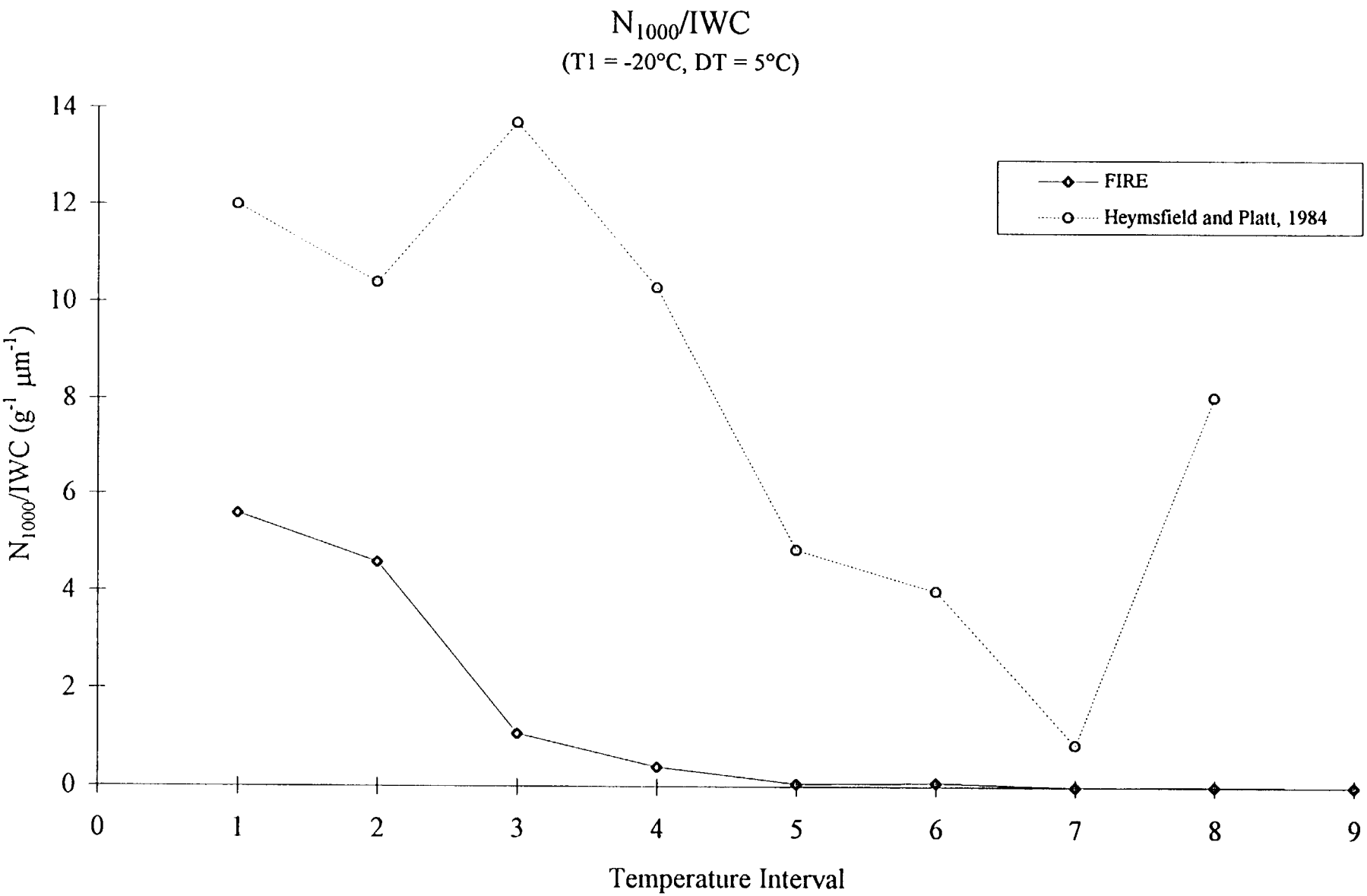
N_{1000}/IWC
(T1 = -20°C, DT = 5°C)
N_{1000}/IWC (g^{-1} μm^{-1})
Temperature Interval
FIRE
Heymsfield and Platt, 1984
0
2
4
6
8
10
12
14
0
1
2
3
4
5
6
7
8
9

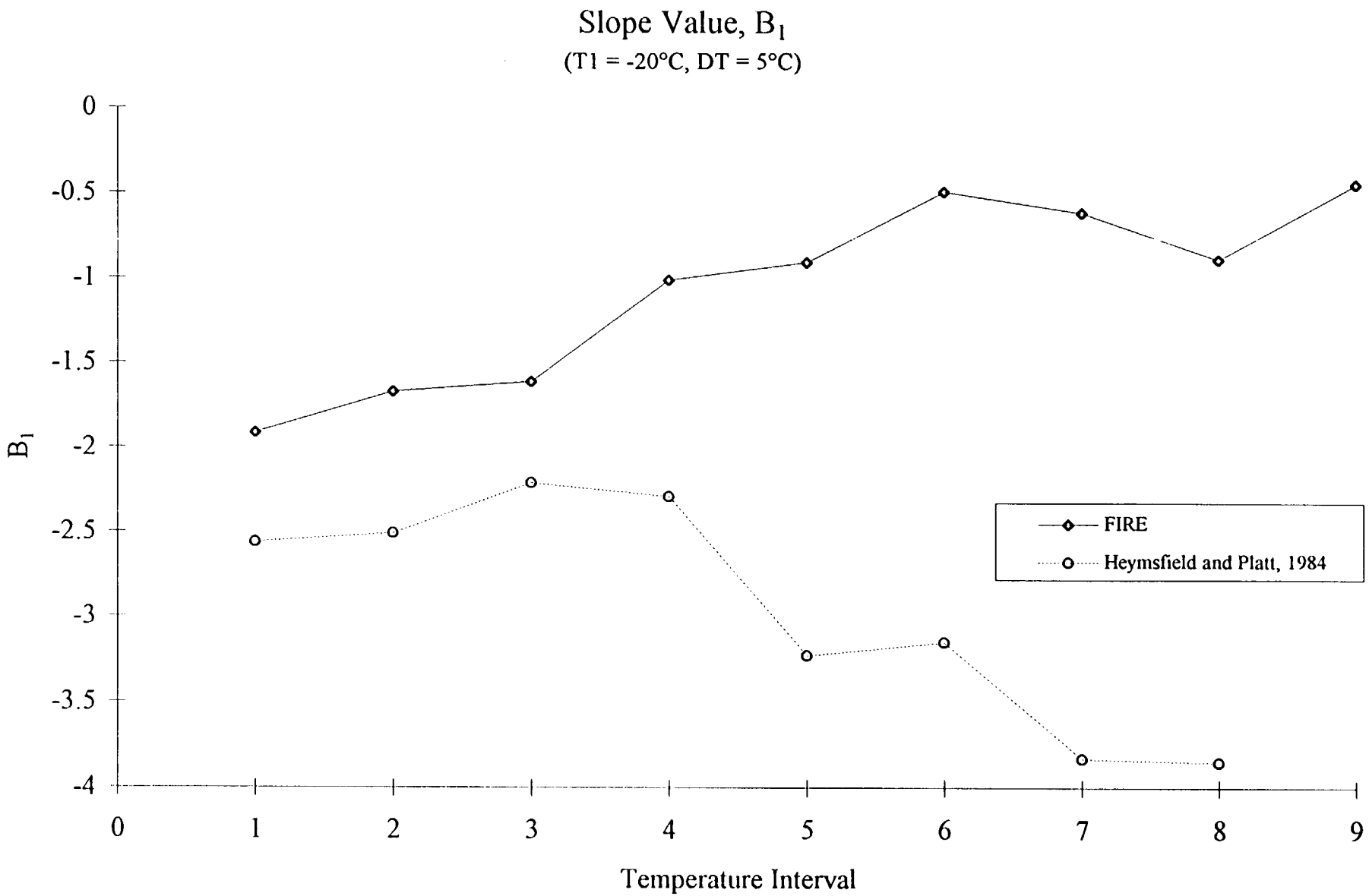
Slope Value, B_1
(T1 = -20°C, DT = 5°C)
B_1
0
-0.5
-1
-1.5
-2
-2.5
-3
-3.5
-4
0
1
2
3
4
5
6
7
8
9
Temperature Interval
FIRE
Heymsfield and Platt, 1984

Slope Value, B_2

(T1 = -20°C, DT = 5°C)

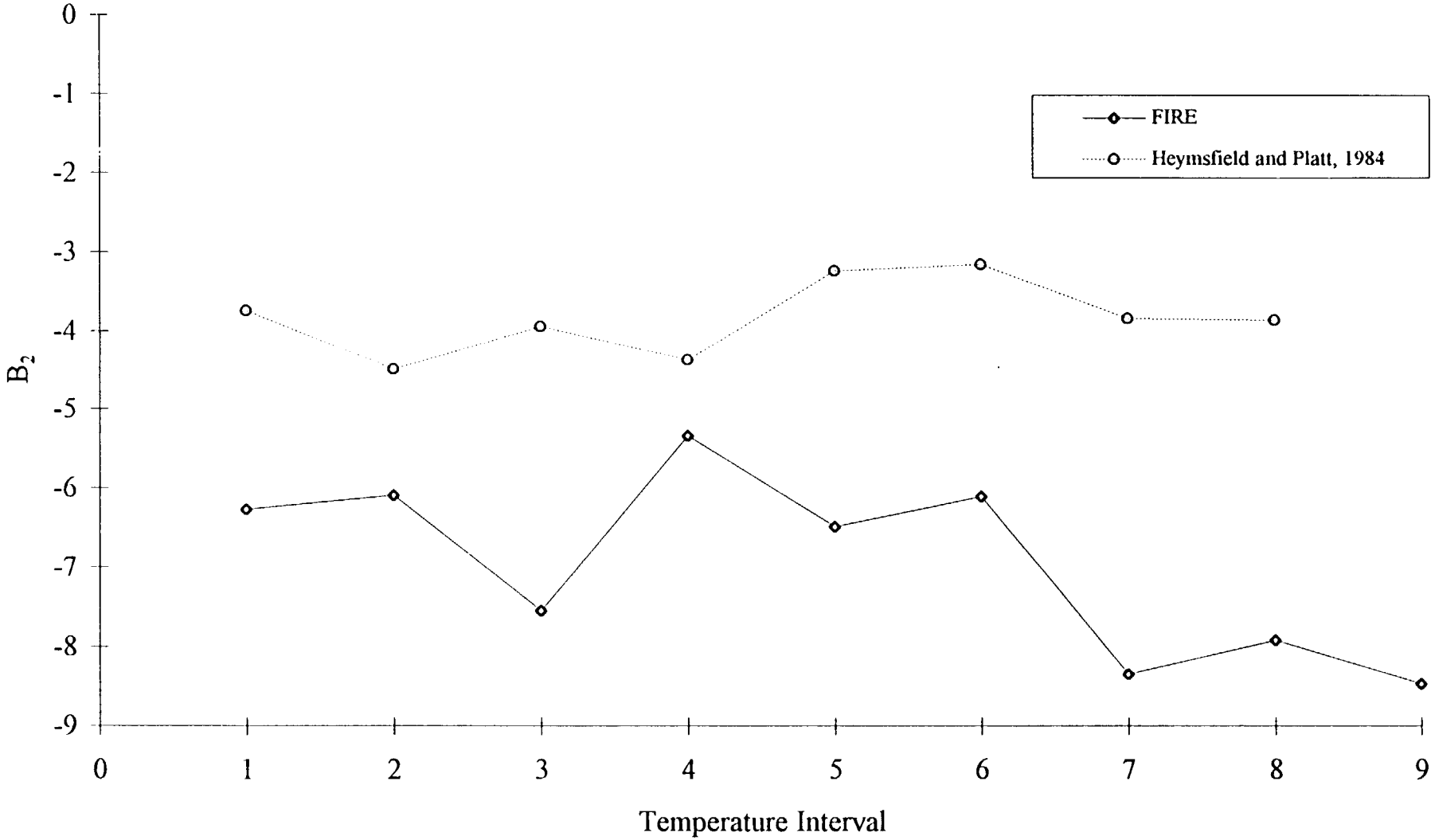

Gamma Distribution Fit to Size Spectra - 1DC and 2DC

by Temperature

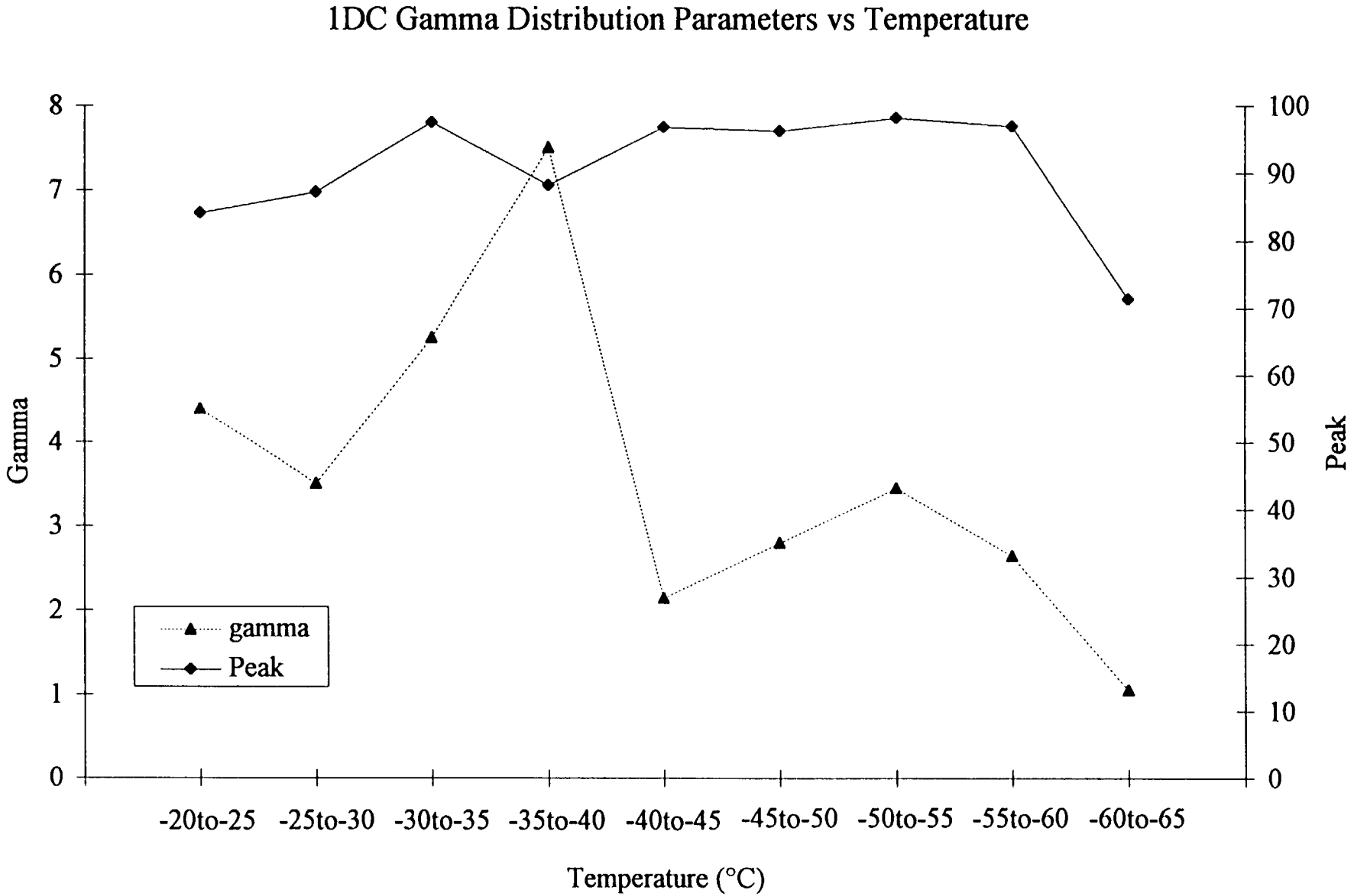
1DC Gamma Distribution Parameters vs Temperature
Gamma
Peak
gamma
Peak
0
1
2
3
4
5
6
7
8
0
10
20
30
40
50
60
70
80
90
100
-20to-25
-25to-30
-30to-35
-35to-40
-40to-45
-45to-50
-50to-55
-55to-60
-60to-65
Temperature (°C)

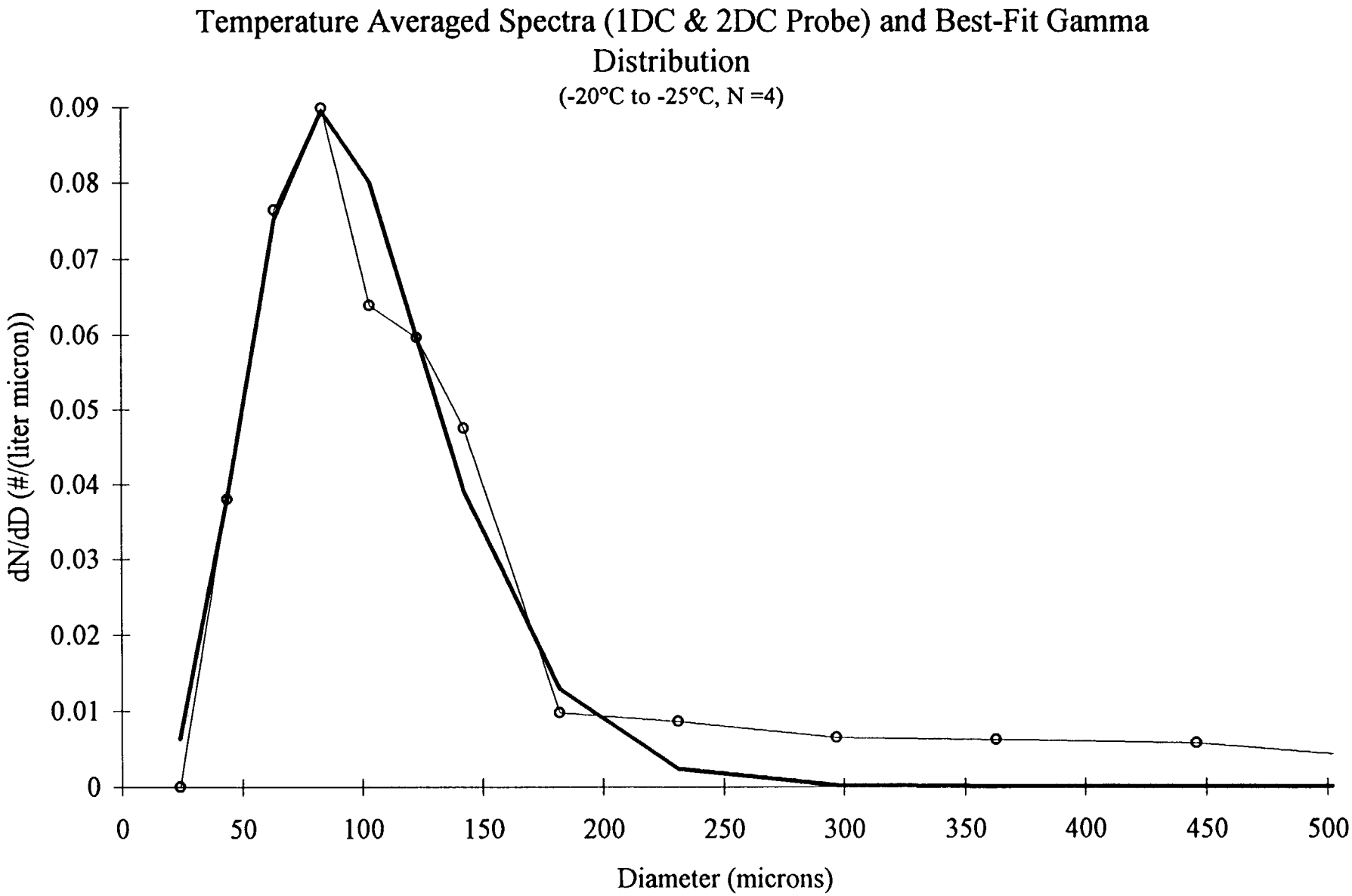
Temperature Averaged Spectra (1DC & 2DC Probe) and Best-Fit Gamma Distribution
(-20°C to -25°C, N =4)
dN/dD (#/(liter micron))
0.09
0.08
0.07
0.06
0.05
0.04
0.03
0.02
0.01
0
0
50
100
150
200
250
300
350
400
450
500
Diameter (microns)

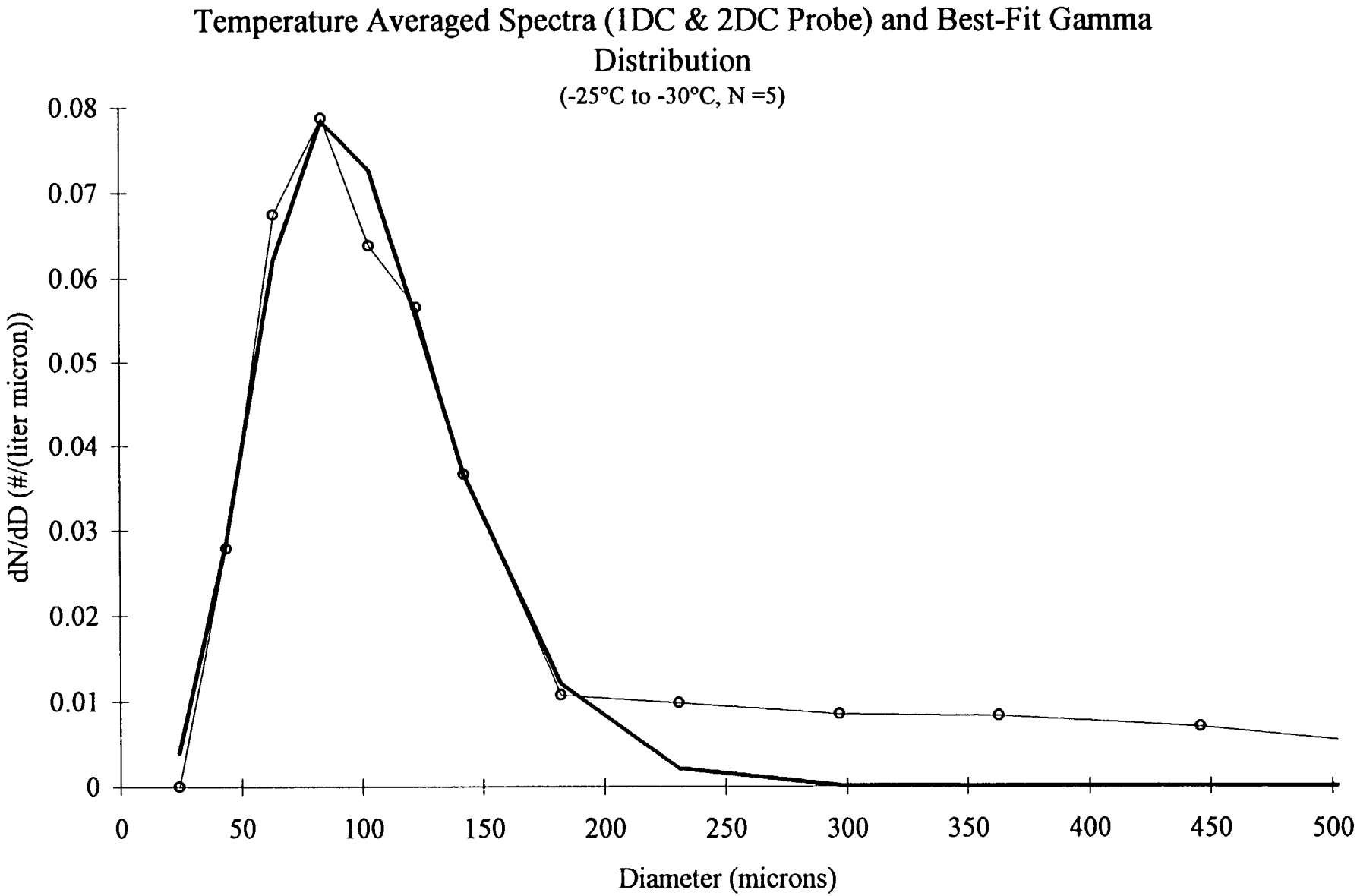
Temperature Averaged Spectra (1DC & 2DC Probe) and Best-Fit Gamma Distribution
(-25°C to -30°C, N =5)
dN/dD (#/(liter micron))
0.08
0.07
0.06
0.05
0.04
0.03
0.02
0.01
0
0
50
100
150
200
250
300
350
400
450
500
Diameter (microns)

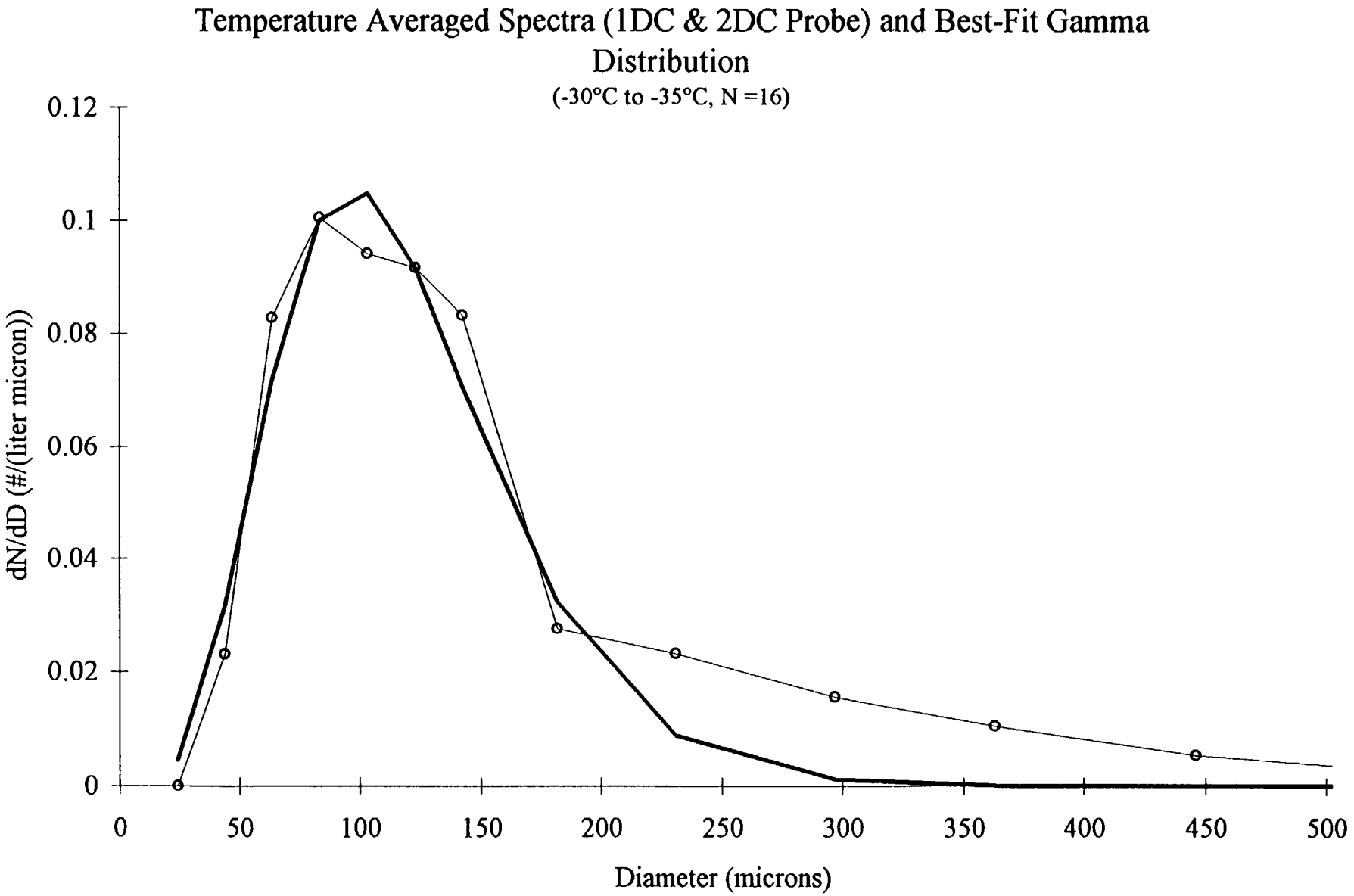
Temperature Averaged Spectra (1DC & 2DC Probe) and Best-Fit Gamma Distribution
(-30°C to -35°C, N =16)
dN/dD (#/(liter micron))
0.12
0.1
0.08
0.06
0.04
0.02
0
0
50
100
150
200
250
300
350
400
450
500
Diameter (microns)

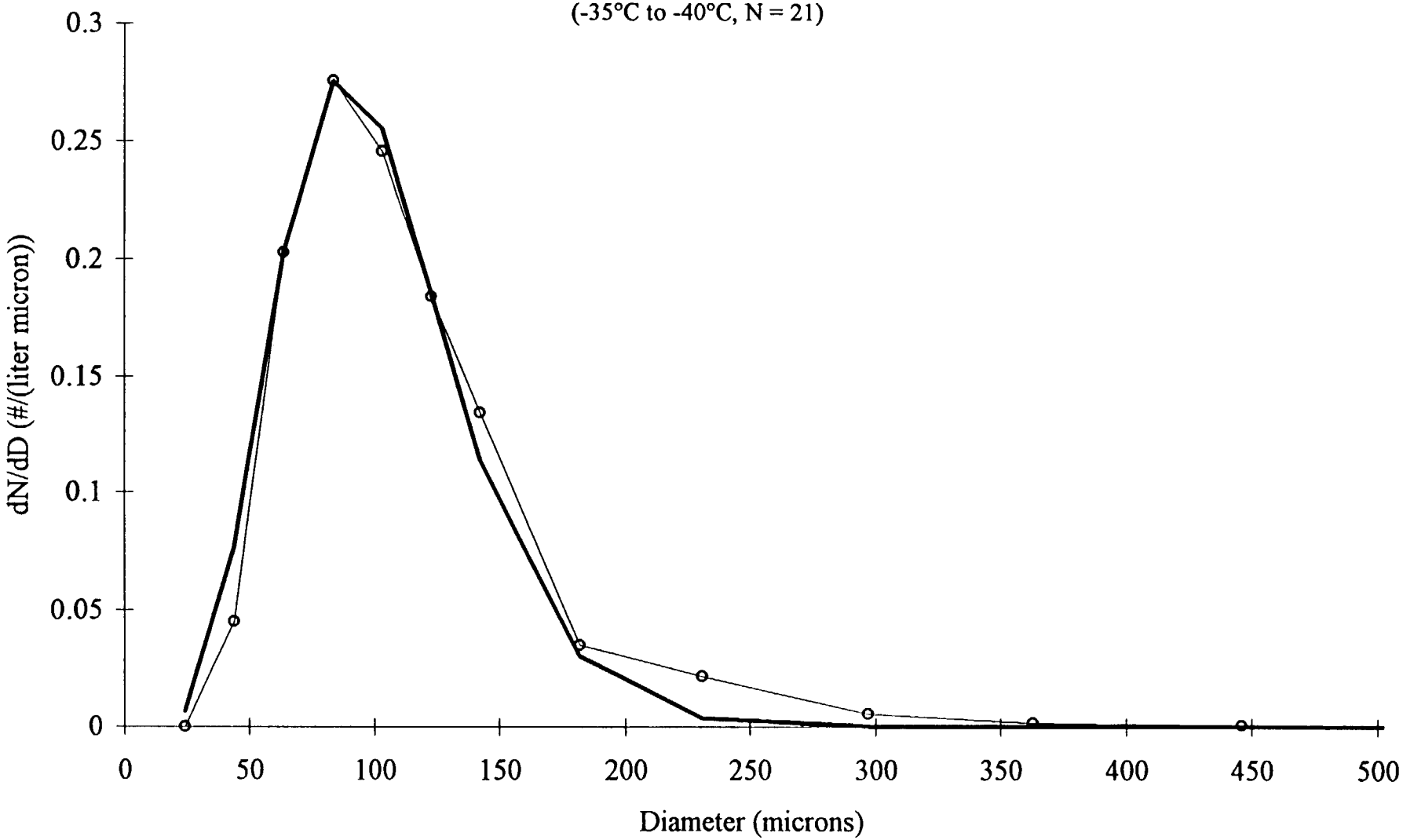
Temperature Averaged Spectra (1DC & 2DC Probe) and Best-Fit Gamma Distribution
(-35°C to -40°C, N = 21)
dN/dD (#/(liter micron))
0.3
0.25
0.2
0.15
0.1
0.05
0
0
50
100
150
200
250
300
350
400
450
500
Diameter (microns)

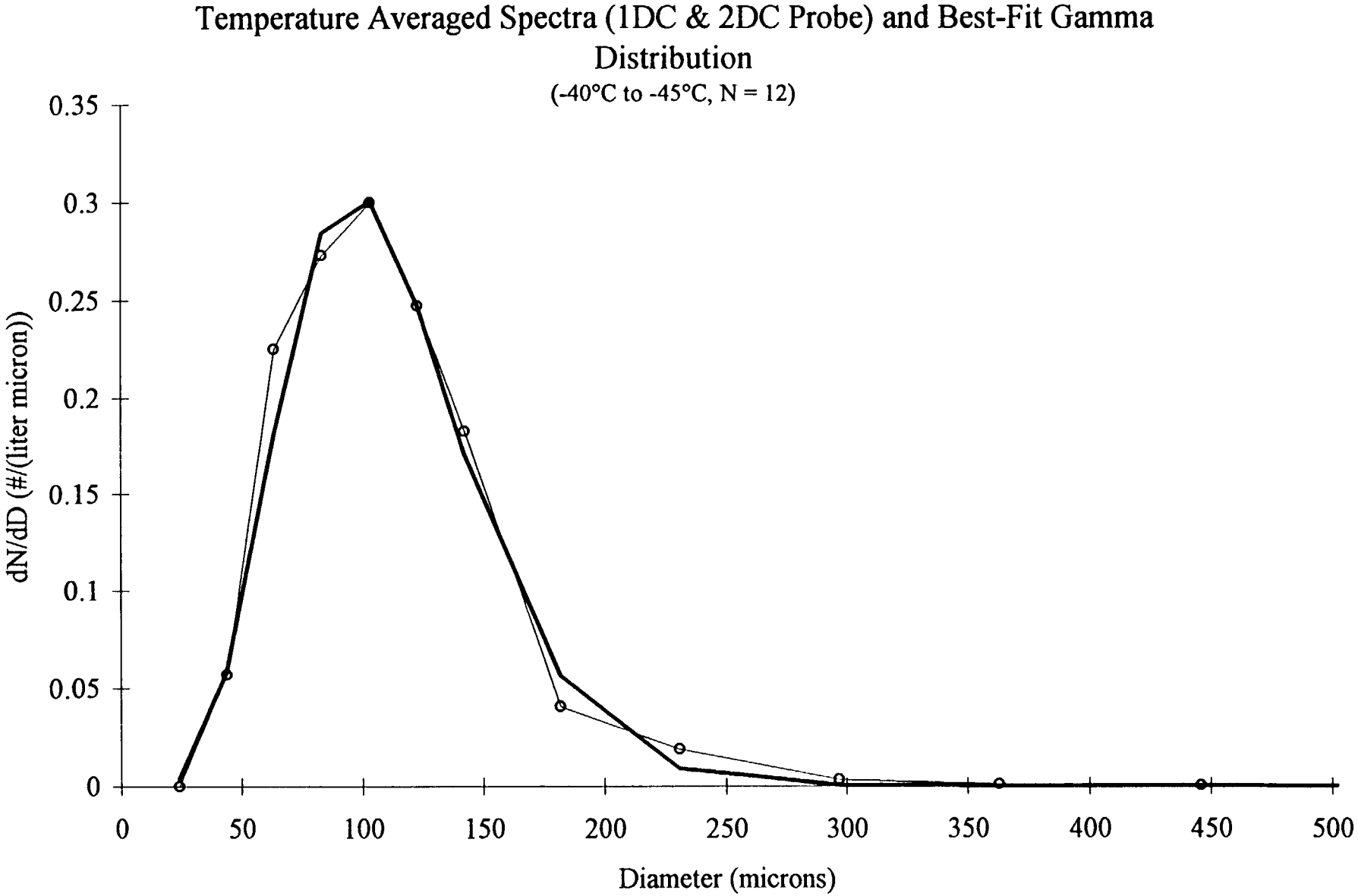
Temperature Averaged Spectra (1DC & 2DC Probe) and Best-Fit Gamma Distribution
(-40°C to -45°C, N = 12)
dN/dD (#/(liter micron))
0.35
0.3
0.25
0.2
0.15
0.1
0.05
0
0
50
100
150
200
250
300
350
400
450
500
Diameter (microns)

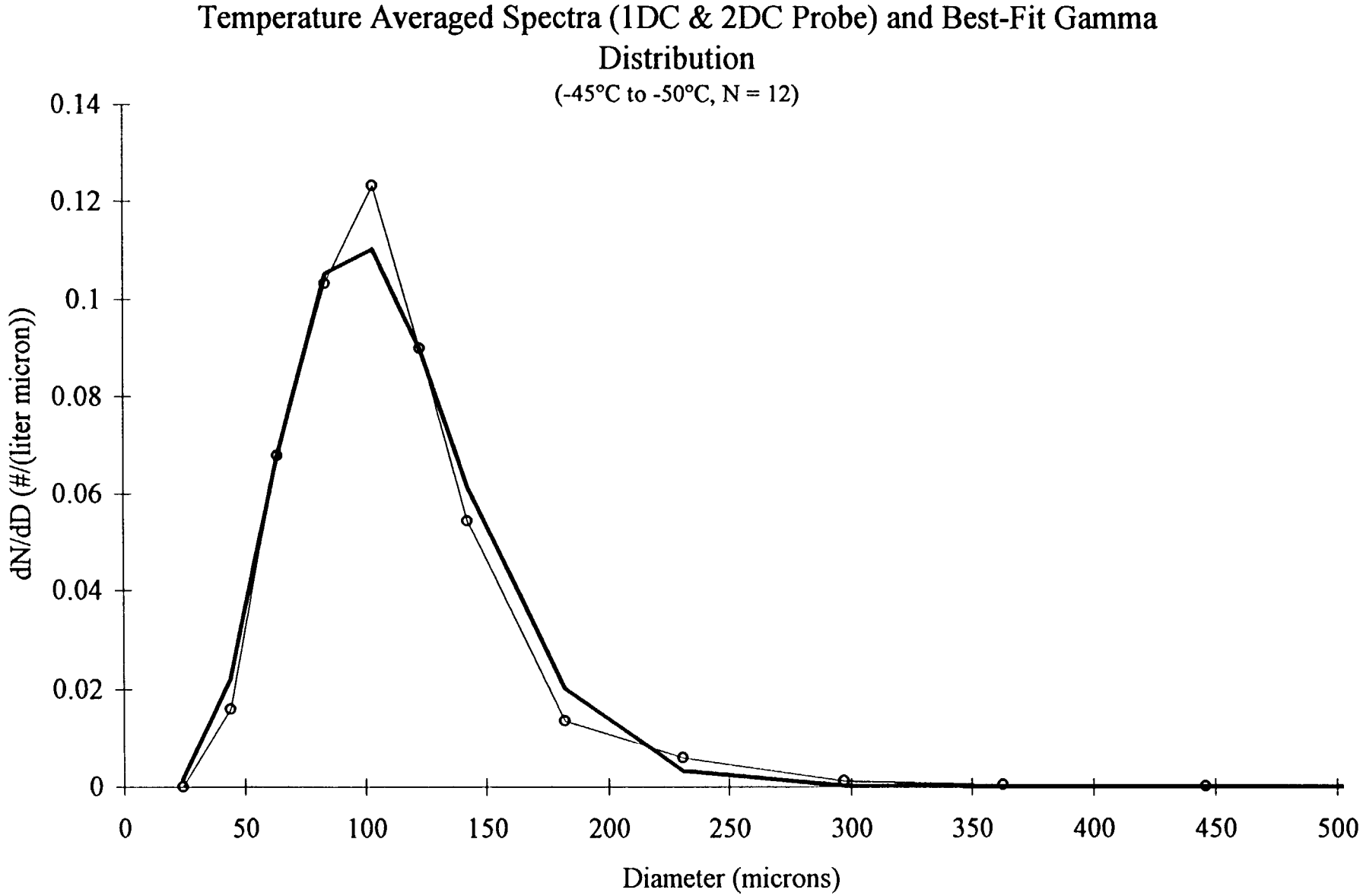
Temperature Averaged Spectra (1DC & 2DC Probe) and Best-Fit Gamma Distribution
(-45°C to -50°C, N = 12)
dN/dD (#/(liter micron))
0.14
0.12
0.1
0.08
0.06
0.04
0.02
0
0
50
100
150
200
250
300
350
400
450
500
Diameter (microns)

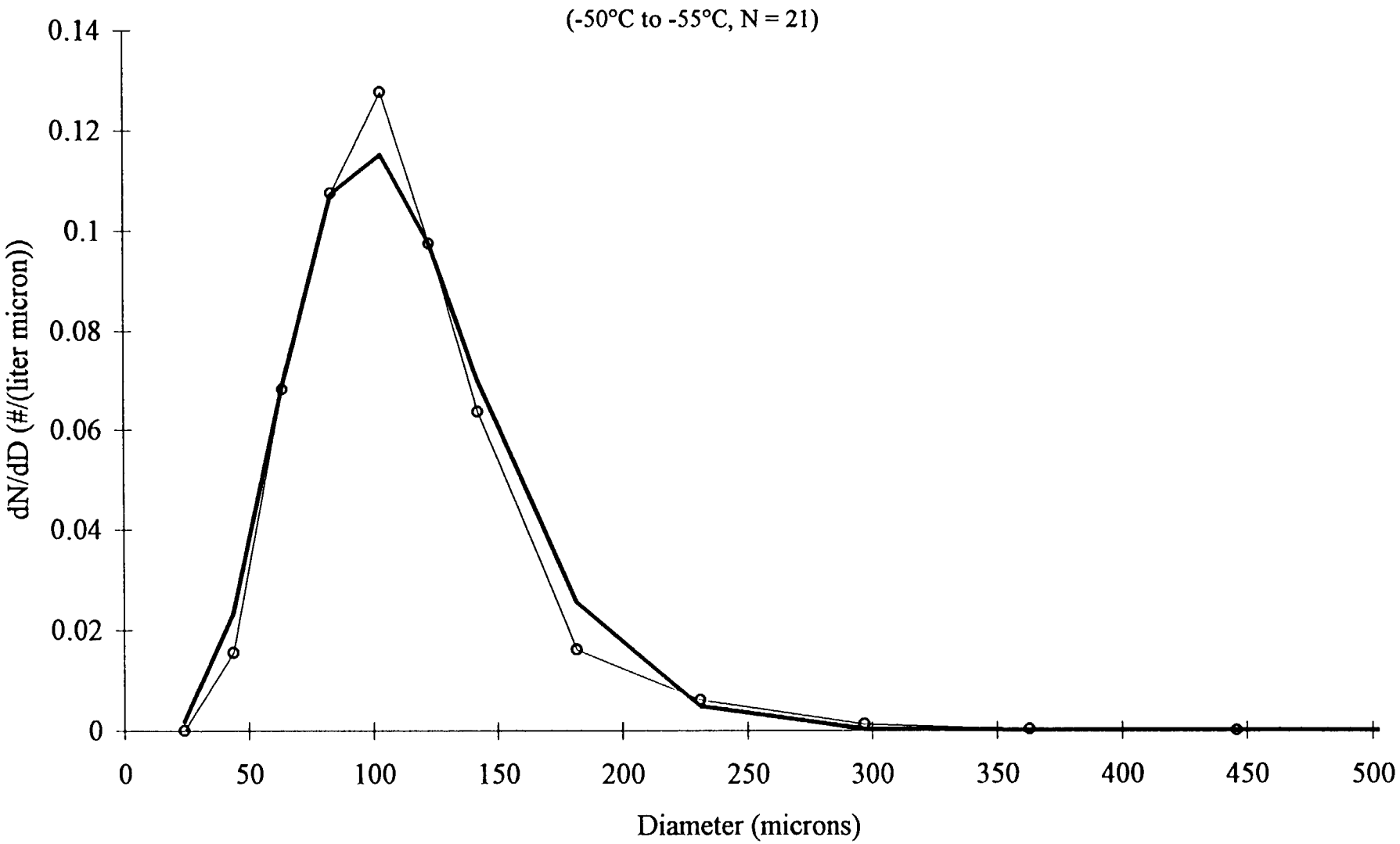
Temperature Averaged Spectra (1DC & 2DC Probe) and Best-Fit Gamma Distribution
(-50°C to -55°C, N = 21)
dN/dD (#/(liter micron))
0.14
0.12
0.1
0.08
0.06
0.04
0.02
0
0
50
100
150
200
250
300
350
400
450
500
Diameter (microns)

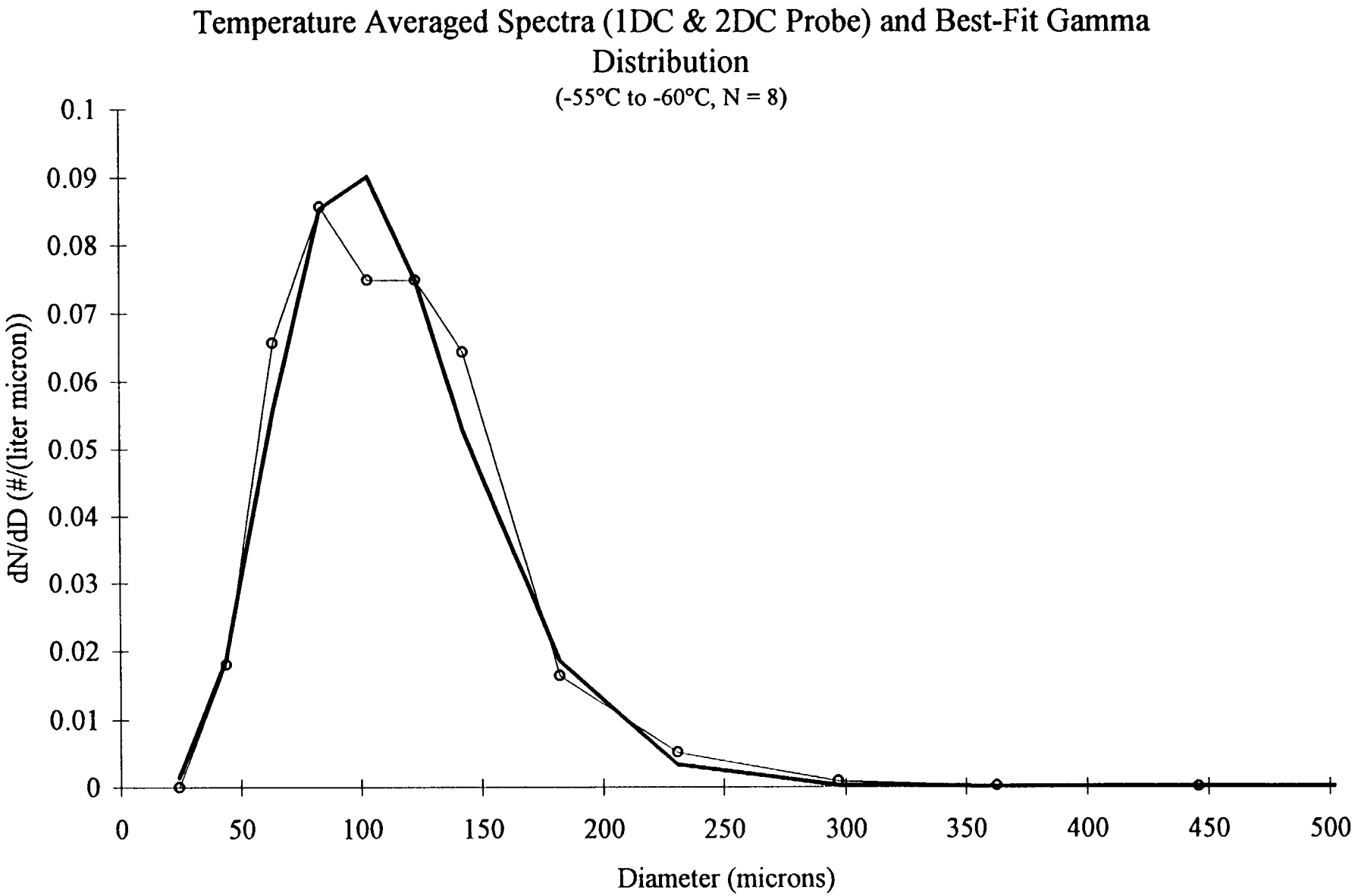
Temperature Averaged Spectra (1DC & 2DC Probe) and Best-Fit Gamma Distribution
(-55°C to -60°C, N = 8)
dN/dD (#/(liter micron))
0.1
0.09
0.08
0.07
0.06
0.05
0.04
0.03
0.02
0.01
0
0
50
100
150
200
250
300
350
400
450
500
Diameter (microns)

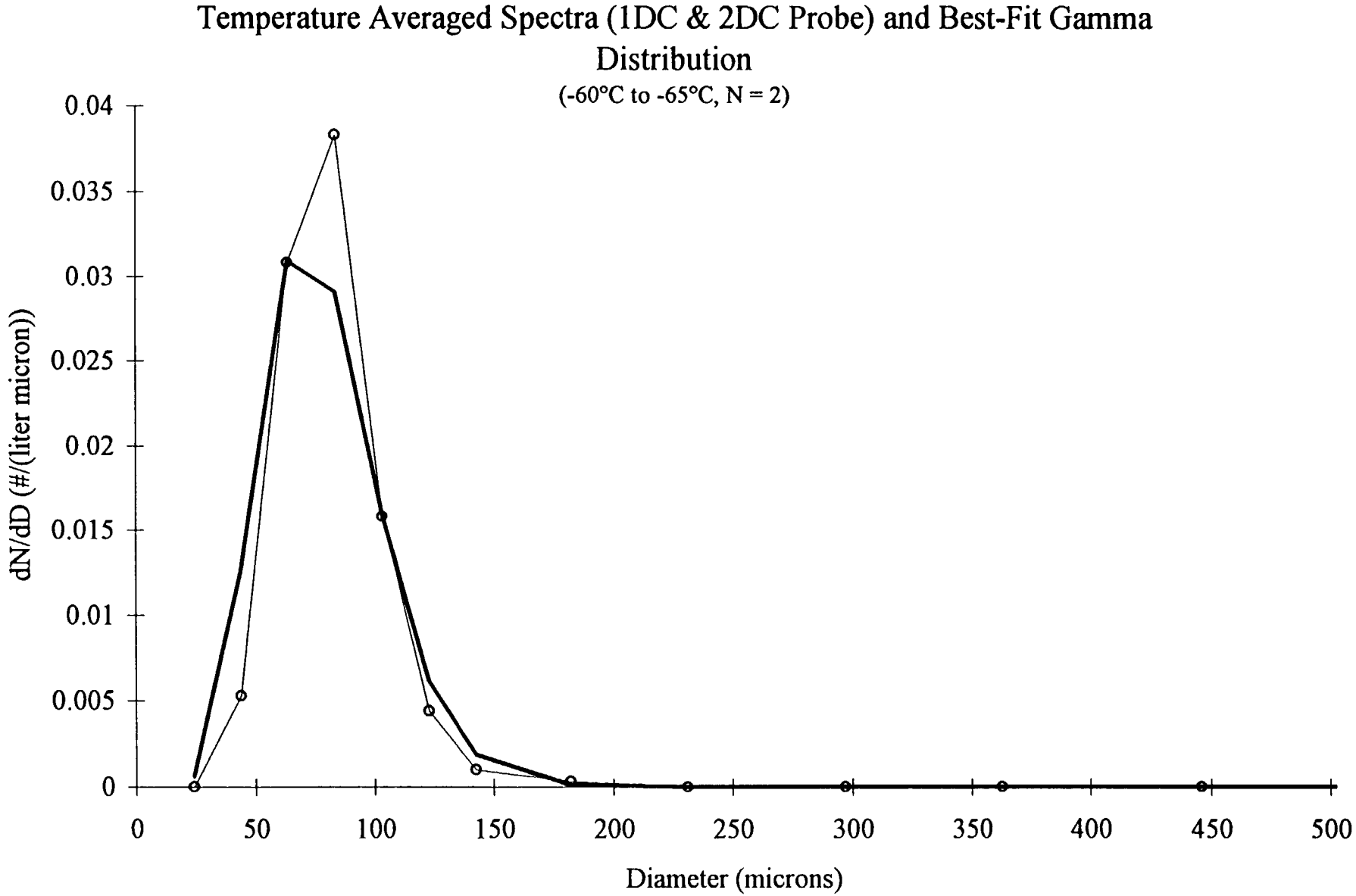
Temperature Averaged Spectra (1DC & 2DC Probe) and Best-Fit Gamma Distribution
(-60°C to -65°C, N = 2)
dN/dD (#/(liter micron))
0.04
0.035
0.03
0.025
0.02
0.015
0.01
0.005
0
0
50
100
150
200
250
300
350
400
450
500
Diameter (microns)

Gamma Distribution Fit to Size Spectra - 1DC and 2DC

by Location in Cloud

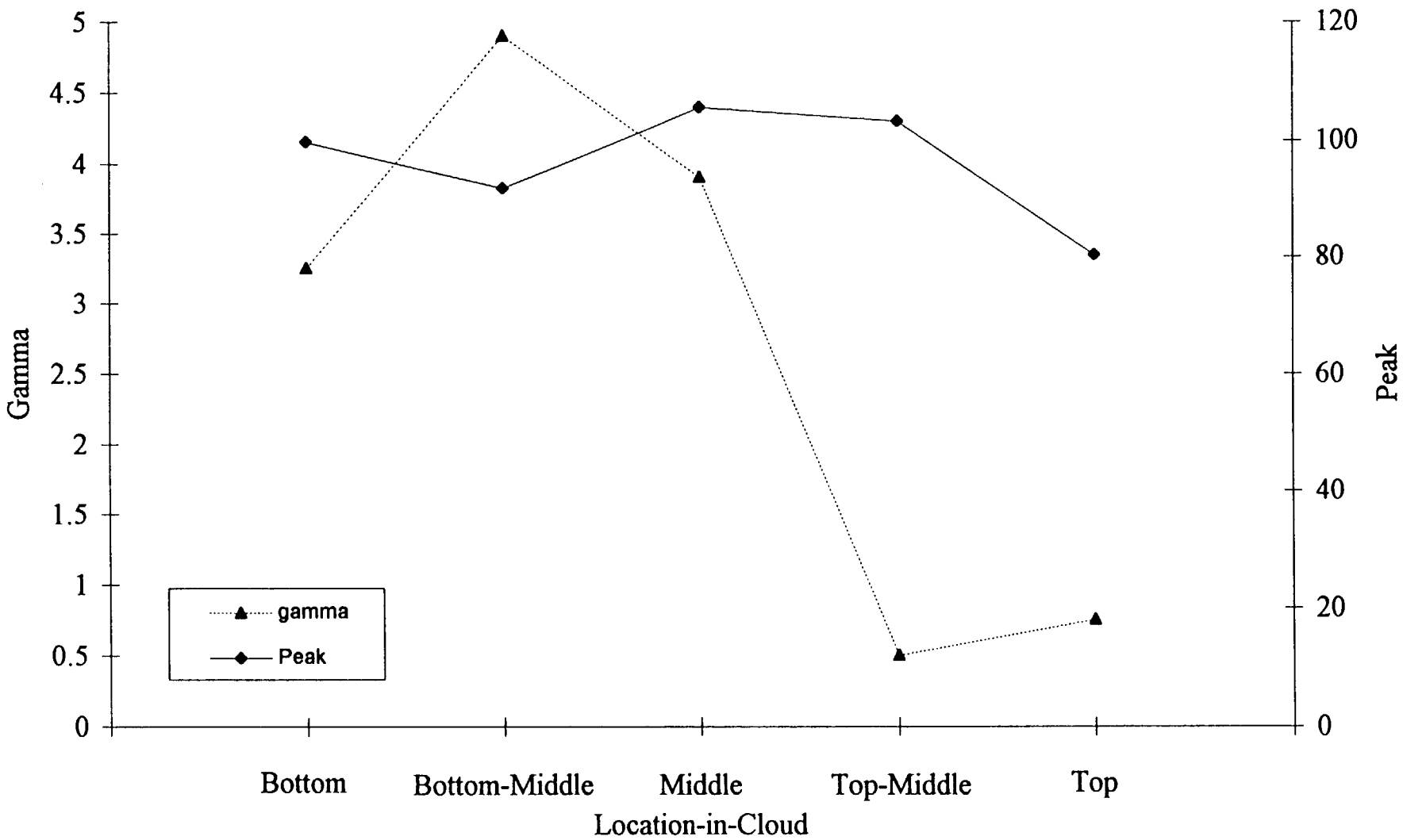
1DC Gamma Distribution Parameters vs Location-in-Cloud
Gamma
Peak
5
4.5
4
3.5
3
2.5
2
1.5
1
0.5
0
120
100
80
60
40
20
0
gamma
Peak
Bottom
Bottom-Middle
Middle
Top-Middle
Top
Location-in-Cloud

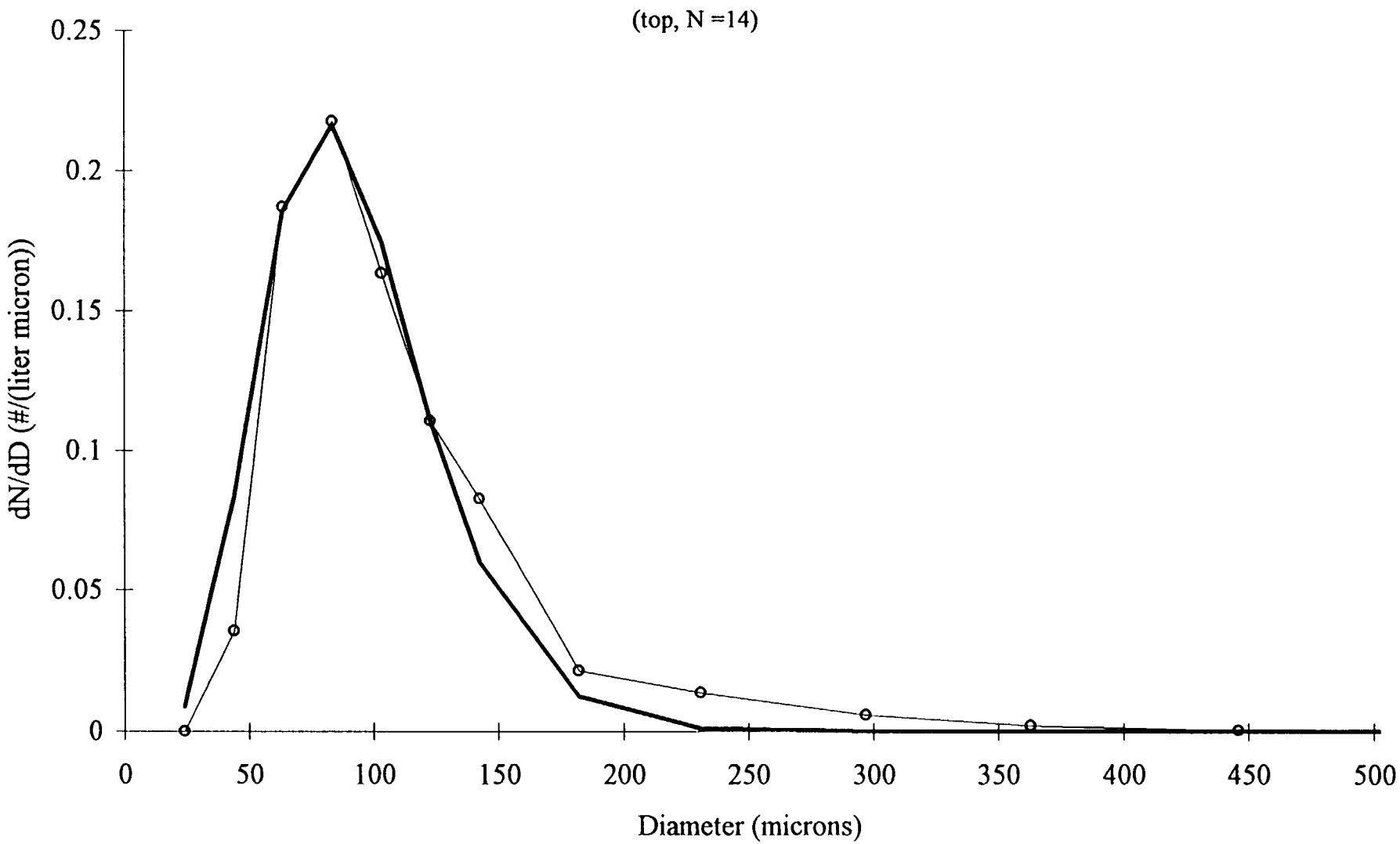
Location in Cloud Averaged Spectra (1DC & 2DC Probe) and Best-Fit Gamma Distribution
(top, N =14)
dN/dD (#/(liter micron))
0.25
0.2
0.15
0.1
0.05
0
0
50
100
150
200
250
300
350
400
450
500
Diameter (microns)

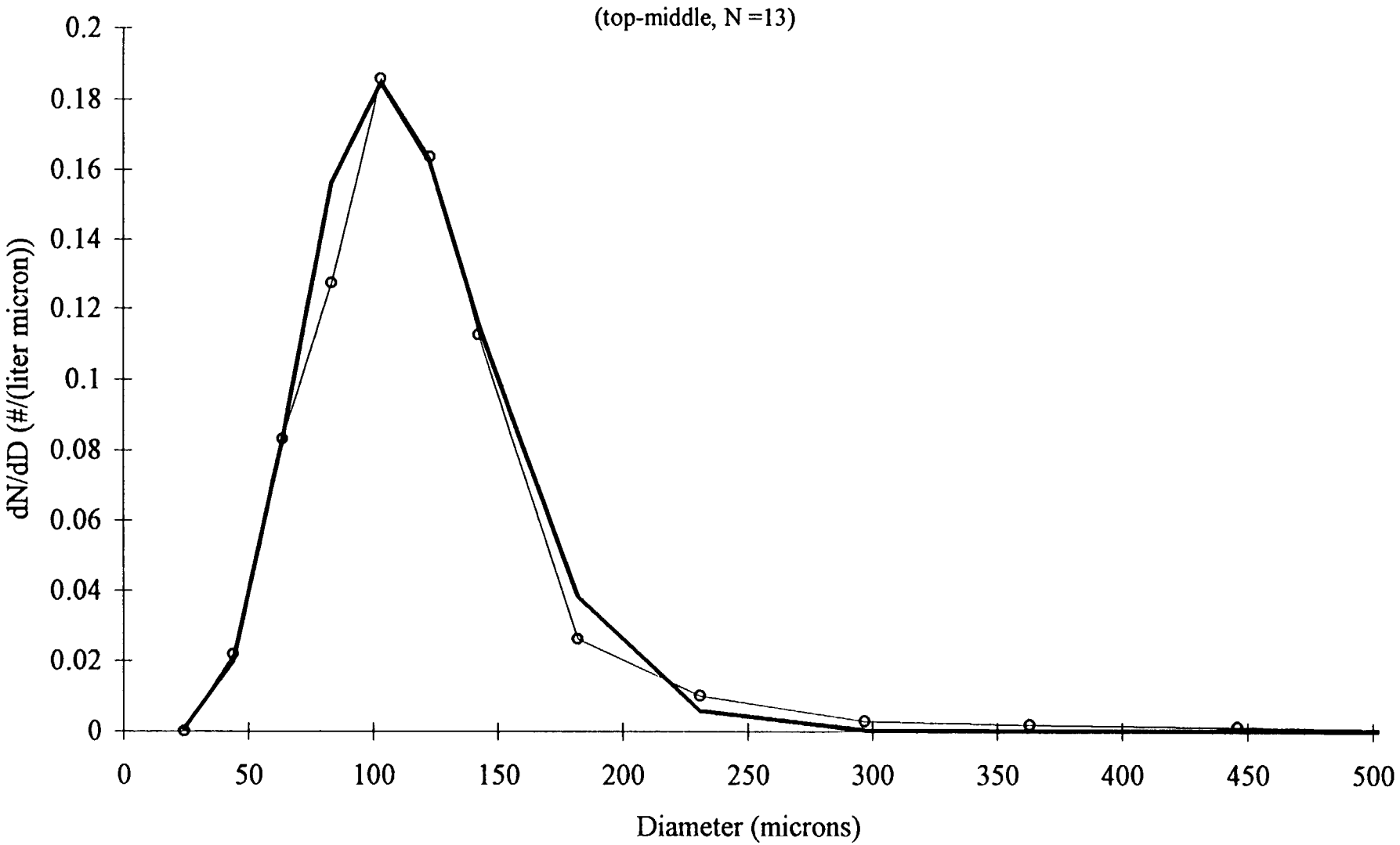
Location in Cloud Averaged Spectra (1DC & 2DC Probe) and Best-Fit Gamma Distribution
(top-middle, N =13)
dN/dD (#/(liter micron))
0.2
0.18
0.16
0.14
0.12
0.1
0.08
0.06
0.04
0.02
0
0
50
100
150
200
250
300
350
400
450
500
Diameter (microns)

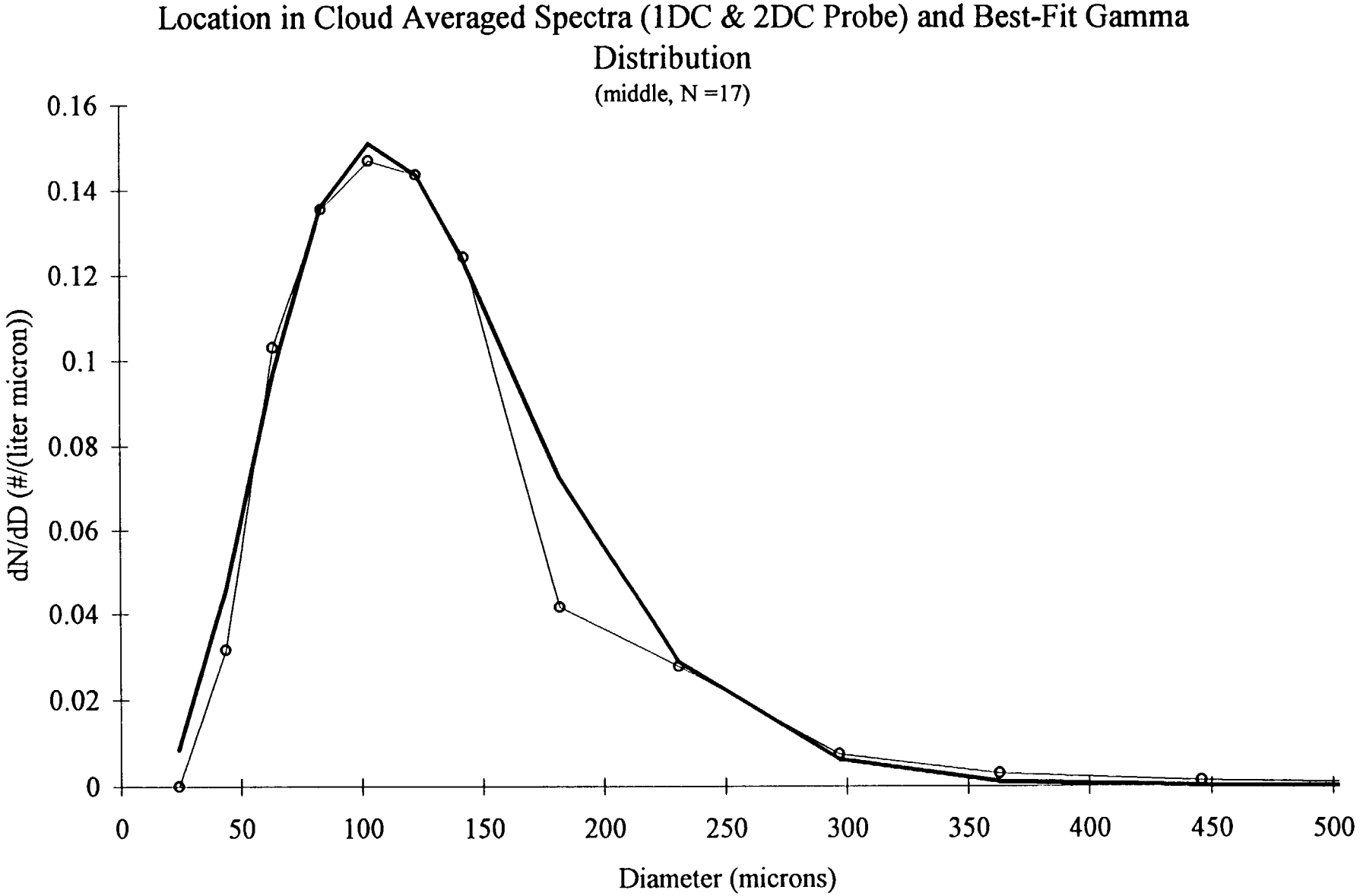
Location in Cloud Averaged Spectra (1DC & 2DC Probe) and Best-Fit Gamma Distribution
(middle, N =17)
dN/dD (#/(liter micron))
0.16
0.14
0.12
0.1
0.08
0.06
0.04
0.02
0
0
50
100
150
200
250
300
350
400
450
500
Diameter (microns)

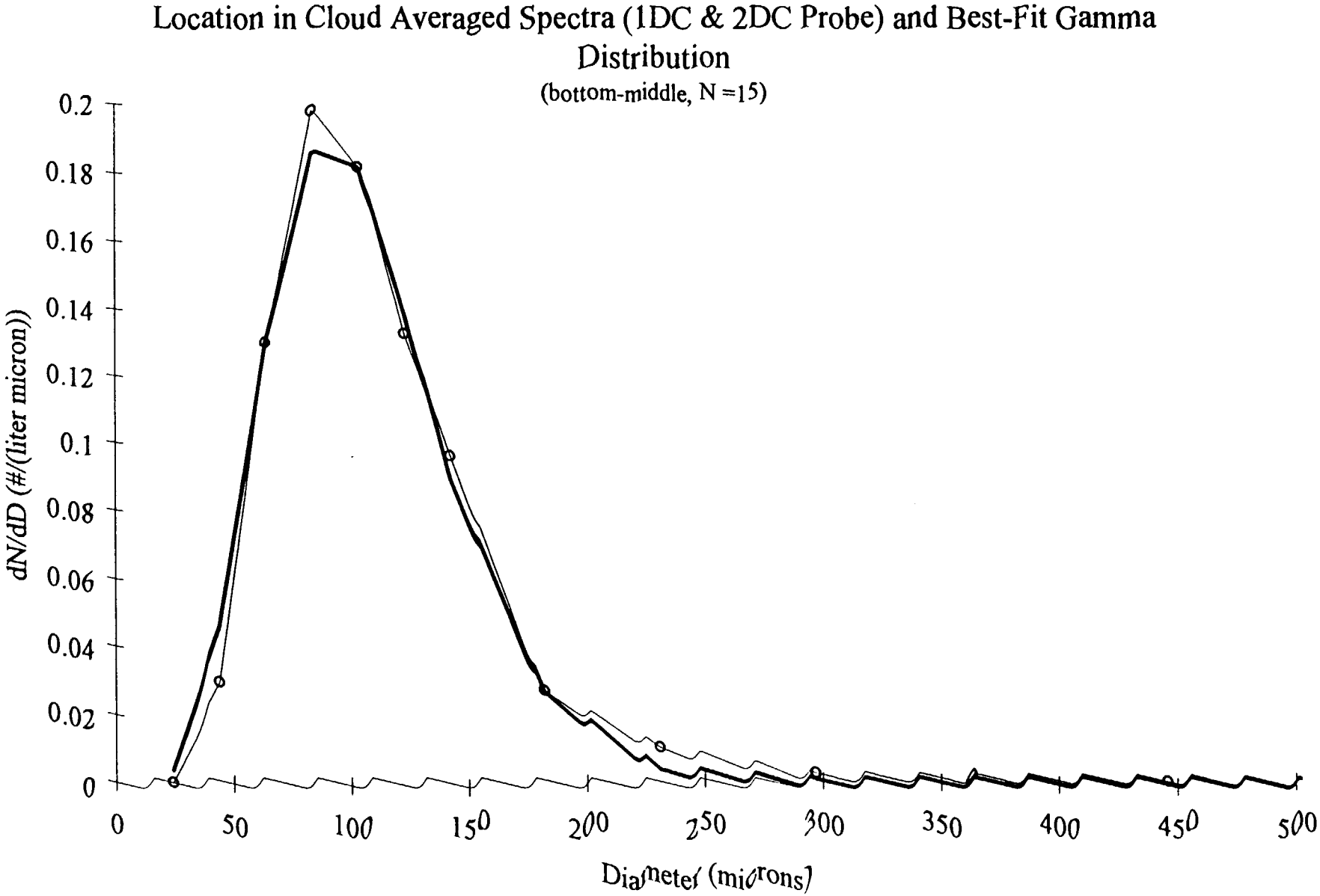
Location in Cloud Averaged Spectra (1DC & 2DC Probe) and Best-Fit Gamma Distribution
(bottom-middle, N =15)
dN/dD (#/(liter micron))
0.2
0.18
0.16
0.14
0.12
0.1
0.08
0.06
0.04
0.02
0
0
50
100
150
200
250
300
350
400
450
500
Diameter (microns)

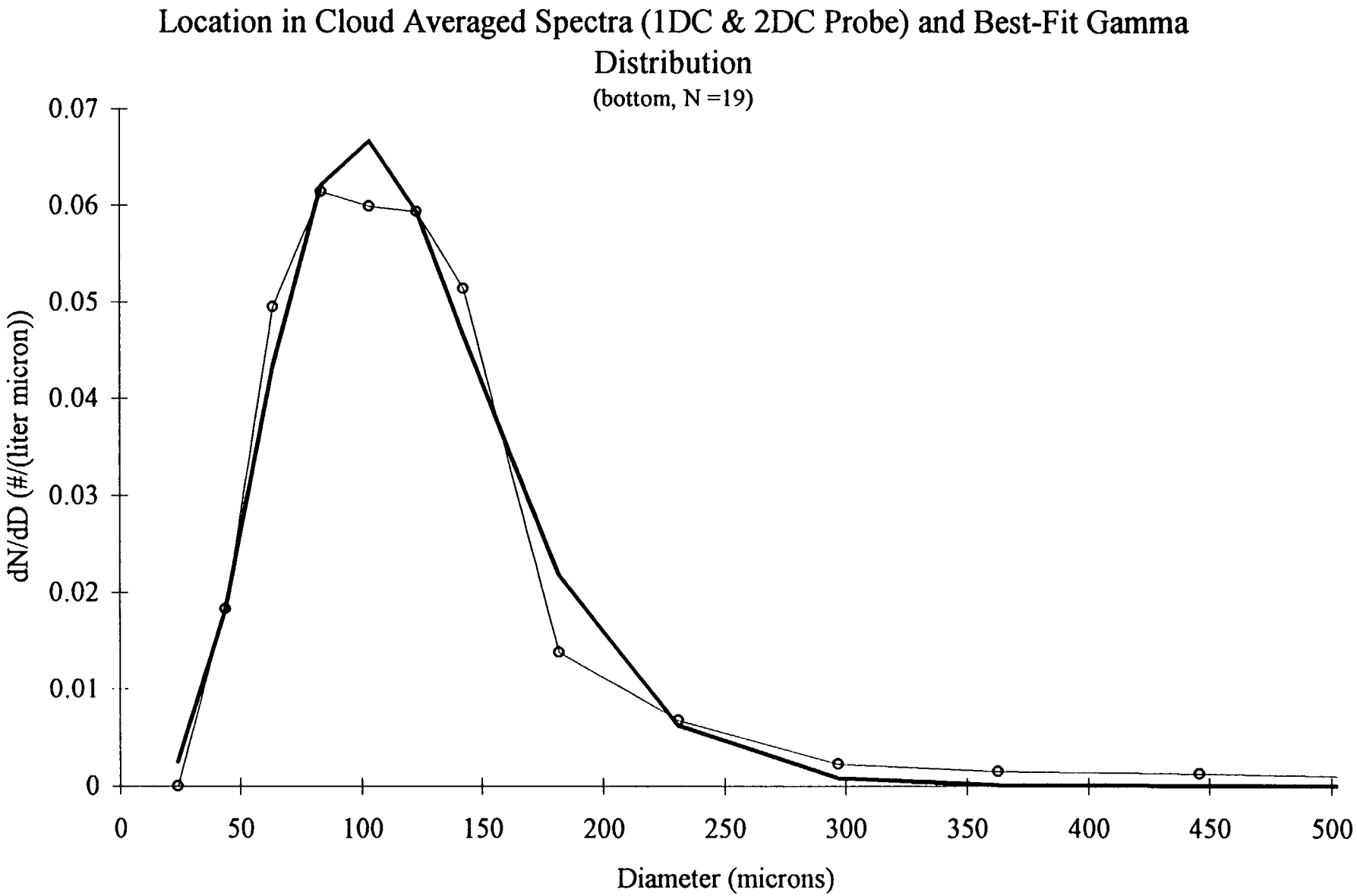
Location in Cloud Averaged Spectra (1DC & 2DC Probe) and Best-Fit Gamma Distribution
(bottom, N =19)
dN/dD (#/(liter micron))
0.07
0.06
0.05
0.04
0.03
0.02
0.01
0
0
50
100
150
200
250
300
350
400
450
500
Diameter (microns)

Gamma Distribution Fit to Size Spectra - Replicator and 2DC

by Temperature

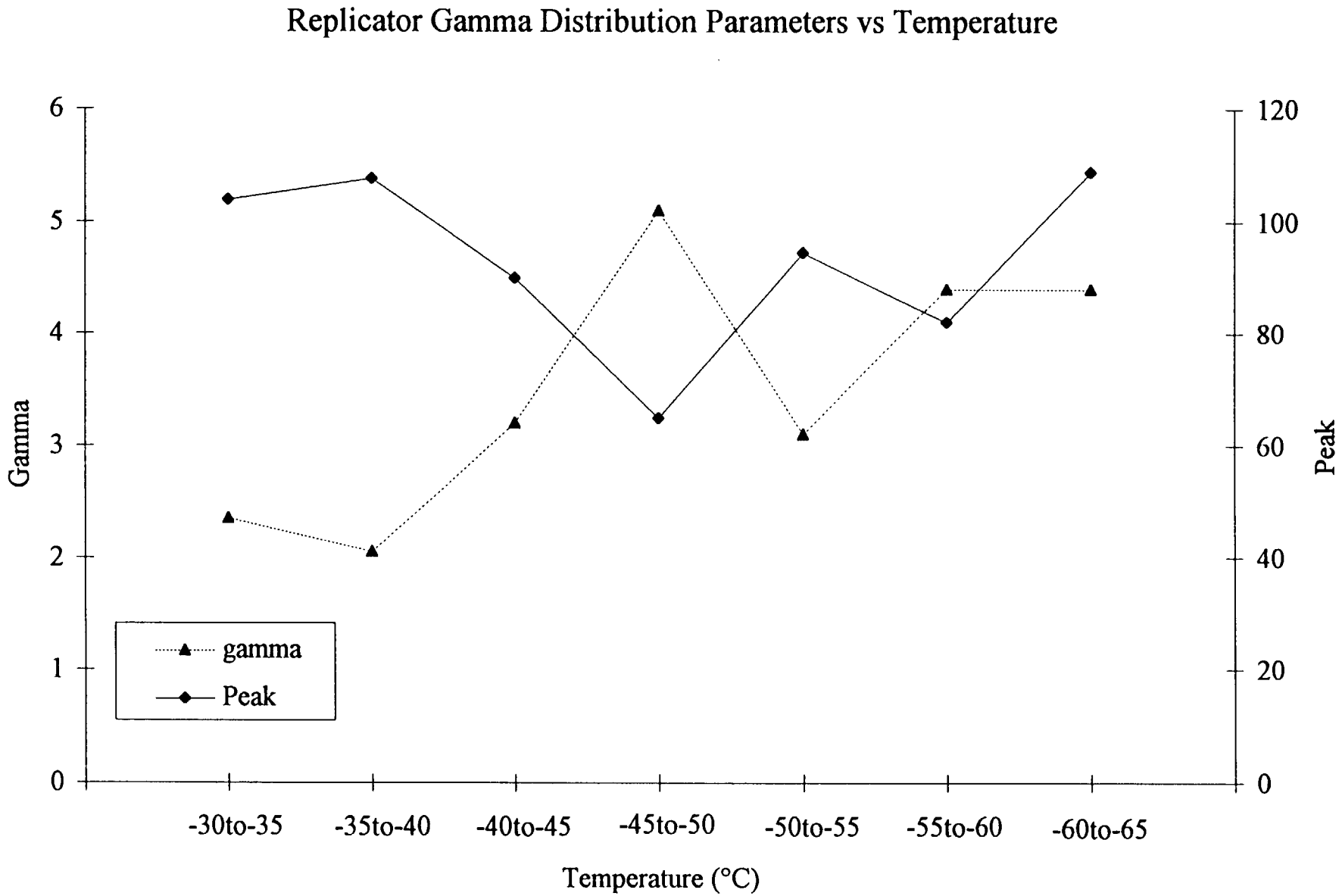
Replicator Gamma Distribution Parameters vs Temperature
Gamma
Peak
6
5
4
3
2
1
0
120
100
80
60
40
20
0
gamma
Peak
-30to-35
-35to-40
-40to-45
-45to-50
-50to-55
-55to-60
-60to-65
Temperature (°C)

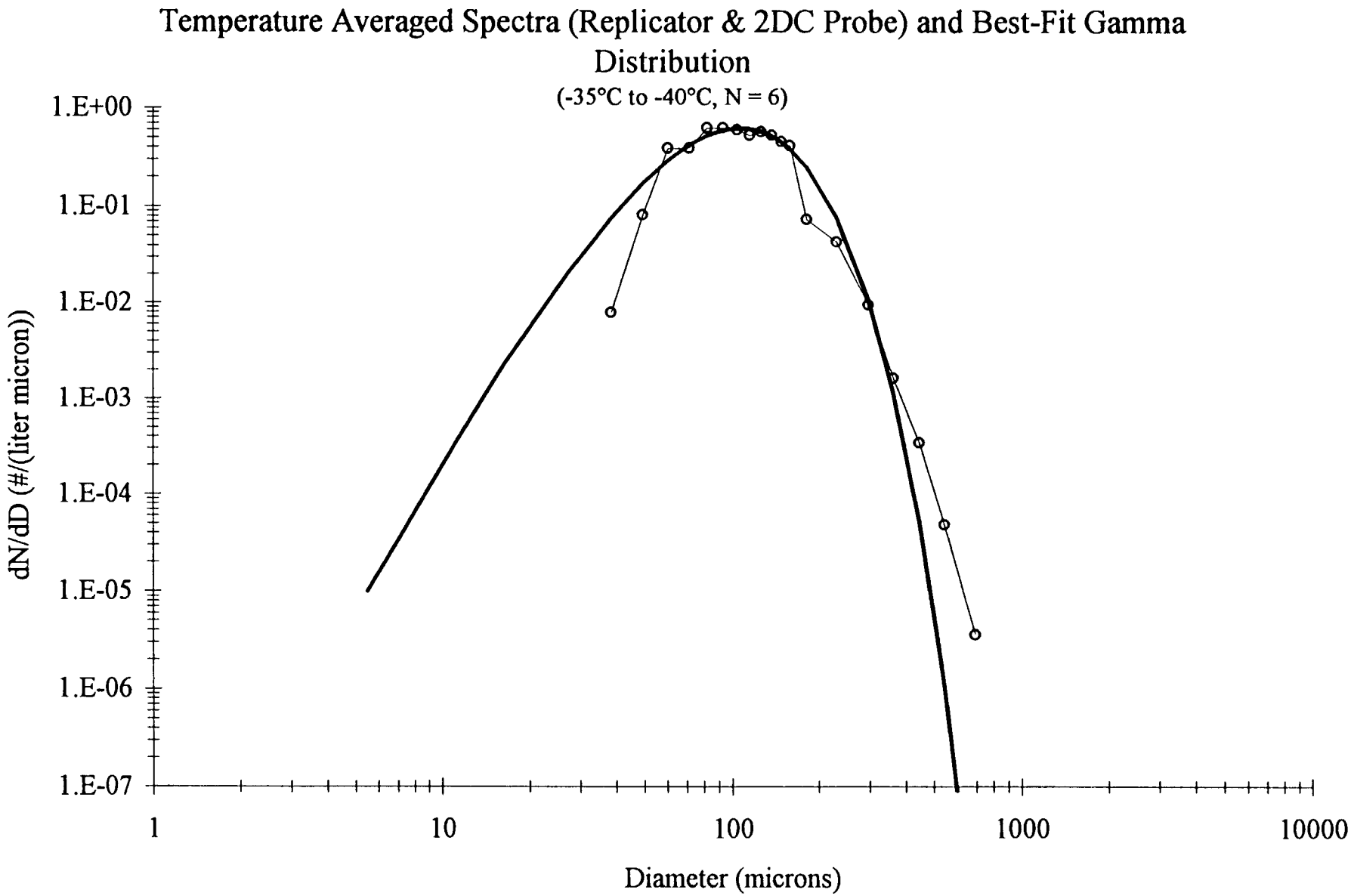
Temperature Averaged Spectra (Replicator & 2DC Probe) and Best-Fit Gamma Distribution
(-35°C to -40°C, N = 6)
dN/dD (#/(liter micron))
1.E+00
1.E-01
1.E-02
1.E-03
1.E-04
1.E-05
1.E-06
1.E-07
1
10
100
1000
10000
Diameter (microns)

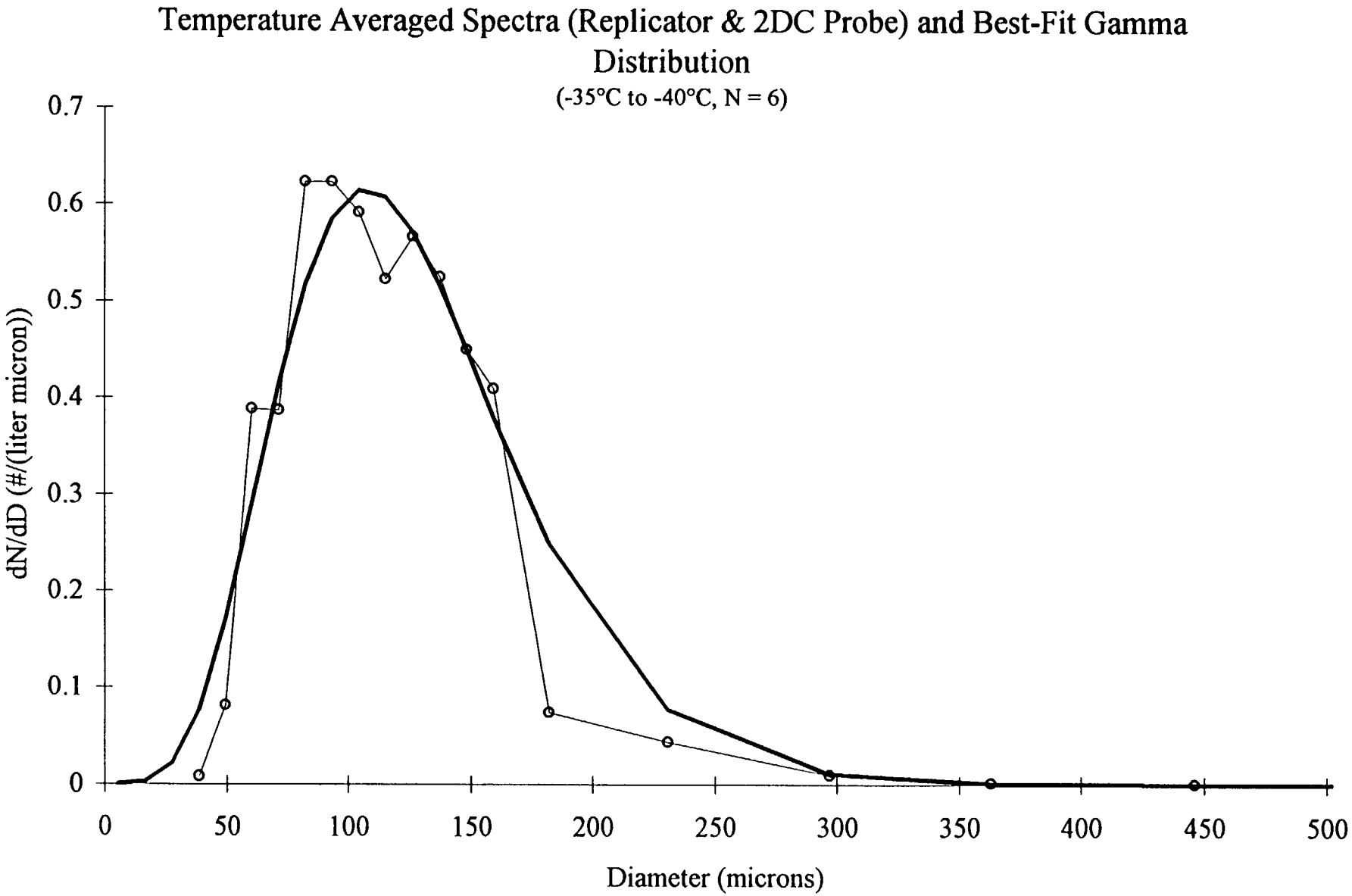
Temperature Averaged Spectra (Replicator & 2DC Probe) and Best-Fit Gamma Distribution
(-35°C to -40°C, N = 6)
dN/dD (#/(liter micron))
0.7
0.6
0.5
0.4
0.3
0.2
0.1
0
0
50
100
150
200
250
300
350
400
450
500
Diameter (microns)

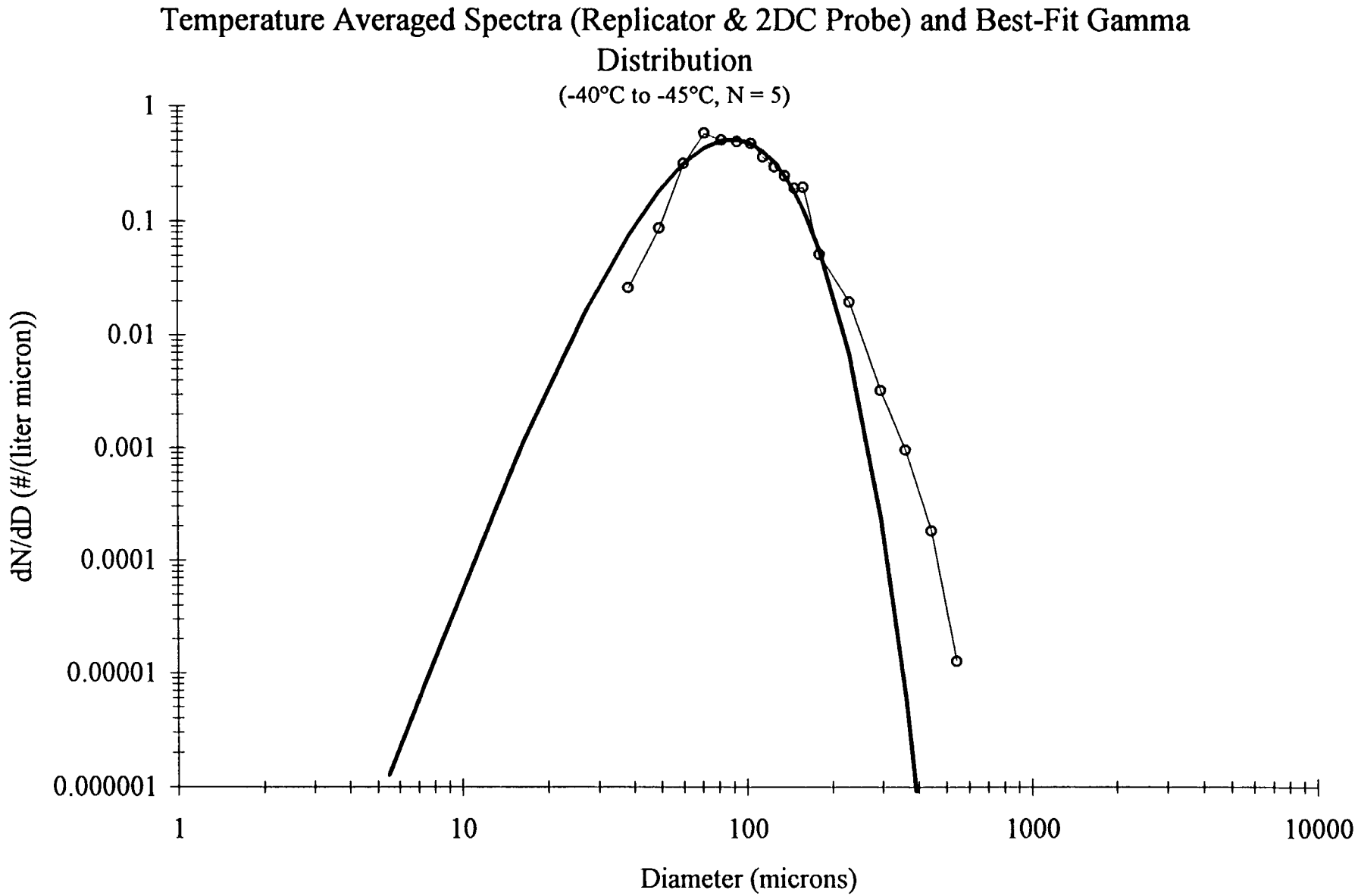
Temperature Averaged Spectra (Replicator & 2DC Probe) and Best-Fit Gamma Distribution
(-40°C to -45°C, N = 5)
dN/dD (#/(liter micron))
1
0.1
0.01
0.001
0.0001
0.00001
0.000001
1
10
100
1000
10000
Diameter (microns)

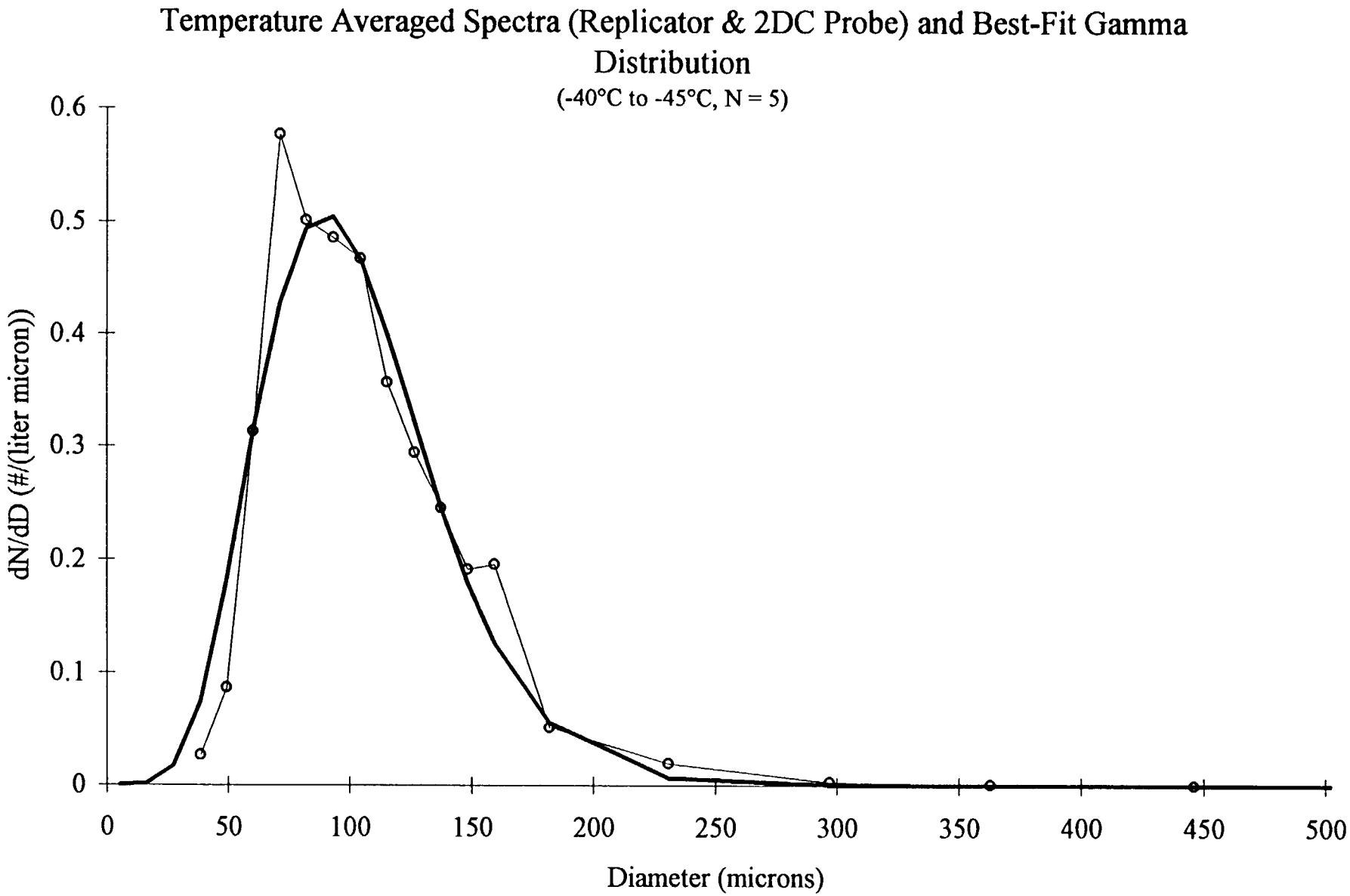
Temperature Averaged Spectra (Replicator & 2DC Probe) and Best-Fit Gamma Distribution
(-40°C to -45°C, N = 5)
dN/dD (#/(liter micron))
0.6
0.5
0.4
0.3
0.2
0.1
0
0
50
100
150
200
250
300
350
400
450
500
Diameter (microns)

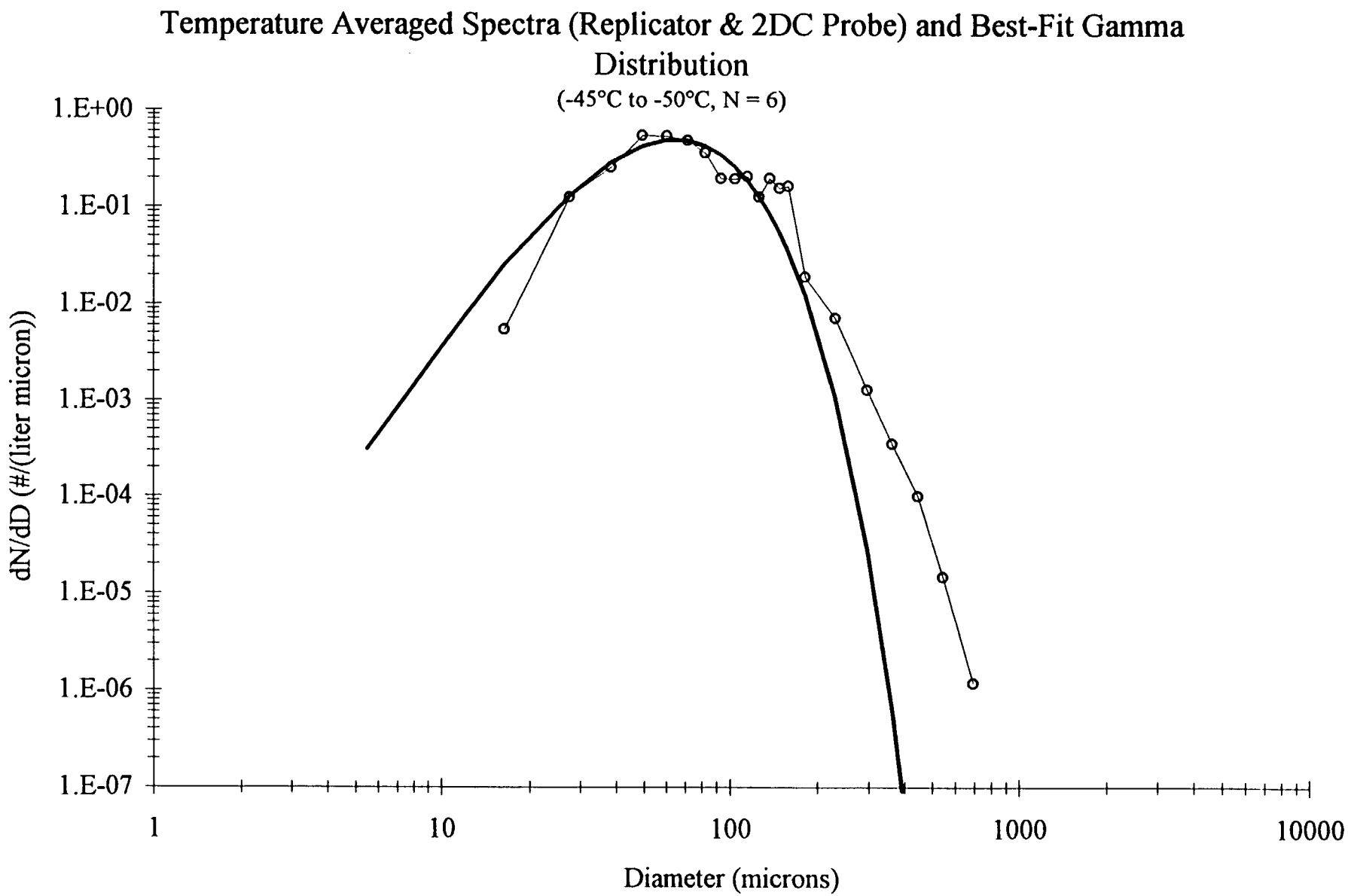
Temperature Averaged Spectra (Replicator & 2DC Probe) and Best-Fit Gamma Distribution
(-45°C to -50°C, N = 6)
dN/dD (#/(liter micron))
1.E+00
1.E-01
1.E-02
1.E-03
1.E-04
1.E-05
1.E-06
1.E-07
1
10
100
1000
10000
Diameter (microns)

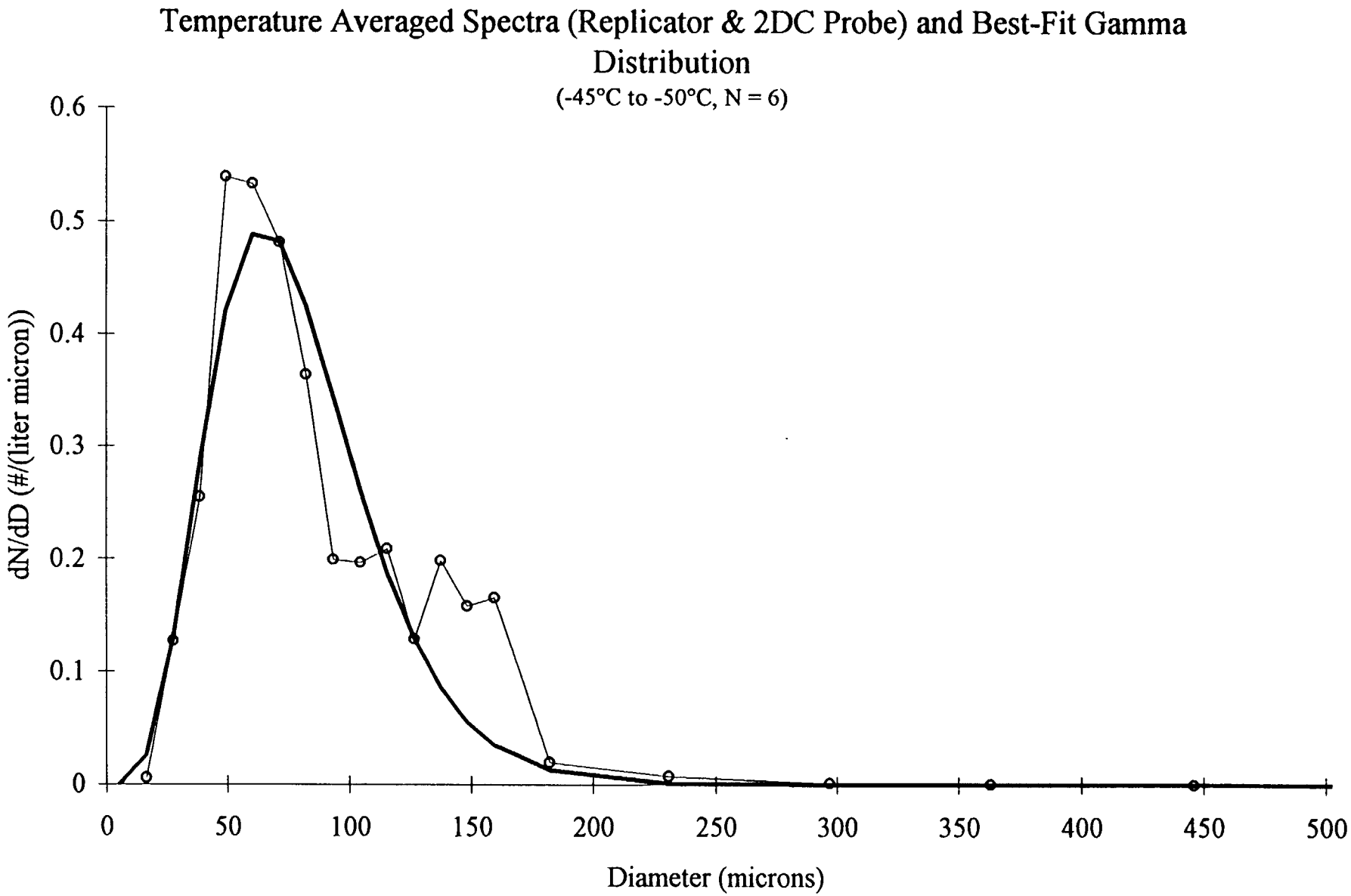
Temperature Averaged Spectra (Replicator & 2DC Probe) and Best-Fit Gamma Distribution
(-45°C to -50°C, N = 6)
dN/dD (#/(liter micron))
0.6
0.5
0.4
0.3
0.2
0.1
0
0
50
100
150
200
250
300
350
400
450
500
Diameter (microns)

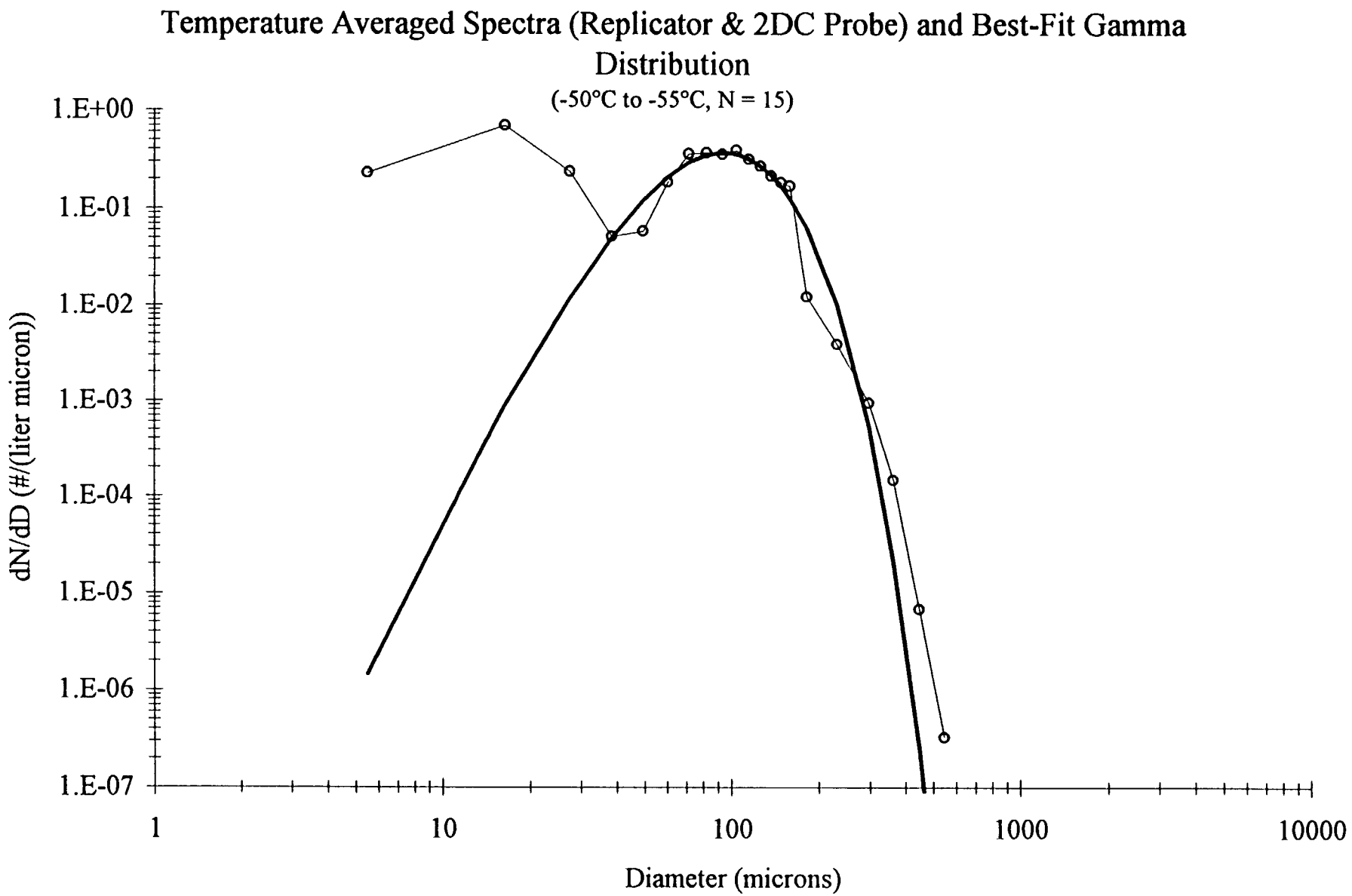
Temperature Averaged Spectra (Replicator & 2DC Probe) and Best-Fit Gamma Distribution
(-50°C to -55°C, N = 15)
dN/dD (#/(liter micron))
1.E+00
1.E-01
1.E-02
1.E-03
1.E-04
1.E-05
1.E-06
1.E-07
1
10
100
1000
10000
Diameter (microns)

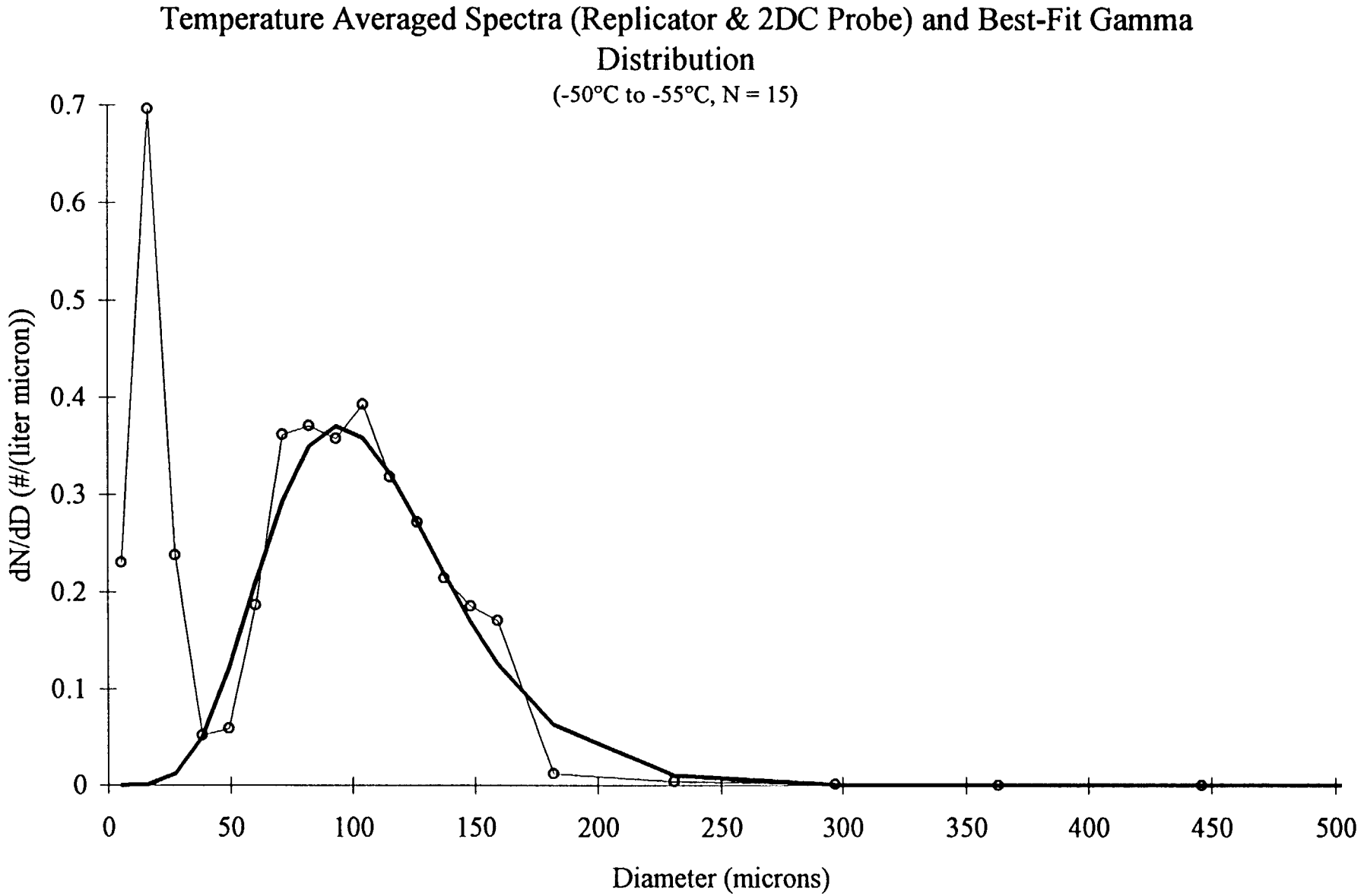
Temperature Averaged Spectra (Replicator & 2DC Probe) and Best-Fit Gamma Distribution
(-50°C to -55°C, N = 15)
dN/dD (#/(liter micron))
0.7
0.6
0.5
0.4
0.3
0.2
0.1
0
0
50
100
150
200
250
300
350
400
450
500
Diameter (microns)

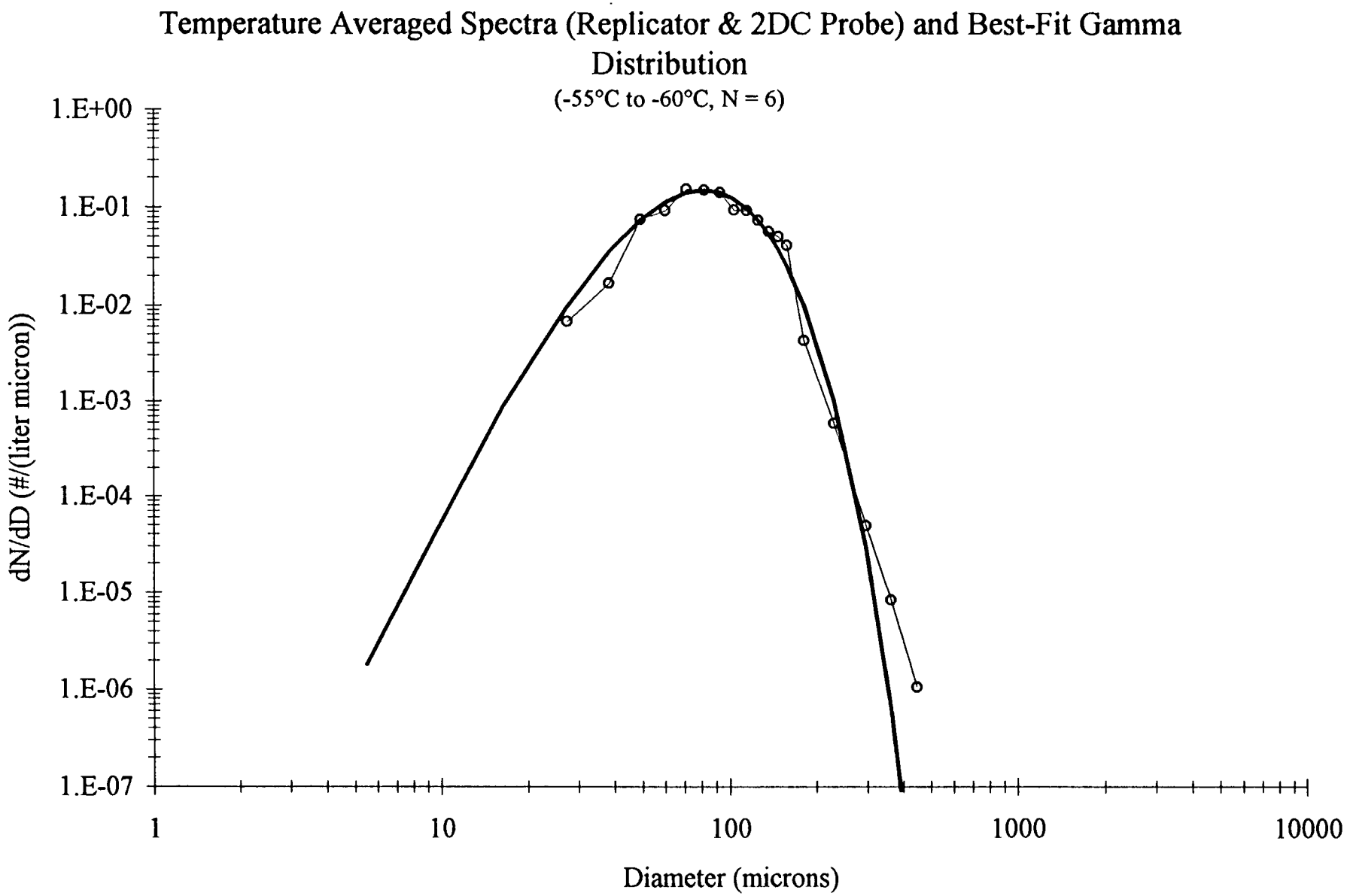
Temperature Averaged Spectra (Replicator & 2DC Probe) and Best-Fit Gamma Distribution
(-55°C to -60°C, N = 6)
dN/dD (#/(liter micron))
1.E+00
1.E-01
1.E-02
1.E-03
1.E-04
1.E-05
1.E-06
1.E-07
1
10
100
1000
10000
Diameter (microns)

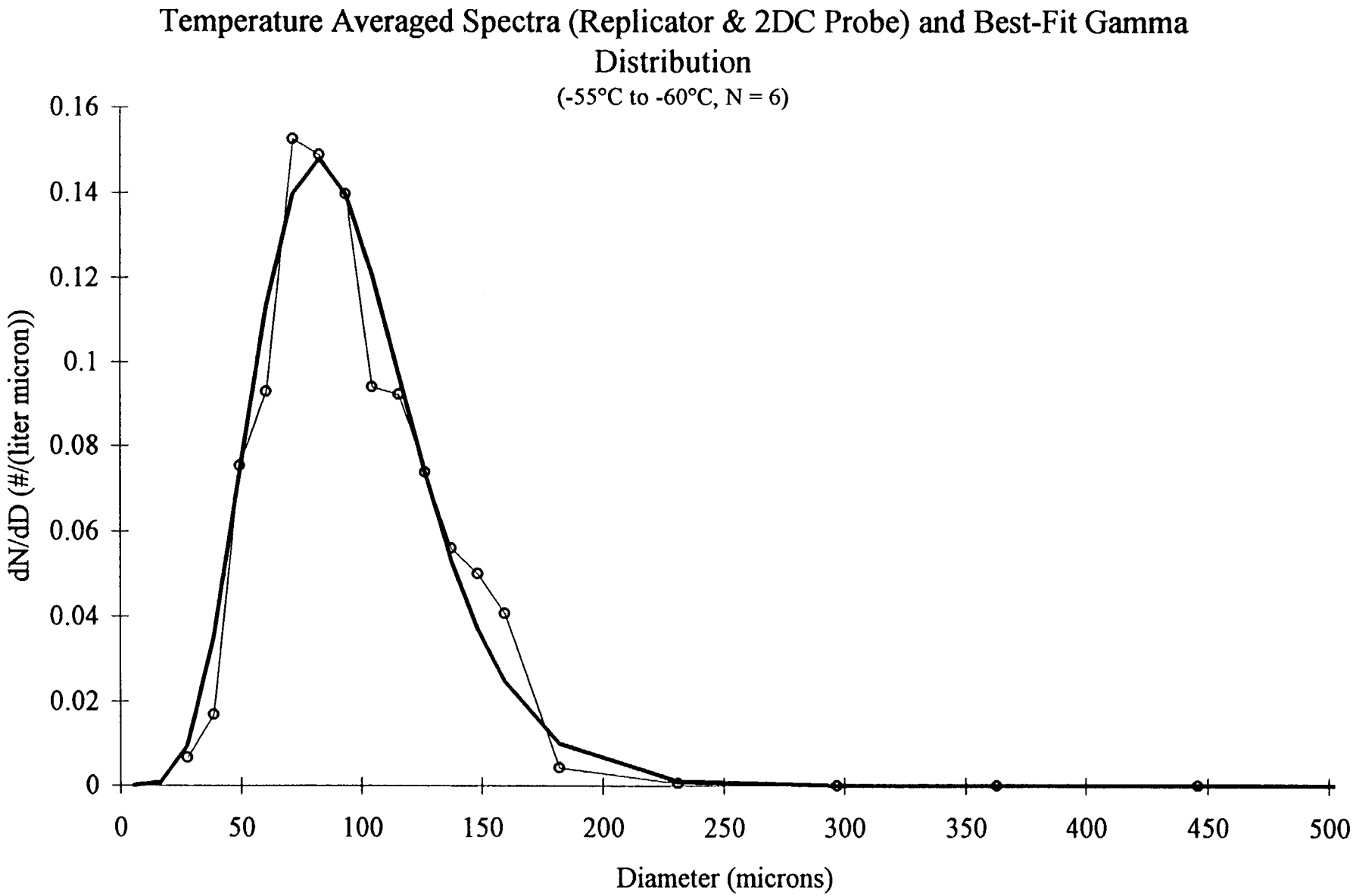
Temperature Averaged Spectra (Replicator & 2DC Probe) and Best-Fit Gamma Distribution
(-55°C to -60°C, N = 6)
dN/dD (#/(liter micron))
0.16
0.14
0.12
0.1
0.08
0.06
0.04
0.02
0
0
50
100
150
200
250
300
350
400
450
500
Diameter (microns)

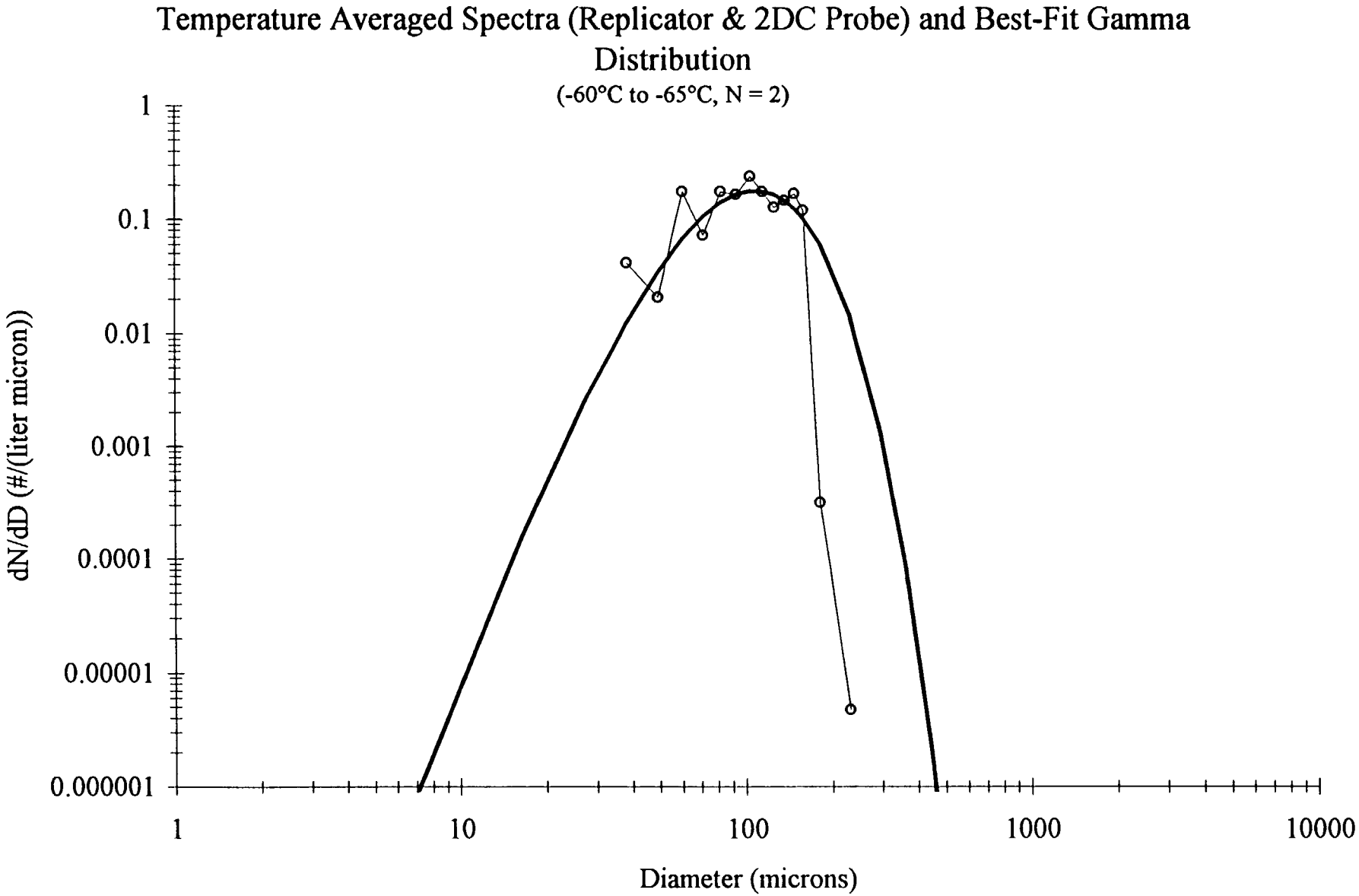
Temperature Averaged Spectra (Replicator & 2DC Probe) and Best-Fit Gamma Distribution
(-60°C to -65°C, N = 2)
dN/dD (#/(liter micron))
1
0.1
0.01
0.001
0.0001
0.00001
0.000001
1
10
100
1000
10000
Diameter (microns)

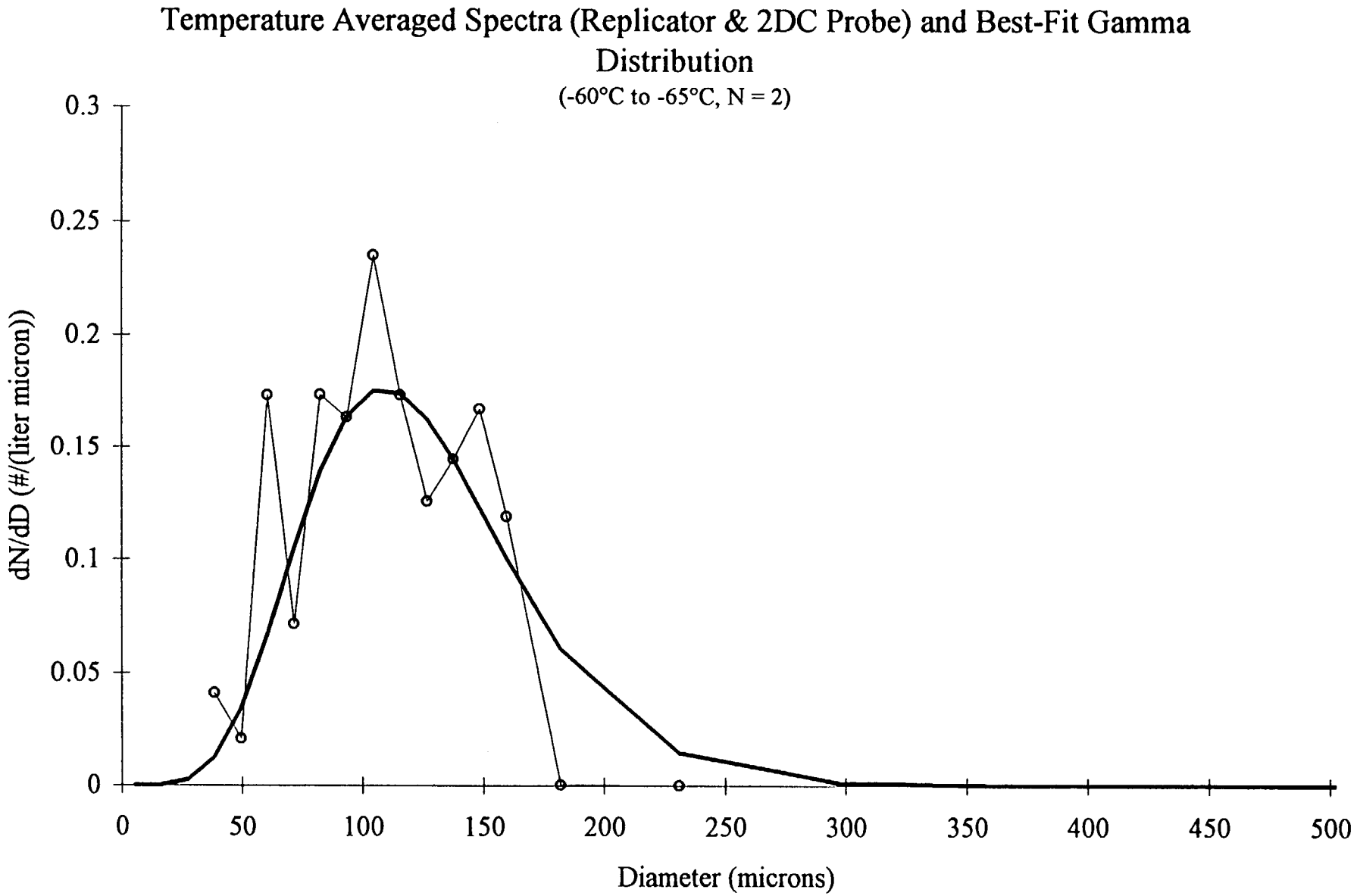
Temperature Averaged Spectra (Replicator & 2DC Probe) and Best-Fit Gamma Distribution
(-60°C to -65°C, N = 2)
dN/dD (#/(liter micron))
0.3
0.25
0.2
0.15
0.1
0.05
0
0
50
100
150
200
250
300
350
400
450
500
Diameter (microns)

Gamma Distribution Fit to Size Spectra - Replicator and 2DC

by Location in Cloud

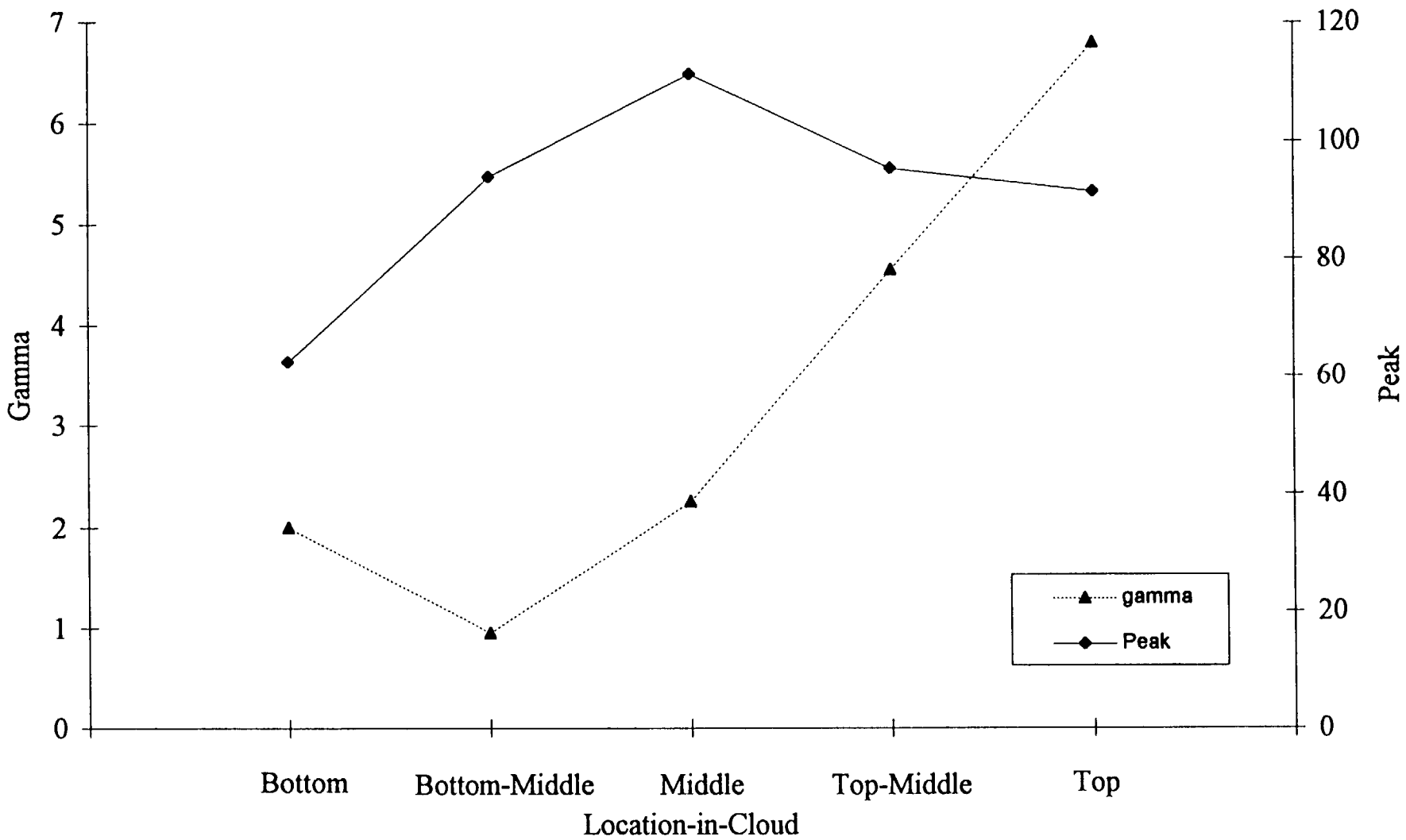
Replicator Gamma Distribution Parameters vs Location-in-Cloud
Gamma
Peak
0
1
2
3
4
5
6
7
0
20
40
60
80
100
120
Bottom
Bottom-Middle
Middle
Top-Middle
Top
Location-in-Cloud
gamma
Peak

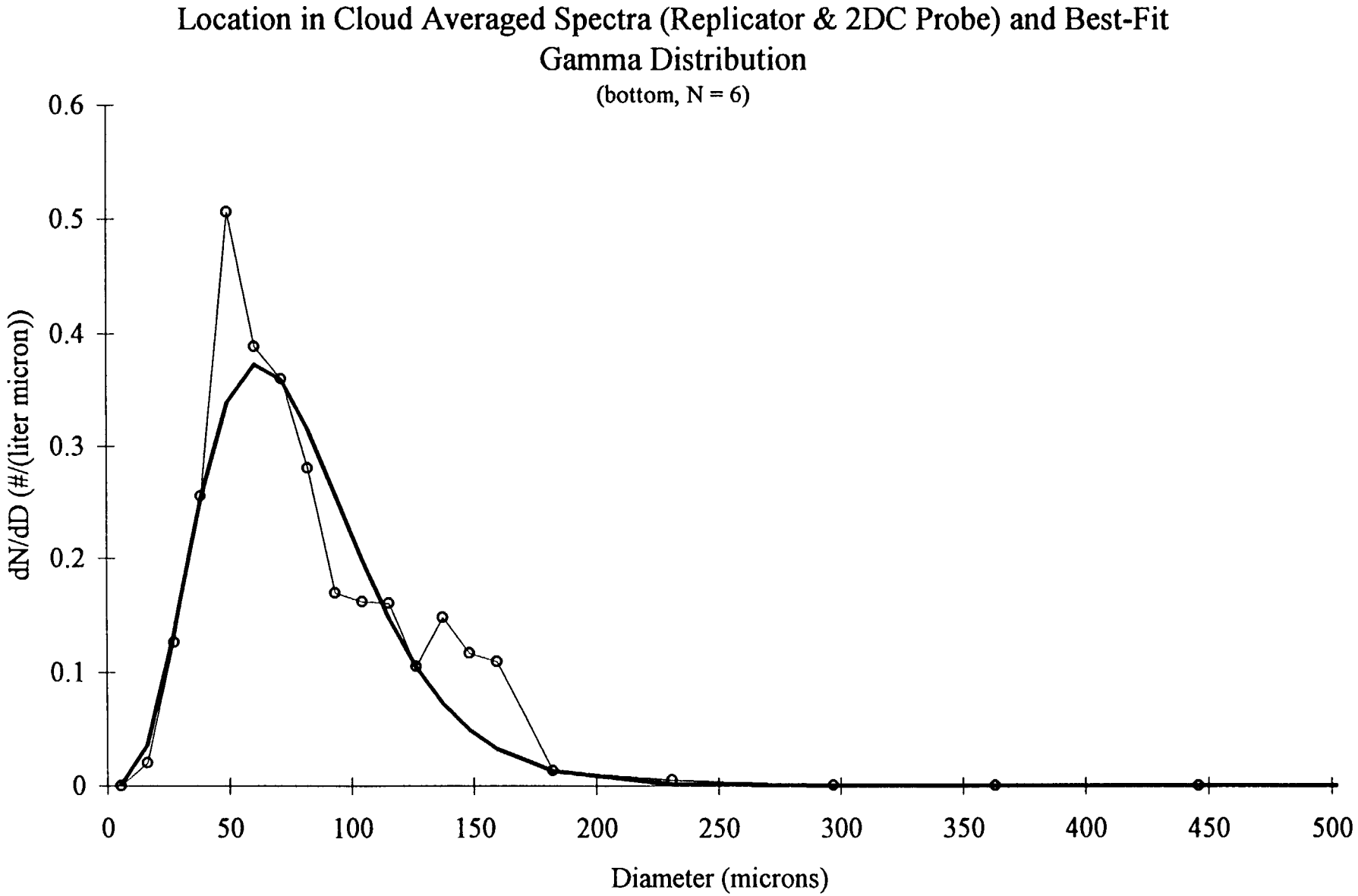
Location in Cloud Averaged Spectra (Replicator & 2DC Probe) and Best-Fit Gamma Distribution
(bottom, N = 6)
dN/dD (#/(liter micron))
0.6
0.5
0.4
0.3
0.2
0.1
0
0
50
100
150
200
250
300
350
400
450
500
Diameter (microns)

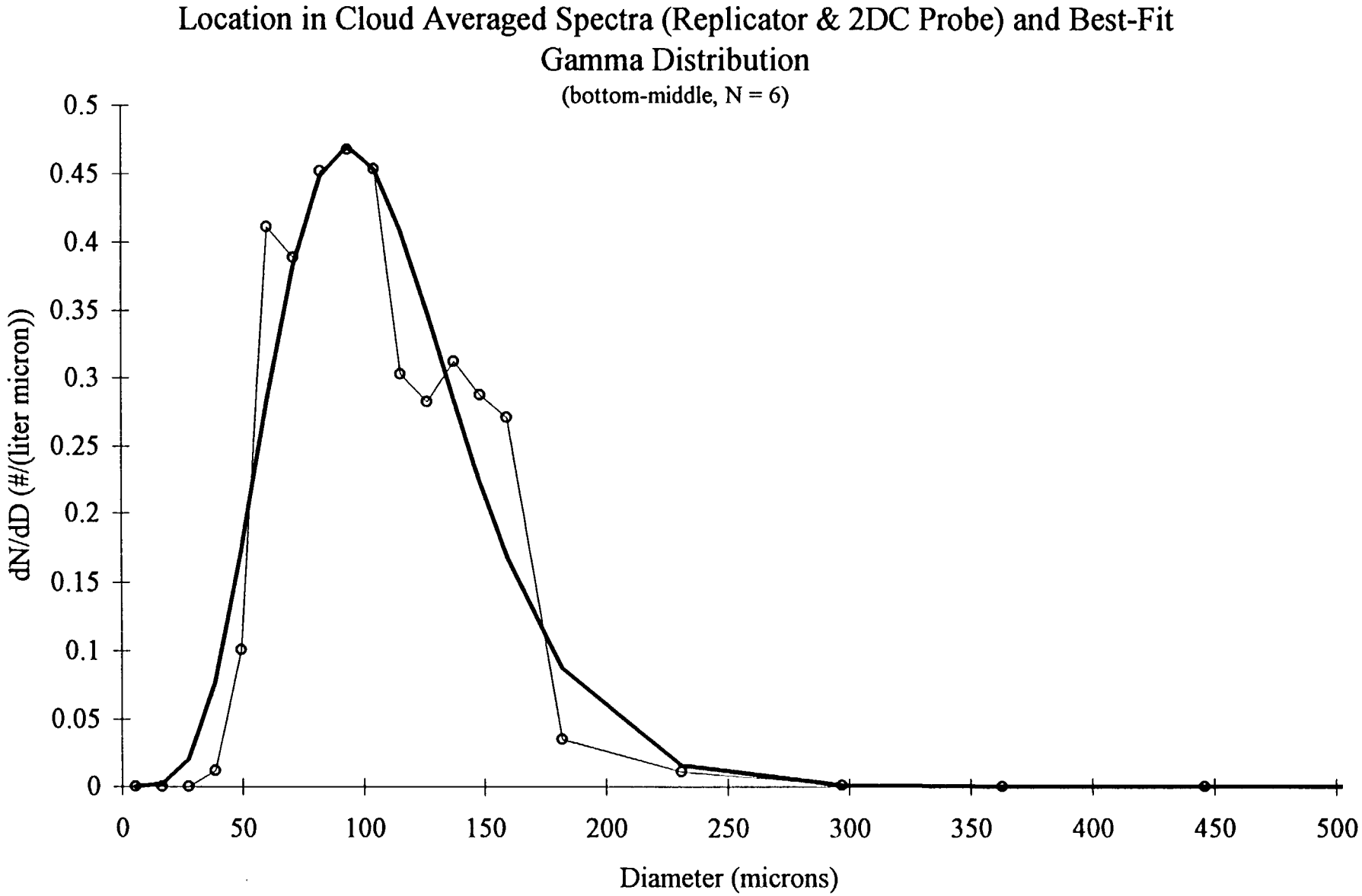
Location in Cloud Averaged Spectra (Replicator & 2DC Probe) and Best-Fit Gamma Distribution
(bottom-middle, N = 6)
dN/dD (#/(liter micron))
0.5
0.45
0.4
0.35
0.3
0.25
0.2
0.15
0.1
0.05
0
0
50
100
150
200
250
300
350
400
450
500
Diameter (microns)

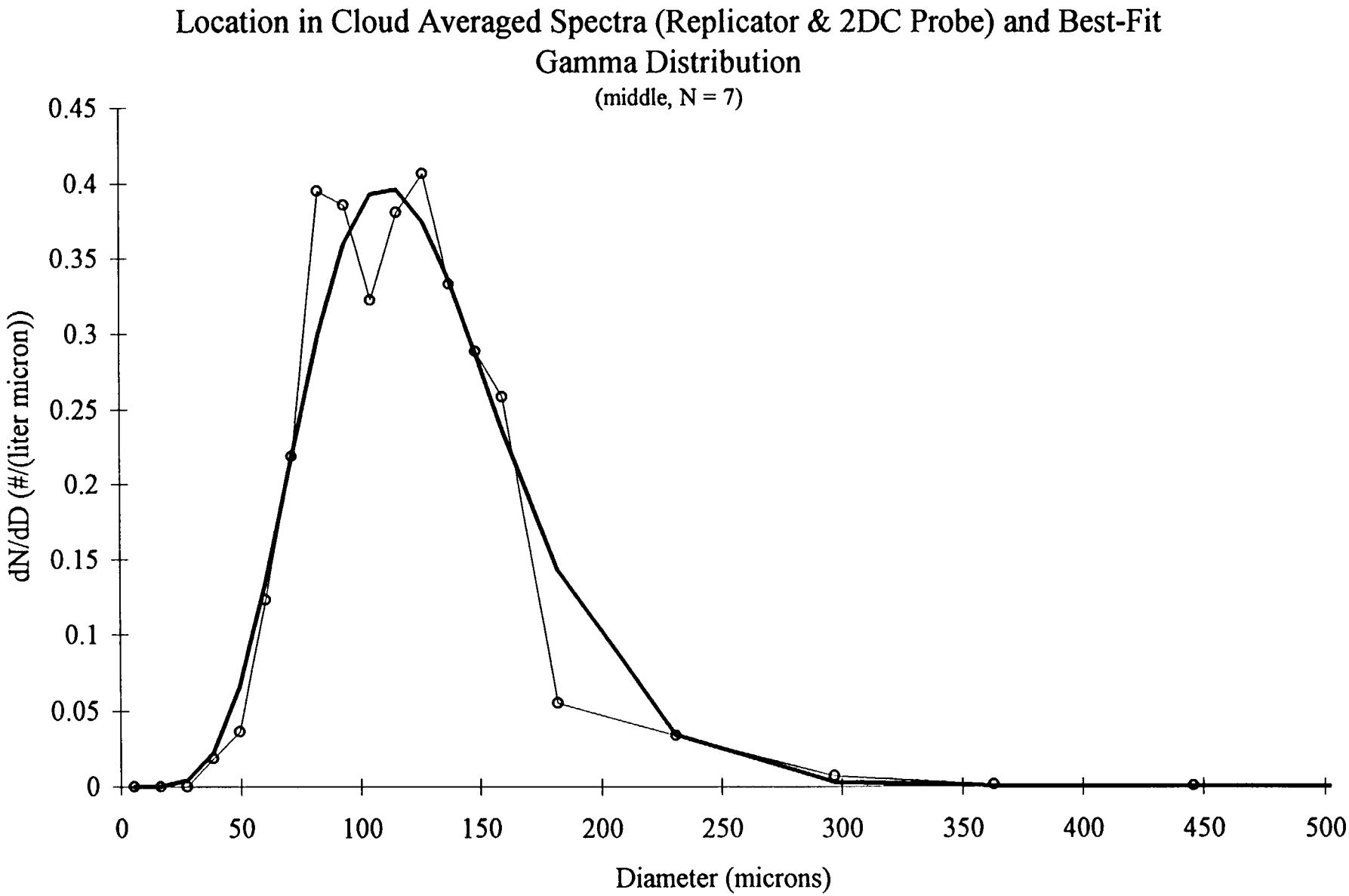
Location in Cloud Averaged Spectra (Replicator & 2DC Probe) and Best-Fit Gamma Distribution
(middle, N = 7)
dN/dD (#/(liter micron))
0.45
0.4
0.35
0.3
0.25
0.2
0.15
0.1
0.05
0
0
50
100
150
200
250
300
350
400
450
500
Diameter (microns)

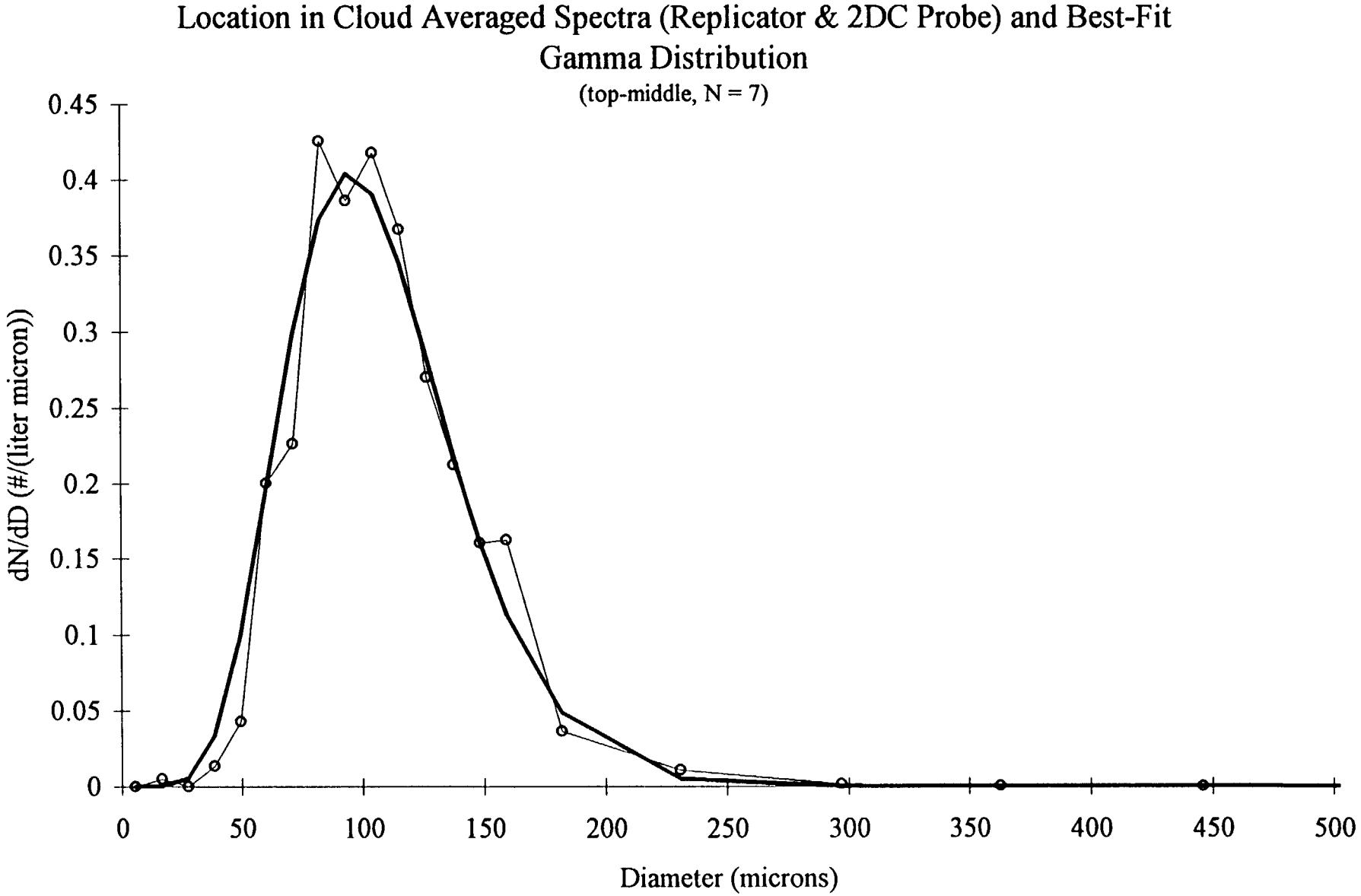
Location in Cloud Averaged Spectra (Replicator & 2DC Probe) and Best-Fit Gamma Distribution
(top-middle, N = 7)
dN/dD (#/(liter micron))
0.45
0.4
0.35
0.3
0.25
0.2
0.15
0.1
0.05
0
0
50
100
150
200
250
300
350
400
450
500
Diameter (microns)

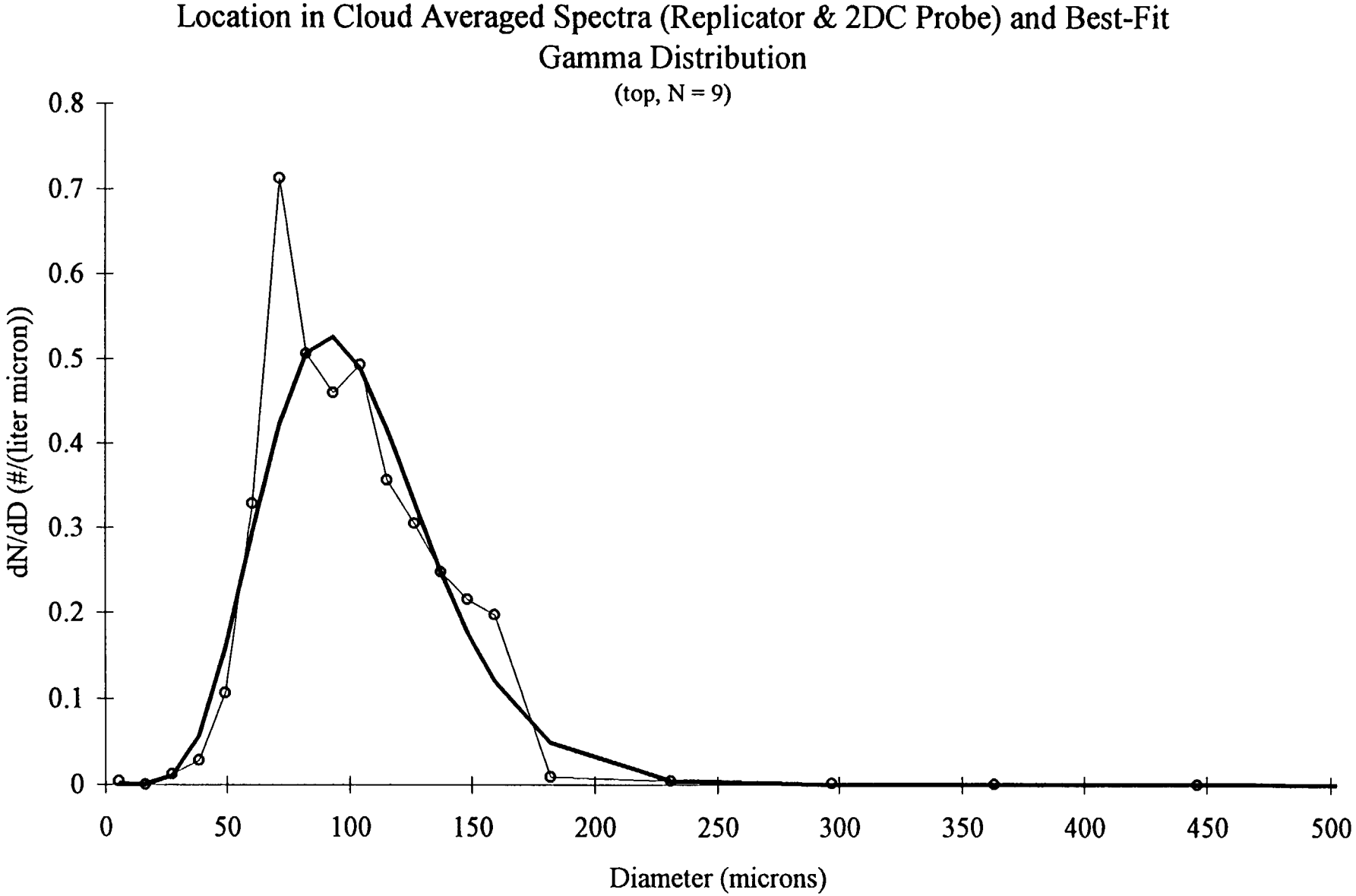
Location in Cloud Averaged Spectra (Replicator & 2DC Probe) and Best-Fit Gamma Distribution
(top, N = 9)
dN/dD (#/(liter micron))
0.8
0.7
0.6
0.5
0.4
0.3
0.2
0.1
0
0
50
100
150
200
250
300
350
400
450
500
Diameter (microns)

Crystal Habit Information

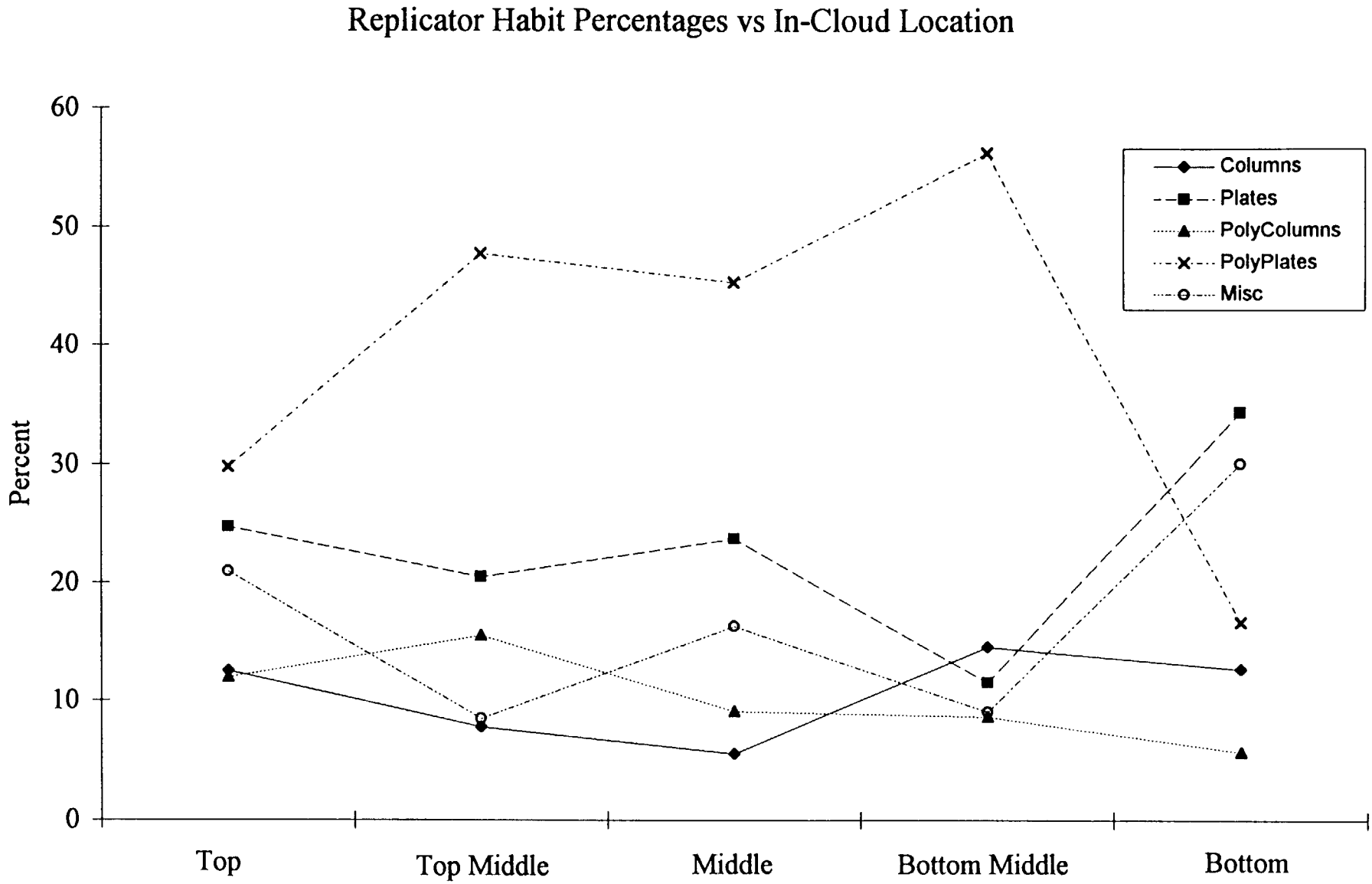
Replicator Habit Percentages vs In-Cloud Location
60
50
40
30
20
10
0
Percent
Top
Top Middle
Middle
Bottom Middle
Bottom
Columns
Plates
PolyColumns
PolyPlates
Misc

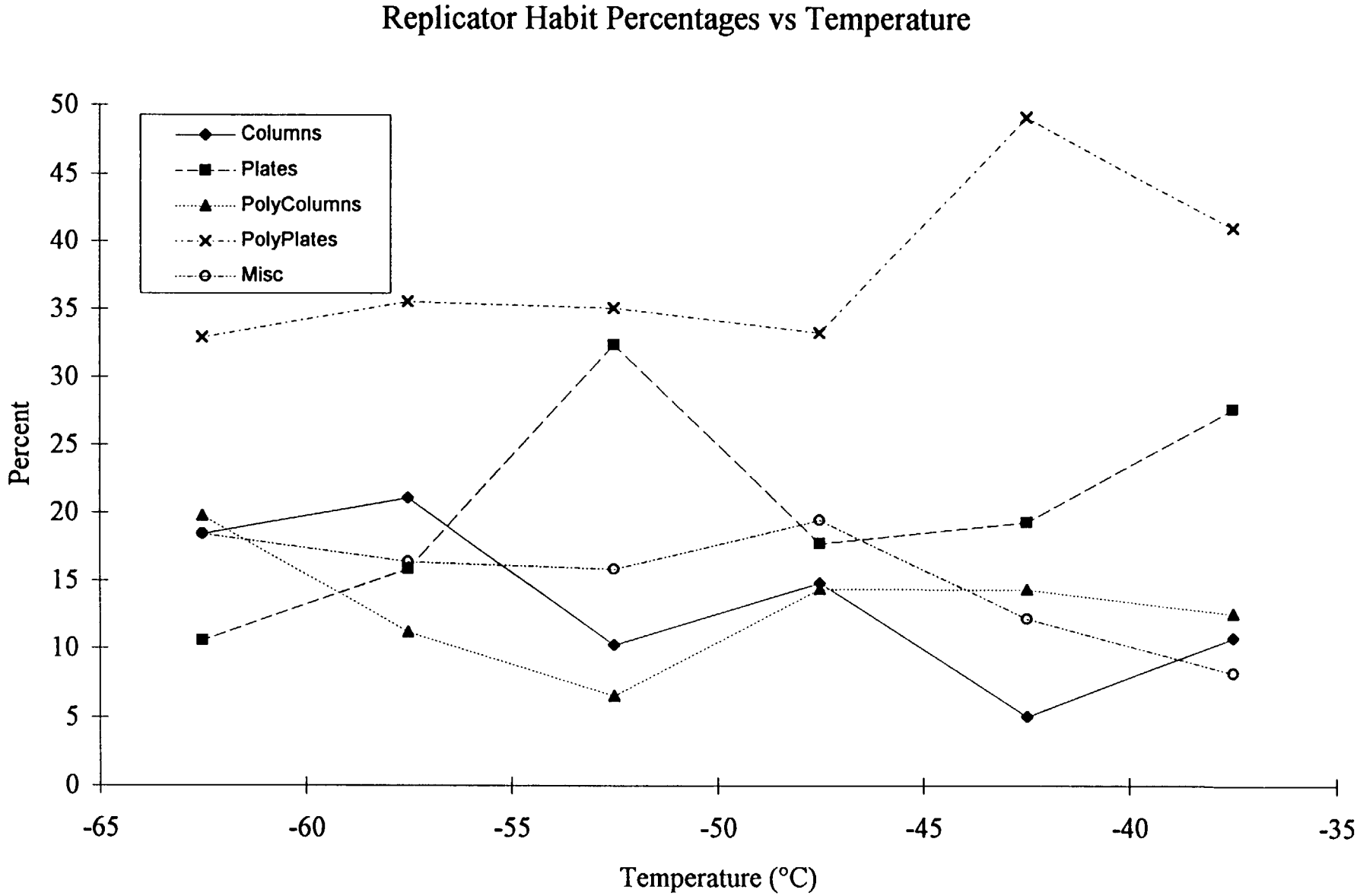
Replicator Habit Percentages vs Temperature
Columns
Plates
PolyColumns
PolyPlates
Misc
Percent
50
45
40
35
30
25
20
15
10
5
0
-65
-60
-55
-50
-45
-40
-35
Temperature (°C)